School of
ENGINEERING
DUKE UNIVERSITY

COMPLIANT ROBOTIC STRUCTURES

First Report to DARPA

June 1, 1984 – May 31, 1985

DEC 0 3 1985

James F. Wilson

Durham, North Carolina 27706

August, 1985

85 11 29 040

COMPLIANT ROBOTIC STRUCTURES

First Report to DARPA

June 1, 1984 – May 31, 1985

James F. Wilson

Department of Civil and Environmental Engineering ✓

Duke University

Durham, North Carolina 27706

August, 1985

REPORT DOCUMENTATION PAGE

Form Approved
OMB No. 0704-0188
Exp Date Jun 30, 1986

1a. REPORT SECURITY CLASSIFICATION	1b RESTRICTIVE MARKINGS
Unclassified	AD-A161897

2a. SECURITY CLASSIFICATION AUTHORITY	3. DISTRIBUTION/AVAILABILITY OF REPORT
	This document is available to the U.S. public through NTIS, Springfield Virginia 22161
2b. DECLASSIFICATION/DOWNGRADING SCHEDULE	

4. PERFORMING ORGANIZATION REPORT NUMBER(S)	5. MONITORING ORGANIZATION REPORT NUMBER(S)
DUKE-CE-001-85-1	

6a. NAME OF PERFORMING ORGANIZATION	6b OFFICE SYMBOL (If applicable)	7a. NAME OF MONITORING ORGANIZATION
Duke University	CE	ONRRR

6c. ADDRESS (City, State, and ZIP Code)	7b. ADDRESS (City, State, and ZIP Code)
Durham, N. C. 27706	Georgia Institute of Technology 2060 O'Keefe Building Atlanta, Georgia 30332

8a. NAME OF FUNDING/SPONSORING ORGANIZATION	8b OFFICE SYMBOL (If applicable)	9. PROCUREMENT INSTRUMENT IDENTIFICATION NUMBER
DARPA (DOD)		MDA903-84-C-0243

8c. ADDRESS (City, State, and ZIP Code)	10. SOURCE OF FUNDING NUMBERS			
	PROGRAM ELEMENT NO.	PROJECT NO.	TASK NO	WORK UNIT ACCESSION NO.
DARPA/DSO 1400 Wilson Blvd. Arlington, Virginia 22209				

11. TITLE (Include Security Classification)

Compliant Robotic Structures

12. PERSONAL AUTHOR(S)
Wilson, James F.

13a. TYPE OF REPORT	13b. TIME COVERED	14. DATE OF REPORT (Year, Month, Day)	15. PAGE COUNT
first year report	FROM 6/1/84 TO 5/31/85	1985, August	

16. SUPPLEMENTARY NOTATION

17. COSATI CODES			18 SUBJECT TERMS (Continue on reverse if necessary and identify by block number)
FIELD	GROUP	SUB-GROUP	Bellows, cylindrical shells, manipulators, nonlinear materials, orthotropic shells, robotics

19. ABSTRACT (Continue on reverse if necessary and identify by block number)

A compliant robotic structure is one or more continuously flexible arms that can be controlled to manipulate objects. A typical arm is comprised of orthotropic tube elements placed end-to-end where each element is designed to move in a particular way (bend, twist or extend) when pressurized.

The results of the first year studies are reported in three chapters. Chapter I focuses on the mechanics and structure of an elephant trunk. Chapter II involves the analysis of computer controlled compliant element systems that bend and coil similar to elephant trunks. Chapter III focuses on the analysis of compliant orthotropic tube elements that can be used as torsion actuators when pressurized.

20 DISTRIBUTION/AVAILABILITY OF ABSTRACT	21. ABSTRACT SECURITY CLASSIFICATION (over)
☒ UNCLASSIFIED/UNLIMITED ☐ SAME AS RPT. ☐ DTIC USERS	unclassified

22a. NAME OF RESPONSIBLE INDIVIDUAL	22b. TELEPHONE (Include Area Code)	22c. OFFICE SYMBOL
William E. Isler	(202) 694-3624	

DD FORM 1473, 84 MAR 83 APR edition may be used until exhausted All other editions are obsolete.

SUMMARY

In the present context, a compliant robotic structure is one or more continually flexible beams whose motion can be controlled to manipulate objects. Typically, a single beam is comprised of many hollow tube elements placed end-to-end, where each tube element moves in a particular way when pressurized with air. Each tube element, made of a reinforced polymeric material, is designed with directional stiffness properties so that tube motion (bending, twisting, extension, coiling) is predictable for a given external loading and internal pressure history. The basic objectives are to develop theories for the motion and control of selected single elements and multiple element systems (beams) to be used a light-weight, fast-acting manipulators.

To meet the objectives, the first year of this three-year project was focused on three separate yet related topics. The first involved studies of an elephant's trunk from the viewpoint of a compliant, continuously flexible manipulator. The relationships among the load-carrying capacity, material (or muscle) properties and trunk geometry were investigated and are reported in Chapter I. Using clues from this animal study, particularly the observations of how a trunk coils around an object and then lifts it, the second study involving the nonlinear mechanics of bending and coiling tube-type element systems was carried out. Those results are reported in Chapter II. The third study employed the linear theory of elasticity to predict the load and deformation behavior of cylindrical tubes with orthotrophy in the form of constant angle helices. The quantative results given in Chapter III show that such a tube element can be used as a torsion actuator, or a manipulator that twists about its longitudinal axis when pressurized.

i

ACKNOWLEDGEMENTS

James F. Wilson

Professor and

Principal Investigator

August, 1985

ii

TABLE OF CONTENTS

I. MECHANICS OF AN ELEPHANT TRUNK:

THEORY AND MEASUREMENTS

ABSTRACT

Elephant trunks are versatile and strong. Their mechanical design may therefore be used as a source of ideas for the design of versatile, strong robotic manipulators. In this paper a mathematical model of an elephant trunk lifting a weight is developed based on assumptions parallel to those used in the analysis of prestressed, linear, composite beams. Data on overall trunk geometry obtained during weight-lifting and data for the trunk muscle distribution at a cross section are used to calculate an apparent tangent modulus for the trunk tissue. During a change in trunk curvature for which the uniform component of longitudinal prestrain remains a constant 30 percent, a typical value for the apparent modulus is of the order of $10^6 N/m^2$. This study represents an initial step toward more refined analyses that rationally relate the loading, the overall trunk geometry and the muscle structure while satisfying equilibrium conditions.

INTRODUCTION

The trunk of an elephant is a tapering muscular structure, completely lacking rigid materials, of nearly circular cross-section. It is versatile and strong; trunks can shorten, extend, bend, and twist, and elephants have been trained to lift and manipulate masses of up to 300 kg with their trunks. This study is part of a larger study exploring the mechanics of trunk motion and strength, and aimed at discovering principles of trunk design that may be used in the design of similar, continuously flexible, versatile, strong robotic manipulators. A further discussion of animal muscular hydrostats and robotic mechanics is given by Wilson (1984).

The purpose of the present study is to correlate original data for the overall geometry of a trunk lifting a load with the reactive forces of the trunk muscles, to measure the average longitudinal strain of a trunk lifting a weight, and then to calculate an apparent modulus of trunk tissue. The apparent modulus is defined as the average tangent modulus for all of the longitudinal and oblique muscle tissue at a given cross section. This average tangent modulus E_a represents the slope of the stress-strain curve in a uni-axial test in which this whole muscle group has a uniform longitudinal pre-strain ϵ_u. The method used to calculate the modulus is one that does not require dissection of the animal involved, and may be used by zoologists interested in the apparent modulus of other animal appendages. This modulus calculated for the trunk may be used as a guide in choosing a material for trunk-like robotic manipulators.

The size and distribution of the trunk's four basic muscle masses--the radial, the longitudinal, and the two oblique layers--probably account for the elephant's ability to grasp and manipulate loads with its trunk. Although the role of each muscle type in trunk movement and load manipulation is not fully

2

understood, it is probable that one can draw parallels to the mechanical behavior of squid tentacles and vertebrate tongues as outlined by Kier (1982). In this case contraction of selected oblique muscles would lead to torsion of the trunk about the longitudinal axis, uniform contraction of radial muscles would lead to uniform trunk lengthening, and contraction of longitudinal and radial muscles, acting separately or together on one side of the trunk, would lead to trunk bending.

In this analysis the longitudinal trunk loads (self-weight and payload) are assumed to be supported solely by the tensions of the longitudinal and oblique muscles. The corresponding longitudinal strain has two components: a relatively larger, uniform, contraction prestrain (observed to be 20 to 35 percent before and during lifting); and a relatively small strain (two percent maximum) due to trunk bending and curvature--as the payload is lifted. In achieving the uniform contraction prestrain, the stress-strain behavior is probably very nonlinear. The tangent modulus (the slope of the stress-strain curve) may increase dramatically since muscles are much stiffer after contraction (Yamada and Evans, 1970). For the small strains associated only with trunk bending and small changes in trunk curvature between two states of lifting the payload, the analysis is based on classical beam theory. That is, the trunk is assumed to be composed of a linear, composite material (the longitudinal and oblique muscles) for which the apparent modulus on the side of the neutral axis under the least muscle tension is the same as the apparent modulus on the other side under the most muscle tension. The apparent modulus of this analysis, then, represents the average value of the tangent modulus for the muscles involved in incremental bending, given a uniform prestrain. The analysis implies that during incremental bending there is no change in chemical structure of the material with load other than the strains imposed on

3

the chemical bonds by the load. Clearly, the trunk of a live elephant may not exactly satisfy all of the assumptions and conditions. However, local variations in the modulus of the components of muscle cells and fibrous connective tissues, and other local variations such as possible shifts in the neutral bending axis and possible nonlinear bending strain distributions, would have little effect on either the average apparent modulus for the load-carrying tissue acting as a group, or on the overall mechanical performance of the trunk. The approach herein represents the first step towards a more refined and accurate analysis of the trunk.

Briefly, the analysis and measurements proceed as follows. As described in the Mathematical Model and Analysis section, a linear strain distribution at a cross section and force equilibrium were used to calculate the location of the neutral axis of the trunk. To do this the cross-sectional areas of muscles were obtained from a drawing of a trunk cross-section and a discussion of detailed trunk morphology presented in the classical study of the elephant's head by Boas and Paulli (1908). The drawing of the cross-section was then estimated to coincide with a particular location along the length of the trunk. At this location the radii of curvature ρ_0 and ρ_1 at two lift positions were measured from films we took of an elephant lifting a known weight with its trunk. The second moment of area of the muscles, I, was determined from the size and distribution of the muscles in the Boas and Paulli cross-section. Based on moment equilibrium, ρ_0, ρ_1, and I were then used, as described below, to calculate the apparent modulus of trunk tissue.

This paper is divided into four parts. In the first two, the Muscle Morphology section and the Lifting Experiments section, we describe the sources of our measured data. We develop our mechanical model of the trunk in the Mathematical Model and Analysis section. We then present our calculated data in the Numerical Results and Discussion section.

4

MUSCLE MORPHOLOGY

Figure 1 presents a schematic drawing adapted from Boas and Paulli (1908) showing the placement and orientation of the four basic muscle masses and the two main tendinous masses in a trunk of _Elephas maximus_, the Asian elephant. Longitudinal sheets of radial muscles radiate from the connective tissue around the two nostrils. These muscles insert dorsally and laterally into tendinous leaves, not shown in this figure, which in turn radiate and connect to a long tendinous sheet, which is shown, covering the dorsal and lateral muscle of the trunk. The outer insertion of the ventral radial muscles is not known. Longitudinal muscles run in the channels formed dorsally and laterally by the radiating muscles. Some of the longitudinal muscles insert into the radiating tendons attached to the radiating muscles, and some end in the center of the trunk where their insertion is less obvious.

Two layers of oblique muscle, oriented in opposite directions and one interior to the other, run down the ventral side of the trunk. Both of these muscle masses are symmetrical about the sagittal plane. The outer layer inserts ventrally along the sides of a long ventral tendon and runs laterally to insert along the sides of the dorso-lateral tendinous sheet. The inner layer inserts ventrally into the inner portion of the ventral tendon, and the lateral insertion of this muscle mass is not known. The orientation of the oblique muscles changes down the length of the trunk. Proximally the outer layer is almost transverse in orientation, but it gradually changes so that distally the fibers run almost longitudinally. The inner layer is exactly the reverse. Proximally, the inner oblique muscle fibers run almost longitudinally and distally they run almost transversely. Both the dorso-lateral and ventral tendons are separated proximally from the skin by a layer of loose connective tissue; further down the trunk they are more intimately connected to the skin.

5
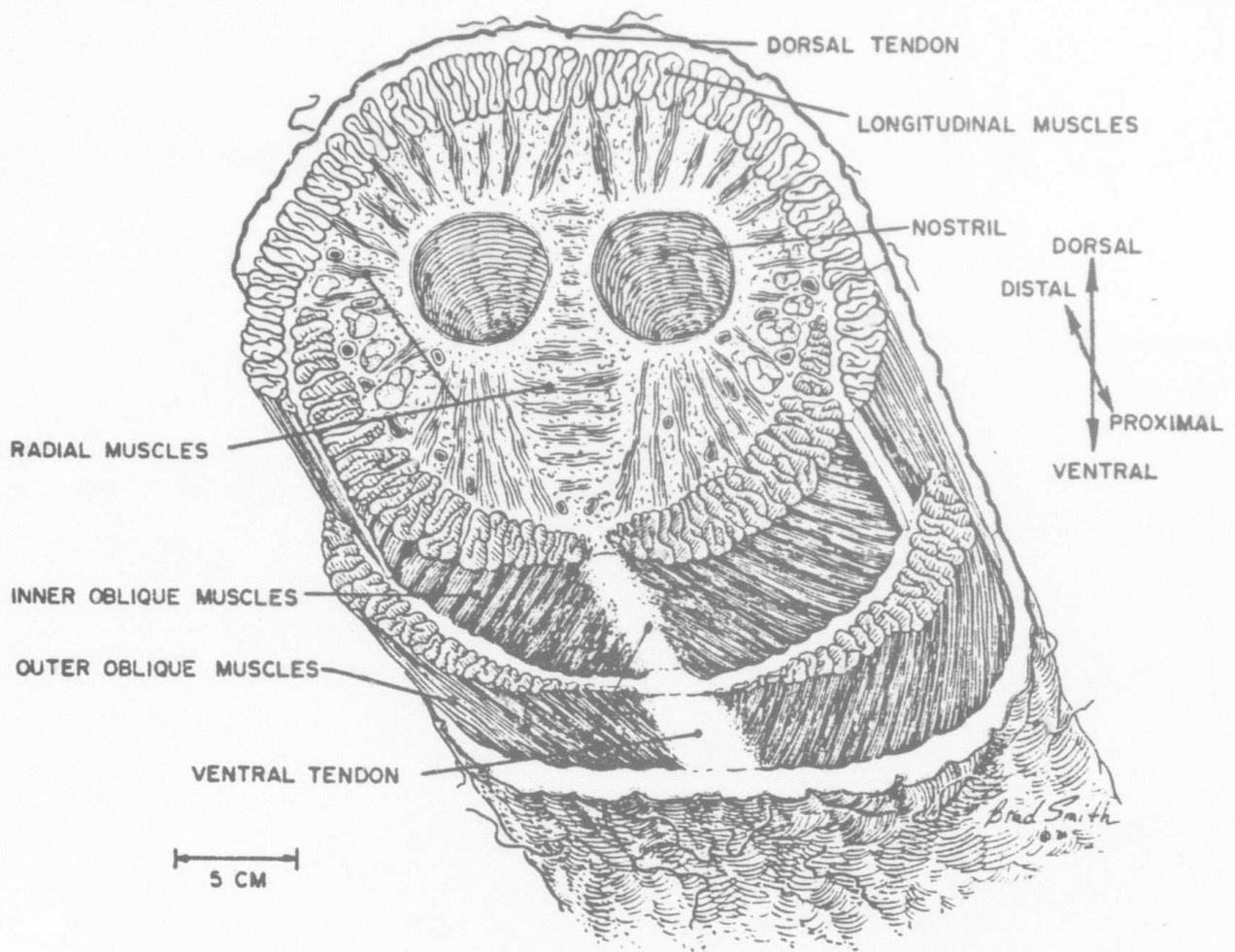
Figure 1   Cross section of an elephant's trunk showing the distribution of muscles (based on information taken from Boas and Paulli (1908) by Brad Smith)

We took 16 mm movies of two mature Asian elephants at the National Zoo in Washington, D.C. This involved filming the trunks while the elephants lifted payloads at the tips of their trunks. These elephants had trunks about 1.5 m long when in a fully extended, relaxed state. The nominal outside diameters of these trunks were about 32 cm at the head and 8 cm at the tip.

For our analysis, we used both data from films and data obtained from drawings of cross-sections of an elephant's trunk from the Boas and Paulli treatise. A composite of such cross-sections is shown in Figure 1. Based on the position of radial muscles below the nostrils, the shape of the nostrils, and the relative thickness of the oblique muscles in cross-section, we deduced that this particular transverse cross-section was located at position A-A along the trunk as shown in scale drawings of photographs, Figures 2. The length scales shown in Figures 1 and 2 are those for the Asian elephant that we filmed. The important assumption we used in deriving the particular numerical results that follow is that the muscle mass distribution for section A-A in Figure 2 is geometrically similar to that of Figure 1.

LIFTING EXPERIMENTS

In preparation for a typical experiment involving a live Asian elephant, white zinc oxide spots were first painted along the midlateral line on the side of the trunk, as shown in Figure 2. Each white spot was located along the trunk at a distance ℓ_i from the spot nearest the head. The trunk was photographed in what appeared to be its longest and fully relaxed state, in a near vertical position.

The sequence of events involving the elephant lifting a payload with the tip of its trunk was recorded using a Canon Scopic 16 mm movie camera situated about 12 m directly to the side of the animal. Trunk motion was in the

7
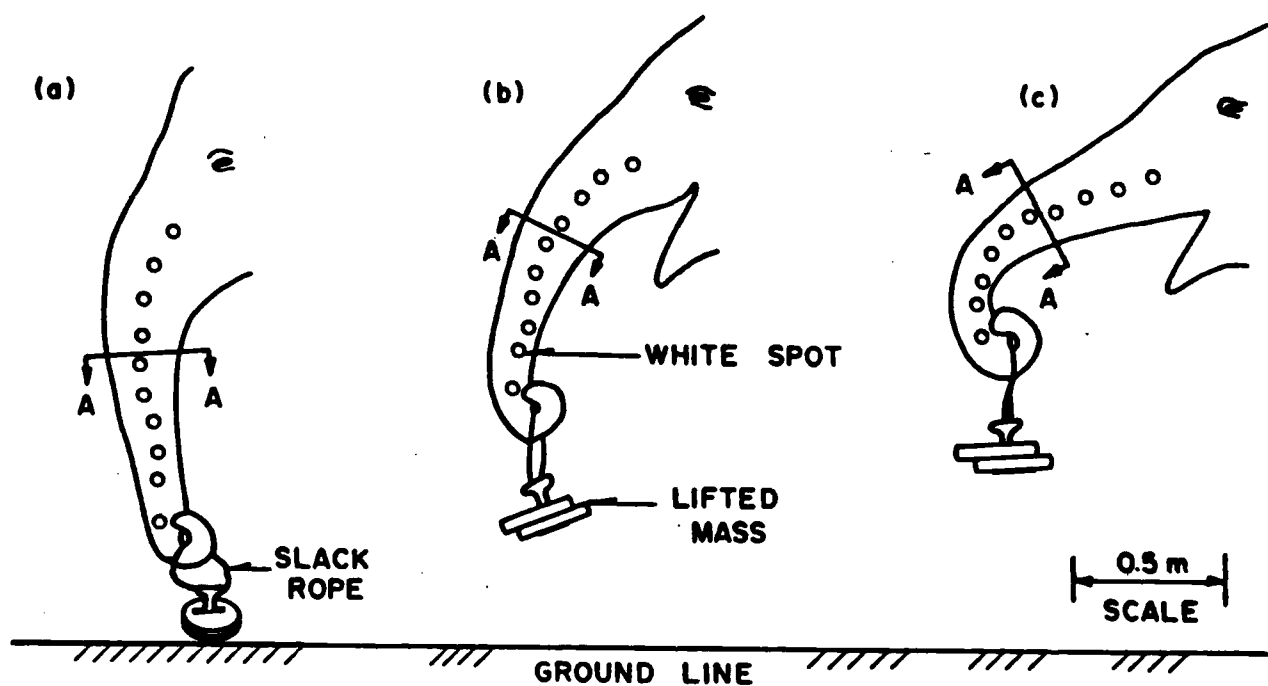
Figure 2   Trunk contracted with payload on ground (a); payload at an
            intermediate position (b); and payload at its highest position
            (c). Traced from projected movie images.

8

vertical plane, parallel to the side of the animal and perpendicular to the plane of movie images. The sequence of events was as follows.

1. The trunk tip looped around the rope attached to a payload mass of 26.2 kg. With the payload still on the ground, the entire trunk shortened and thickened before lifting, resulting in the configuration of Figure 2a. The average longitudinal contracted strain ϵ_u was deduced by comparing the locations of the trunk spots in the relaxed and contracted states. That is, each spot moved from its relaxed position ℓ_i by an amount $\Delta\ell_i$ as depicted by the insert of Figure 3. The results are plotted as circles in Figure 3, from which the slope or initial strain before lifting was deduced by a least squares straight line fit as $\epsilon_u = -24.4\%$, a nearly uniform value along the trunk.

2. The coiled trunk tip stretched a bit while the elephant lifted its head and dragged the payload along the ground.

3. The payload was lifted by an upward motion of the head, accompanied by a further shortening of the trunk, and a further curling motion of the whole trunk. Figures 2b and 2c depict the trunk with the payload lifted to an intermediate and the highest position. The average value of ϵ_u for these last two positions based on the data of Figure 3 were -31.5% and -33.0% respectively.

A careful study of enlarged prints from the film showed that the radius of curvature ρ traced by the white dots in the plane of motion changed significantly. The values of ρ and the corresponding uncertainties in measurement $\pm \Delta\rho$ at section A-A of the trunk were measured as $\rho_0 = 1.18$ m $\pm$ 0.06 m and $\rho_1 = 1.67$ m $\pm$ 0.25 m, corresponding respectively to the intermediate and highest positions of the trunk shown in Figure 2. The analysis that follows relates these bending strains to the radius of curvature.

9
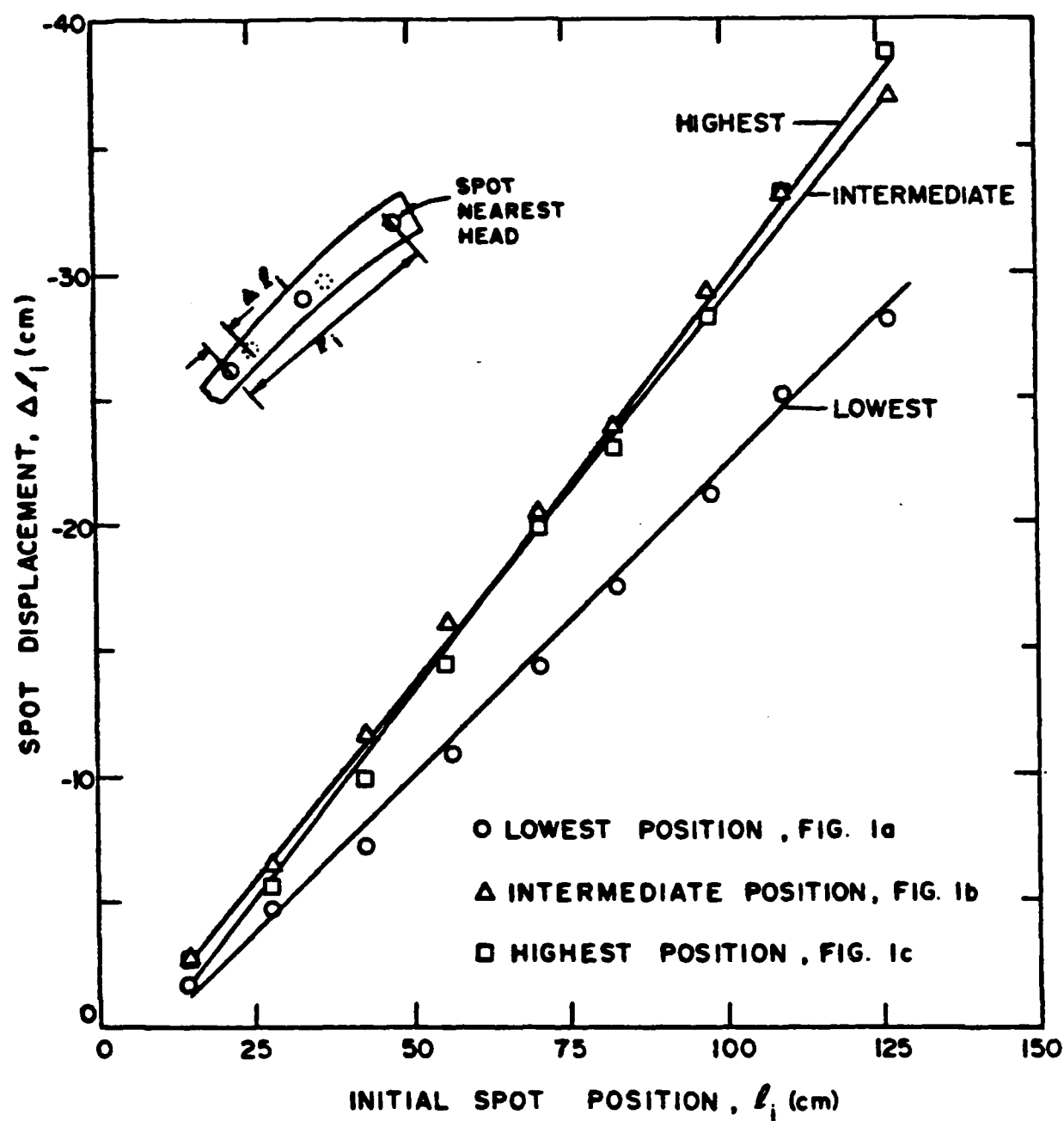
Figure 3   Straight lines indicate uniform trunk·contraction (constant gradient of deformation) for the three conditions of Figure 2.

10

MATHEMATICAL MODEL AND ANALYSIS

The purpose of this section is twofold: to define a rational, static, mathematical model of the trunk muscle system that supports both the trunk load and payload and to calculate the apparent elastic modulus of the trunk at section A-A when the trunk is between the two positions shown in Figure 2b and 2c. A few simplifying assumptions are needed. First, the longitudinal strain ϵ_x due only to trunk curvature ρ has a linear distribution from dorsal to ventral. That is

$$\epsilon_x = -\frac{y}{\rho} \tag{1}$$

where Figure 4 depicts this strain at position y from the neutral axis of bending. This linear strain distribution superimposed on the uniform contractual strain ϵ_u from muscle pretension gives the total strain at the trunk cross section. Second, in comparison to this total strain distribution, it is reasonable to assume that $\epsilon_y = \gamma_{xy} = 0$, where ϵ_y is the normal strain along the y direction and γ_{xy} is the transverse shear strain due to changes in the bending moment and curvature along the trunk. These assumptions, which are consistent with elementary beam theory, lead to an expression for the normal strain ϵ_θ along the length of each oblique muscle inclined at an acute angle θ with the longitudinal axis (Figure 3 and 4) or

$$\epsilon_\theta = \epsilon_x \cos^2\theta \tag{2}$$

Equation (2) follows from the strain transformation equations derived, for instance, by Timoshenko and Goodier (1951), where ϵ_y and γ_{xy} are zero.

The third assumption is that the longitudinal tensile stress in each muscle mass is linear with its longitudinal contracted strain, or

$$\sigma_x = -E_a \epsilon_x; \qquad \sigma_\theta = -E_a \epsilon_\theta \tag{3}$$

where σ_x and σ_θ are the normal stresses for the longitudinal muscles and

11

oblique muscles, respectively. Here, E_a is the apparent elastic modulus of the muscle mass, which is assumed to be the same for each muscle type.

The fourth assumption is that only the muscles carry the stresses set up by the trunk's own mass and by the payload. Thus, the tissue surrounding the muscles, although following the linear strain distribution, has a negligible stiffness compared to the stiffness of the activated muscles. A consequence of these assumptions is that the neutral axis in bending does not shift for small changes in trunk curvatures. The accuracy of these assumptions is not known.

At a typical cross section such as A-A in Figure 4, the condition of force equilibrium in the x direction, or perpendicular to this transverse section, must be met. This equilibrium condition establishes the location of the neutral axis $y=0$, or the plane along which the muscle strain due to trunk curvature alone is always zero. Force equilibrium is expressed as:

$$\int_{A_x} \sigma_x \, dA_x + \int_{A_0} \sigma_\theta \cos^2\theta \, dA_0 = 0 \tag{4}$$

where A_x is the total transverse cross sectional area for the longitudinal muscles and A_0 is the total observed cross sectional area of the oblique muscles projected on the same transverse cross section (the $x=0$ plane). From Figure 5, it is observed that for the oblique muscles the cross section area element normal to σ_θ is $dA_0 \cos\theta$, that the corresponding force is $\sigma_\theta \cos\theta \, dA_0$, and the component of this force projected along x is thus $\sigma_\theta \cos^2\theta \, dA_0$, which leads to the second integral on the left in Equation (4). With Equations (1), (2) and (3), Equation (4) is rewritten as

$$\int_{A_x} y \, dA_x + \int_{A_0} y \cos^4\theta \, dA_0 = 0 \tag{5}$$

A practical way to locate the neutral axis is as follows. As shown in Figure 4, the neutral axis at $y = 0$ is located at a distance $\bar{z}$ from a datum

12
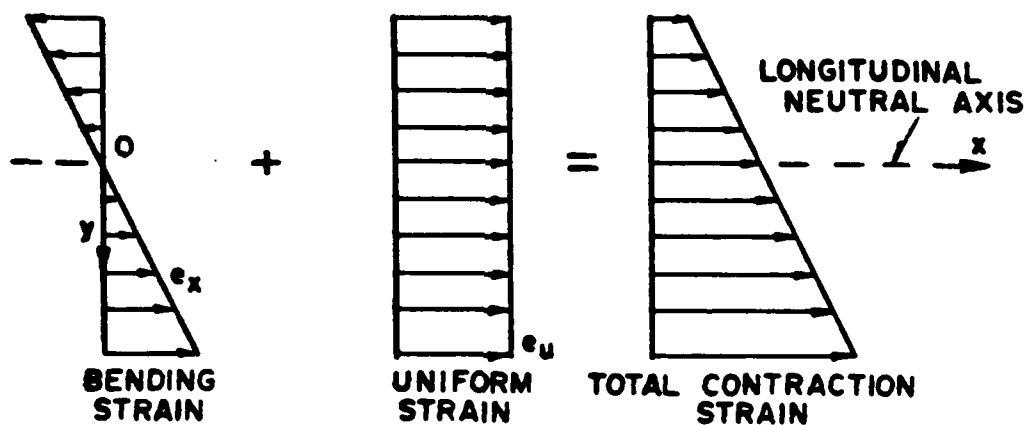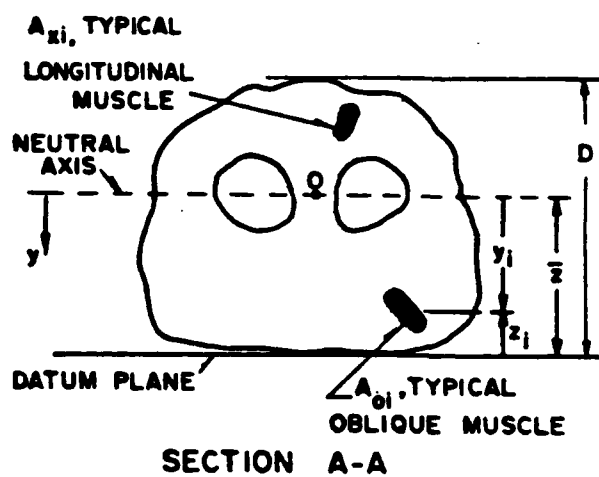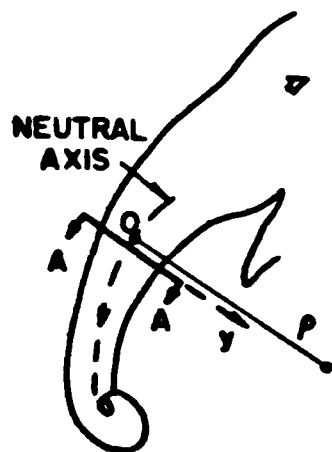
Figure 4. Definitions of trunk geometry and longitudinal strain.
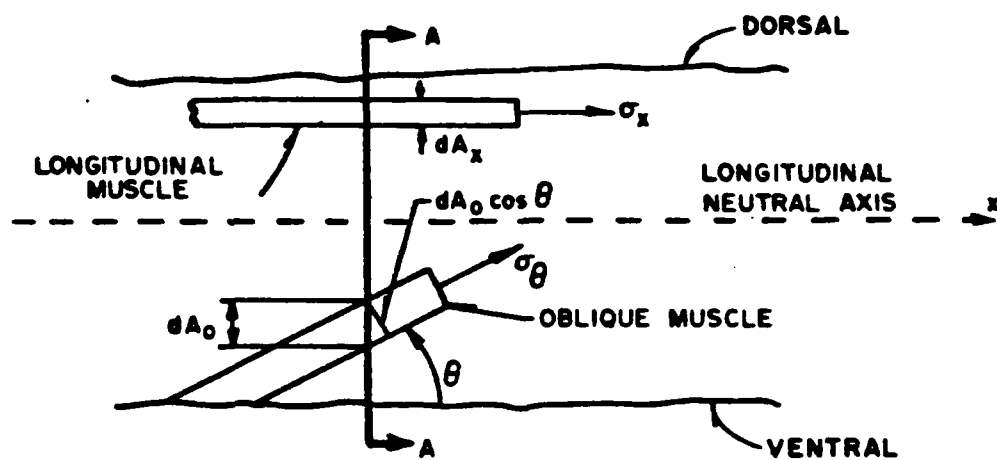
Figure 5. Stress and orientation of a typical oblique muscle.

axis chosen as the ventral edge. If the centroid of the area for each muscle i of area A_{xi} or A_{oi} is located at $y = y_i$, then the centroidal distance z_i from the datum axis is defined as

$$z_i = \bar{z} - y_i \tag{6}$$

When Equation (6) is combined with Equation (5), with the differential areas replaced by the areas A_{xi} and A_{oi}, and the integrals replaced by finite sums, the result is a practical formula for locating the neutral axis. That is

$$\bar{z} = \frac{\sum_{i=1}^{N} z_i A_{xi} + \sum_{i=1}^{M} z_i A_{oi} \cos^4 \theta_i}{\sum_{i=1}^{N} A_{xi} + \sum_{i=1}^{M} A_{oi} \cos^4 \theta_i} \tag{7}$$

where there are N longitudinal muscles and M oblique muscles at a cross section. Care must be taken to use the correct angles for the oblique muscle areas. For instance, for section A-A of Figure 5, $\theta = \theta_i = 29.1$ deg for the inner oblique muscles and $\theta = \theta_i = 34.1$ deg for the outer oblique muscles.

Having located the neutral axis, the bending strain distribution can be calculated from Equation (1) if the radius of curvature is known. Of interest here is the _change_ in the bending strain distribution between two loading states at section A-A. For instance, the difference in longitudinal muscle strain $\Delta\epsilon_x$ for a trunk configuration in its highest position (Figure 2c) for $\rho = \rho_1$ and in its intermediate position (Figure 2b) for $\rho = \rho_0$ is

$$\Delta\epsilon_x = -\frac{y}{\rho_1} - \left(-\frac{y}{\rho_0}\right) = -\frac{y}{\bar{\rho}} \tag{8}$$

where

$$\frac{1}{\bar{\rho}} = \frac{\rho_0 - \rho_1}{\rho_0 \rho_1} \tag{9}$$

At a fixed location y, the change in strain $\Delta\epsilon_\theta$ in a typical oblique muscle will always be less than $\Delta\epsilon_x$, or from Equation (2)

15

$$\Delta\epsilon_\theta = -\frac{y}{\bar{\rho}} \cos^2\theta \tag{10}$$

Accompanying these strain changes $\Delta\epsilon_x$ and $\Delta\epsilon_\theta$ during lifting are corresponding changes in the normal stress distributions, $\Delta\sigma_x$ and $\Delta\sigma_\theta$. These are the muscle reactions in response to shifts in two types of external loads causing moments at section A-A. One of these loads is due to the trunk mass segment m_t (below section A-A to the tip) which causes a differential moment of $m_t g(d_1-d_0)$. The other load is due to the payload mass m_p which causes a differential moment $m_p g(e_1-e_0)$. The load offset distances d_0, d_1, e_0 and e_1 are defined in the free body sketches of Figure 6. For moment equilibrium at Section A-A, it follows that

$$m_t g(d_1-d_0) + m_p g(e_1-e_0) = \int_{A_x} y\, \Delta\sigma_x dA_x + \int_{A_0} y\, \Delta\sigma_\theta \cos^2\theta dA_0 \tag{11}$$

Here $\Delta\sigma_x\, dA_x$ and $\Delta\sigma_\theta \cos^2\theta\, dA_0$ are the changes of the x-directed forces in the longitudinal and oblique muscles, respectively, which, when multiplied by their moment arms y and integrated over section A-A, leads to Equation (11). Invoking the linear relationships of Equations (3), along with Equations (2), (8), and (10), the differential stresses become

$$\Delta\sigma_x = -E_a\, \Delta\epsilon_x = E_a \frac{y}{\bar{\rho}} \tag{12}$$

$$\Delta\sigma_\theta = E_a\, \Delta\epsilon_\theta = E_a \frac{y}{\bar{\rho}} \cos^2\theta \tag{13}$$

With Equations (12) and (13), Equation (11) can be solved for the apparent modulus, or

$$E_a = \frac{\bar{\rho}}{I} [m_t g(d_1-d_0) + m_p g(e_1-e_0)] \tag{14}$$

where $\bar{\rho}$ is given by Equation (9) and I, the second moment of the muscle area with respect to the neutral axis (y=0), is

16
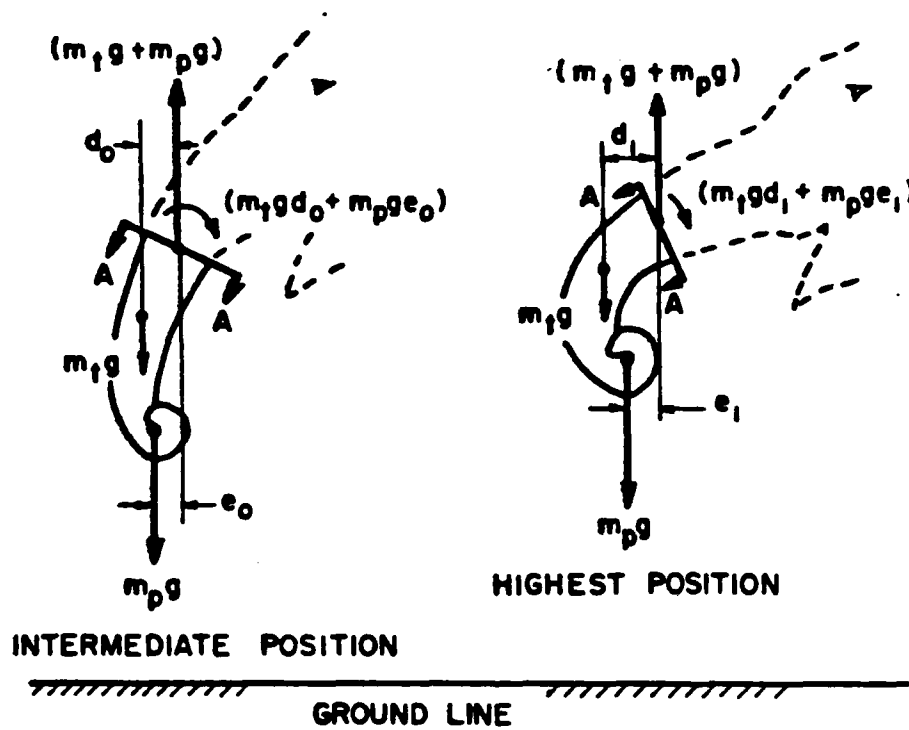
Figure 6. Free body sketches of a contracted trunk at
two positions.

17

$$I = \int_{A_x} y^2 \, dA_x + \int_{A_0} y^2 \cos^4\theta \, dA_0 \qquad (15)$$

With a knowledge of the muscle morphology as shown in Figure 1, along with trunk curvatures and the loading terms, the apparent modulus E_a may be calculated from Equations (14) and (15). Then the differential stress and strain distributions due only to a curvature change may be calculated from Equations (12) and (13). The appropriate measurements and typical numerical results are now discussed.

NUMERICAL RESULTS AND DISCUSSION

To obtain the desired numerical results, a clear and properly scaled outline of the longitudinal and oblique muscle areas at Section A-A is needed. Such a drawing, deduced from the Boas and Paulli treatise (1908) is shown in Figure 7. This muscle distribution and the measured data listed in Table 1 were used to calculate the apparent trunk modulus. The geometry of Figure 7 was scaled to match the cross section A-A of our subject animal's trunk, for which the section height D (Figure 4) was measured from photographs as 24 cm. Of the 150 muscle areas shown in Figure 7, 78 are longitudinal, 51 are inner oblique (θ = 29.1 deg), and 21 are outer oblique (θ = 34.1 deg). Using a fine grid overlay, each muscle area or projected area and its respective centroidal distance to the datum plane was calculated. The total areas A_x and A_0 are given in Table 2. With the values of θ measured from drawings in the Boas and Paulli treatise (1908), $\bar{z}$ was calculated from Equation (7) as 12.0 cm. Since D = 24 cm, the neutral axis lies at the mid-height of this cross section. The value of I was then calculated by numerically integrating Equation (15), yielding I = 4270 cm^4. Of course, these numerical results, although precisely calculated to three significant figures, are only as accurate as the artist's original drawings of the muscle distributions.

18
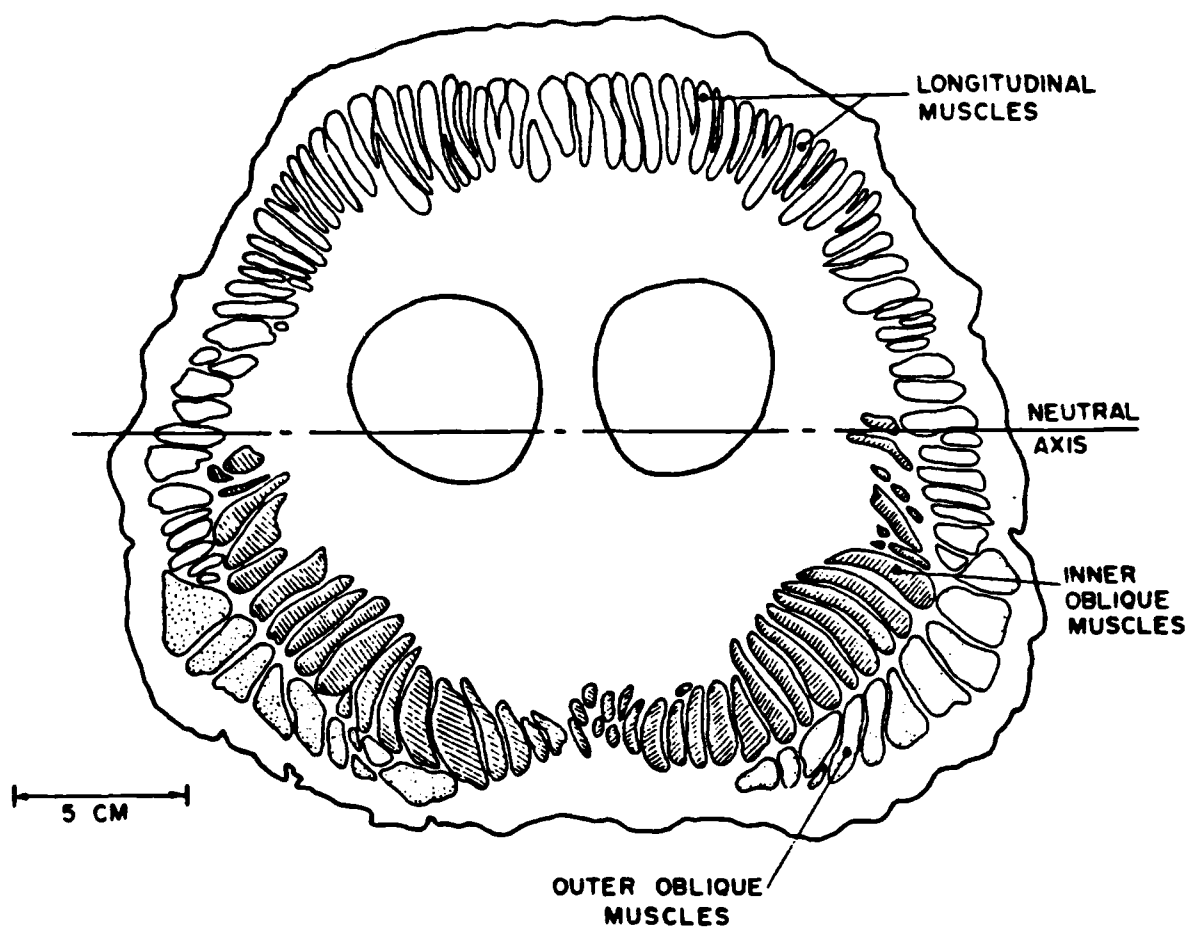
Figure 7. Idealized muscle distribution used for calculations (adapted from Boas and Paulli, 1908).

Table 1 - Summary of Measured Data

Symbol and Value	Meaning
$D = 24$ cm	trunk height (y direction) at section A-A
$d_0 = 5.0$ cm	offset distance of m_t (intermediate), Fig. 6a
$d_1 = 8.0$ cm	offset distance of m_t (highest), Fig. 6b
$e_0 = 9.29$ cm	offset distance of m_p (intermediate), Fig. 6a
$e_1 = 13.27$ cm	offset distance of m_p (highest), Fig. 6b
ℓ_i, $\Delta \ell_i$	spot locations, plotted in Fig. 3
$m_p = 26.2$ kg	mass of payload
$m_t = 16.37$ kg	mass of trunk from tip to section A-A
$M = 78$	number of longitudinal muscles at section A-A
$N = 72$	number of oblique muscles at section A-A
$\gamma = 1180$ kg/m^3	mass density of trunk
$\theta = 29.1$ deg	inclination of inner oblique muscles, Fig. 5
$\theta = 34.1$ deg	inclination of outer oblique muscles, Fig. 5
$\rho_0 = 118$	radius of curvature of section A-A, Fig. 6A
$\rho_1 = 167$	radius of curvature at section A-A, Fig. 6b
$\Delta \rho_0 = \pm 6$ cm	uncertainty of ρ_0 measurement
$\Delta \rho_1 = \pm 25$ cm	uncertainty of ρ_1 measurement

Table 2 - Summary of Calculated Data

Symbol and Value	Meaning	Equation or Figure
$A_x = 54.6$ cm^2	area of all longitudinal muscles on x=0 plane	Fig. 7
$A_o = 185.7$ cm^2	projected area of all oblique muscles on x=0 plane (inner oblique: 160 cm^2; outer oblique: 25.7 cm^2)	Fig. 7
$E_a = 1.33 \times 10^6$ N/m^2	apparent modulus of trunk	Eq. (14)
$\Delta E_a = \pm 0.532 \times 10^6$ N/m^2	uncertainty in E_a	Eq. (16)
$I = 4270$ cm^4	area moment of all muscles	Eq. (15)
$\bar{z} = 12.0$ cm	location of neutral axis	Fig. 4
$\Delta \sigma_x = 3.22 \times 10^4$ N/m^2	max. stress change, longitudinal muscle	Eq. (12)
$\Delta \sigma_\theta = 2.23 \times 10^4$ N/m^2	max. stress change, inner oblique muscle	Eq. (13)
$\Delta \sigma_\theta = 2.37 \times 10^4$ N/m^2	max. stress change, outer oblique muscle	Eq. (13)
$\Delta \epsilon_x = 0.0242$	max. strain change, longitudinal muscle	Eq. (8)
$\Delta \epsilon_\theta = 0.0168$	max. strain change, inner oblique muscle	Eq. (10)
$\Delta \epsilon_\theta = 0.0178$	max. strain change, outer oblique muscle	Eq. (10)
$\epsilon_u = -0.244$	uniform strain, lowest position	Fig. 3
$\epsilon_u = -0.315$	uniform strain, intermediate position	Fig. 3
$\epsilon_u = -0.330$	uniform strain, highest position	Fig. 3
$\bar{\rho} = -402$ cm	differential curvature	Eq. (9)

21

The external moments at section A-A due to the payload and the trunk mass were measured for the trunk in two different positions: the intermediate and the highest positions shown in Figures 2 and 6. The reason for choosing these two positions was that the uniform component of longitudinal trunk strain was nearly the same for both positions (ε_u was 0.315 and 0.330, respectively). Thus, the radii of curvature ρ_0 and ρ_1 as measured from photographs did not need to be corrected to account for changes in ε_u. The importance of highly accurate measures of these radii to an accurate calculation of the apparent modulus will be discussed below.

The quantities defining the differential moment between the selected trunk positions are enclosed in the square brackets of Equation (14). Measurements were made for each of these quantities. The payload mass m_p was 26.2 kg. The offset distances e_0 and e_1 for this load, as well as the volume segment of the trunk from tip to section A-A, were deduced from photographs (see Figure 6). The centroidal distances d_1 and d_2 for this volume segment were calculated assuming that the volume was a series of right, truncated cones. The volumes of the two nostrils, deduced from the Boas and Paulli treatise, were treated as voids. The product of this volume segment and the trunk's mass density then gave the value $m_t = 16.37$ kg. Our measurements of the mass density, made on selected samples from different areas of a dead elephant's trunk, yielded an average mass density of 1180 kg/m^3, with a maximum variation of 8 percent among samples.

The remaining quantity needed to calculate E_a given by Equation (14) is the differential curvature $\bar{\rho}$. This is defined by Equation (9) in terms of the radii of curvatures ρ_0 and ρ_1 at section A-A. Accurate measures of these radii were more difficult to deduce from enlarged photographs than the data previously discussed. More closely spaced and more carefully aligned white

22

spots along the trunk would lead to better measurements. In the present case, $\rho_0 = 118 \pm 6$ cm and $\rho_1 = 167 \pm 25$ cm, showing an uncertainty of 5 percent and 15 percent, respectively. For the nominal values of the radii, Equation (9) gave $\bar{\rho} = -402$ cm.

Using the measured data discussed above and summarized in Table 1, the apparent modulus was calculated from Equation (14), or $E_a = 1.33 \times 10^6$ N/m^2. It is interesting to note that this modulus compares favorably with the tangent modulus of human Sartorius muscle (1.77×10^6 N/m^2) and dog Rectus abdominis muscle (4.0×10^6 N/m^2) at prestrains of 60 to 65 percent, as estimated from data presented by Yamada and Evans (1970). Also, this modulus agrees within 10 percent with Young's modulus of a commercially available, synthetic rubber, Type A60B*.

Further calculations lead to the differential strain distributions in the longitudinal muscles, $\Delta\epsilon_x$, and in the oblique muscles, $\Delta\epsilon_\theta$, and their corresponding differential stresses, $\Delta\sigma_x$ and $\Delta\sigma_\theta$. The maximum value for each of these quantities was calculated from Equations (8), (10), (12) and (13) based on the maximum distance y extending from the neutral axis to the centroid of the most outlying muscle. The numerical results summarized in Table 2 reveal that the maximum differential muscle strains range from about 1.7 to 2.5 percent, and the maximum differential stresses range from about 2.2 $\times 10^4$ to 3.2×10^4 N/m^2. In fact, at any chosen distance y from the neutral axis, calculations showed rather narrow ranges for the differential strains and differential stresses among the three types of muscles. It is apparent that the muscles do a good job in sharing the load at this cross section.

Given the validity of the mathematical model, for which the main assumptions were the linearity of strain over the cross section and the linear

---

*Manufactured by The Lord Corporation, Erie, PA.

23

stress-strain law, the accuracy of the numerical results were found to depend strongly on the accuracy of ρ_0 and ρ_1. These were the most uncertain of all of the measured parameters. The analysis of Kline and McClintock (1953) may be used to show just how sensitive the calculation of E_a is to the measured uncertainties $\Delta\rho_0$ and $\Delta\rho_1$ of ρ_0 and ρ_1, respectively. The corresponding uncertainty in E_a, or ΔE_a for these two parameters only is given by

$$\Delta E_a = \left[\left(\frac{\partial E_a}{\partial \rho_0} \Delta\rho_0 \right)^2 + \left(\frac{\partial E_a}{\partial \rho_1} \Delta\rho_1 \right)^2 \right]^{1/2} \qquad (16)$$

When $\bar{\rho}$ from Equation (9) is substituted into Equation (14) and the result is differentiated according to Equation (16), the result is

$$\frac{\Delta E_a}{E_a} = \frac{1}{\rho_0 \rho_1 |\rho_0 - \rho_1|} \left(\rho_1^4 \Delta\rho_0^2 + \rho_0^4 \Delta\rho_1^2 \right)^{1/2} \qquad (17)$$

With the nominal values of the radii and their deviations as listed in Table 1, the numerical value of $\Delta E_a/E_a$ calculated from Equation (17) is 0.40. Thus, for relatively small uncertainties in radii (5 percent and 15 percent), the uncertainty in the apparent modulus is 40 percent, where $E_a = 1.33 \times 10^6$ H/m^2 $\pm 0.532 \times 10^6$ H/m^2.

Further studies are now underway that involve microscopic studies of muscle morphology at different cross sections in a dead elephant's trunk, and also the direct measurements of tensile properties of connective tissue. As further data becomes available, the present mathematical model may be refined. Thus, more exact connections may be deduced among the trunk's system parameters including its external loading, its overall shape during lifting, its muscle distribution, and the mechanical properties of its muscles. The results may provide clues to future mechanical designs of continuously flexible robotic manipulators made of polymeric materials.

NOMENCLATURE

A_o total area of oblique muscles projected on the $x=0$ plane

A_{oi} projected area of i-th oblique muscle on the $x=0$ plane

A_x total cross sectional area of longitudinal muscles in the $x=0$ plane

A_{xi} cross sectional area of i-th longitudinal muscle on the $x=0$ plane

D trunk height in y direction at section A-A

d_o, d_1 moment arms of m_t, Figure 6

E_a apparent modulus of trunk

ΔE_a uncertainty in E_a

e_o, e_i moment arms for m_p, Figure 6

g gravitational constant

I second moment of muscle cross sectional areas, Equation (15)

ℓ_i distance of the i-th spot, Figure 3

M number of oblique muscles at a cross section

m_p mass of pay load lifted at trunk tip

m_t mass of trunk from tip to section A-A, Figure 6

N number of longitudinal muscles at a cross section

x longitudinal coordinate along trunk's neutral axis

y, y_i transverse coordinates measured from neutral axis, Figure 4

z_i transverse coordinate of i-th muscle, Figure 4

$\bar{z}$ location of neutral axis from ventral, Figure 4

γ_{xy} transverse shear strain

ϵ_x normal strain in longitudinal muscles

ϵ_y normal strain along y

ϵ_θ normal contraction strain in oblique muscles

ϵ_u uniform trunk contraction strain

$\Delta \ell_i$ displacement of i-th spot along longitudinal axis

25

$\Delta\epsilon_x$ differential longitudinal strain due to trunk curvature change

$\Delta\epsilon_\theta$ differential strain in oblique muscles due to trunk curvature change

θ acute inclination angle of oblique muscles with the x-axis

θ_i value of θ for the i-th oblique muscle

ρ radius of curvature of trunk's neutral axis

ρ_0 value of ρ at section A-A, intermediate load position

$\Delta\rho_0$ uncertainty in ρ_0

ρ_1 value of ρ at section A-A, highest load position

$\Delta\rho_1$ uncertainty in ρ_1

ρ differential radius of curvature, Equation (9)

σ_x normal tensile stress in longitudinal muscles

σ_y normal stress in transverse direction

σ_θ normal tensile stress in oblique muscles

$\Delta\sigma_x$ differential stress corresponding to $\Delta\epsilon_x$

$\Delta\sigma_\theta$ differential stress corresponding to $\Delta\epsilon_\theta$

REFERENCES

Boas, J. E. V., and Paulli, S. (1908) The Elephant's Head: Studies in the Comparative Anatomy of the Head of the Indian Elephant and Other Mammals, Part I, Gustav Fisher, Jena, 1-79.

Kier, W. M. (1982) The functional morphology of the musculature of squid (loliginidae) arms and tentacles, Journal of Morphology, 12, 179-192.

Kline, S. J. and McClintock, F. A. (1953) Describing uncertainties in single-sample experiments, Mechanical Engineering, January, 3-11.

Timoshenko, S. and Goodier, J. N. (1951) Theory of Elasticity, McGraw-Hill, NY, 14-17.

Wilson, J. F. (1984) Robotic mechanics and animal morphology, Robotics and Artificial Intelligence, NATO ASI Series F11, M. Brady, ed., Springer-Verlag, Berlin, 419-443.

Yamada, H. and Evans, F. G., editors (1970), Strength of Biological Materials, Williams and Wilkins, Baltimore, MD, 95-96.

II. MECHANICS OF A CONTINUOUS MANIPULATOR MADE OF A NONLINEAR, COMPOSITE MATERIAL

ABSTRACT

This research deals with the analysis of light weight, flexible and fast moving robotic arms. A typical arm consisting of hollow cylindrical elements, bends and coils around a load and moves it to the desired position by varying the internal pressures in the individual elements. The theoretical derivations relating arm positions and loading incorporate nonlinear material properties and large deflections. A learning program is developed that stores information about arm motion, information that is used in subsequent manipulations to achieve efficient lifting scenarios. Typical numerical results for arm designs will be verified experimentally in the near future.

INTRODUCTION

Robots are programmed machines designed to carry out desired tasks for humans [1,2]. Their use in the industry is rapidly increasing and extensive research is underway with the aim of improving their capabilities. Robots can be used to efficiently carry out routine tasks without making the mistakes that a human would because of fatigue. Also robots can be used in environments which are harmful to the health of humans.

Mechanically most of the present day robots have arms consisting of rigid members connected by hinged or pivoted joints. To move such an arm precisely, the movements of its various members have to be coordinated. Such robots are slow-acting because of the inertia of the members and the time required to compute and control position.

A different approach using a light-weight, highly flexible, fast moving arm is made in this research. Such an arm is analogous to an elephant's trunk which has been analyzed recently [3]. It was observed that trained elephants can efficiently coil their trunks around heavy loads and lift them to desired positions. The present study simulates the action of an elephant's trunk within the limits of structural feasibility. The robotic arm is a continuous manipulator of rubber or polymeric material, consisting of hollow cylindrical elements joined end to end. The elements are selectively reinforced so that they bend, twist or extend when pressurized. Theoretical derivations and computer programs are written to evaluate the internal pressure required in each of the elements such that the arm can coil around a load and lift it to a desired position.

This research also deals with another important aspect of robotics. As machines cannot reason or think like humans, the robot has to be programmed to anticipate the various options or remedial measures, in advance of motion. Thus some aspects of Artificial Intelligence are incorporated into this research. A new Learning Program evaluates the end moments to be applied to

29

each of the elements in order to lift and position the end load. This program's database is updated appropriately each time the program is run, thereby increasing the apparent knowledge and efficiency of the program in performing load positioning calculations.

The theoretical derivations for the mechanical behavior of the pressurized elements, the programming logic, and some numerical results for a typical, flexible robotic arm are discussed.

ANALYSIS OF A TYPICAL ELEMENT

The geometry of a typical element is shown in Figure 1. It is a thin walled cylinder with the ends sealed and with reinforcement on the underside. The element is modelled as a cantilever beam of a nonlinear material. As in [4], finite deflections are considered. Given the applied end moment due to internal pressure, the horizontal and vertical deflections of the end of the beam are evaluated. The radius of curvature of the deflected beam is also computed. In this analysis, [5] was also used.

The hollow, cylindrical section is made out of a synthetic, nonlinear material for which the stress strain relationship is as follows

$$\sigma = A\varepsilon + B\varepsilon^{1/n}$$

where A, B and n are material constants.

The synthetic material can withstand high strains (up to 200%) without failure. The reinforcement is made of high strength steel shim or synthetic fibers with high tensile strength (Kevlar, for instance) as shown in Figure 2. The reinforcement provides the strength to the structure. The neutral axis for the composite element passes through the reinforcement because its stiffness is much greater in magnitude than that of the synthetic cylindrical section. For this reason with the application of internal pressure and thus an end moment, the element bends as shown in Figure 1. The reinforcement is assumed to be a linear material.

30
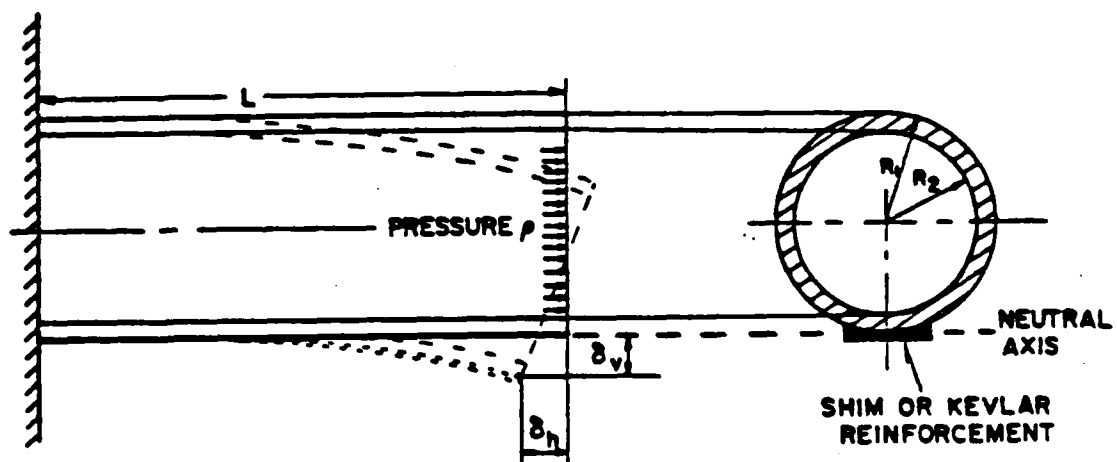
Figure 1. Bending of element due to internal pressurization.
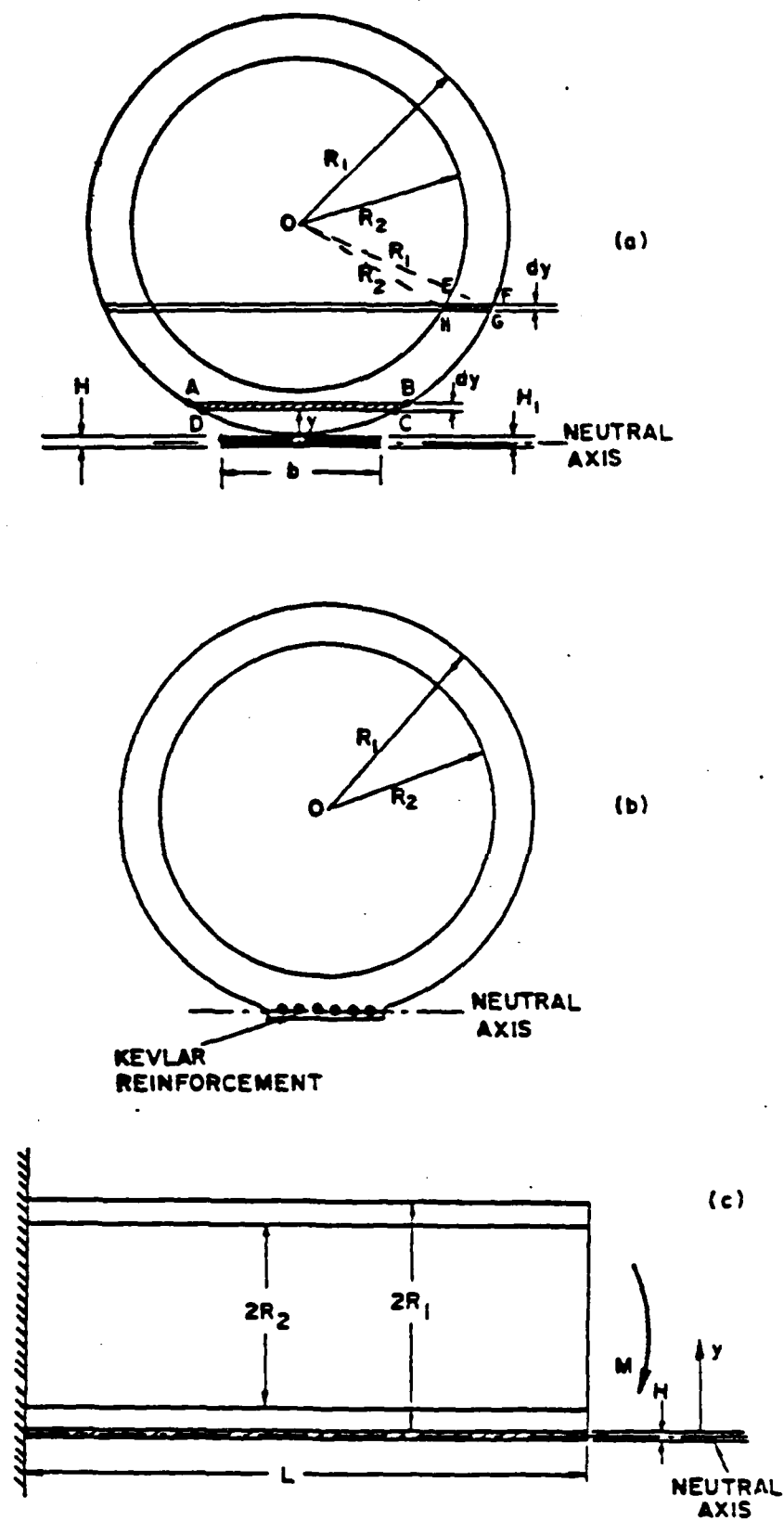
Figure 2. Cross-sectional views of element with shim (a); and with Kevlar reinforcement (b); side view (c).

Because the cylindrical part of the composite element is made up of a nonlinear composite material, the position of the neutral axis varies and has to be computed for each stress distribution across the section. Given an applied end moment M_a, the following iterative steps are required to calculate the position of the neutral axis.

a. Choose an initial position of the neutral axis.

b. Compute the radius of curvature ρ for the deflected element for the chosen position of the neutral axis.

c. Compute the moment of resistance M_c of the section for the computed ρ and the chosen position of the neutral axis.

d. If the following inequality holds for a specified tolerance limit ε

$$\left| \frac{M_a - M_c}{M_a} \right| < \varepsilon$$

then the iterations stop. Otherwise a new position of neutral axis is chosen and steps (b) to (d) are repeated. See Appendix A for the details of calculation.

Derivation of End Deflection Formulae

After the position of the neutral axis and the radius of curvature have been determined for the given end moment, the end deflections are computed in the following manner.

We know the moment curvature relationship as given by equation (A.21 in Appendix A). The equation is repeated here as follows

$$M_c = (\frac{1}{\rho}) \alpha + (\frac{1}{\rho}) \beta + (\frac{1}{\rho})^{1/n} {}_\eta$$

On rearranging the terms we get

33

$$\frac{1}{\rho} = \frac{M_c - \xi}{\alpha + \beta} \tag{1}$$

where

$$\xi = \left(\frac{1}{\rho}\right)^{1/n} \eta$$

$$\frac{1}{\rho} = \frac{y''(x)}{\{1 + [y'(x)]^2\}^{3/2}} \tag{2}$$

Equating Equations (1) and (2) we get

$$\frac{y''(x)}{\{1 + [y'(x)]^2\}^{3/2}} = \frac{M_c - \xi}{\alpha + \beta} \tag{3}$$

Equation (3) is a second order differential equation which can be integrated directly with respect to x to yield

$$\frac{y'(x)}{\{1 + [y'(x)]^2\}^{1/2}} = \frac{(M_c - \xi)}{(\alpha + \beta)} x + c_1$$

The constant of integration, c_1, can be evaluated using the fact that $y'(0) = 0$. Thus $c_1 = 0$ and

$$\frac{y'(x)}{\{1 + [y'(x)]^2\}^{1/2}} = \frac{(M_c - \xi)}{(\alpha + \beta)} x$$

Solving for $y'(x)$ yields

$$y'(x) = \frac{(M_c - \xi)x}{\sqrt{(\alpha + \beta)^2 - (M_c - \xi)^2 x^2}} \tag{4}$$

By integrating once more one obtains

$$y(x) = \frac{(\alpha + \beta) - [(\alpha + \beta)^2 - (M_c - \xi)^2 x^2]^{1/2}}{(M_c - \xi)} \tag{5}$$

where the constant of integration has been evaluated using the condition that $y(0) = 0$.

34

To evaluate the horizontal deflection, δ_h, at the free end of the beam, as shown in Figure 3, the equation for the arc length is used. The total length then is

$$L = \int_0^{L-\delta_h} \sqrt{1 + [y'(x)]^2} \; dx \qquad (6)$$

From Equations (5) and (6) we obtain

$$L = \int_0^{L-\delta_h} \frac{\alpha + \beta}{\sqrt{(\alpha + \beta)^2 - (M_c - \xi)^2 x^2}} \; dx \qquad (7)$$

This integral can be evaluated using the trignometric substitution.

$$x = \frac{\alpha + \beta}{M_c - \xi} \sin \theta \qquad (8)$$

$$dx = \frac{\alpha + \beta}{M_c - \xi} \cos \theta \; d\theta \qquad (9)$$

From Equation (8)

$$\theta = \sin^{-1}\left[x \; \frac{(M_c - \xi)}{(\alpha + \beta)}\right]$$

when

$$x = L - \delta_h$$

$$\theta_{(at \; x=L-\delta_h)} = \bar{\theta} = \sin^{-1}\left[(L - \delta_h) \; \frac{(M_c - \xi)}{(\alpha + \beta)}\right] \qquad (10)$$

Using Equations (9) and (10) from Equation (7) we get

$$L = \int_0^{\bar{\theta}} \frac{(\alpha + \beta)^2 \cos \theta}{(M_c - \xi)\sqrt{(\alpha + \beta)^2 - (\alpha + \beta)^2 \sin^2\theta}} \; d\theta$$

$$= \frac{(\alpha + \beta)}{(M_c - \xi)} \int_0^{\bar{\theta}} d\theta$$

$$= \frac{(\alpha + \beta)}{(M_c - \xi)} \sin^{-1}\left[(L - \delta_h) \; \frac{(M_c - \xi)}{(\alpha + \beta)}\right. \qquad (11)$$

35
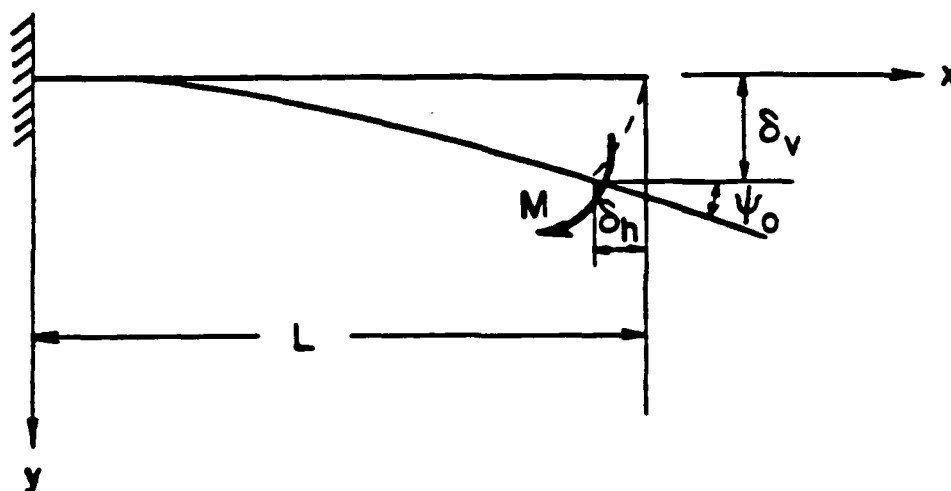
Figure 3.   Cantilever beam subjected to an end moment.

ANALYSIS OF MOTION AND LOAD-CARRYING CAPACITY OF A

CONTINUOUS MANIPULATOR ARM

The manipulator arm is made up by joining a number of the 'typical' elements, end to end. The desired capability of the arm determines the size and number of elements in the arm. The last few elements, (3 in our model) coil around the load, whereas the remaining elements help in the lifting of the load. Refer to Figure 4b.

Given an applied end moment, as shown in the previous chapter, we can evaluate the end deflections, and thus the end coordinates of the element with respect to the local coordinate axis system of the element. These end coordinates are transferred from local to global coordinate axis system by using a transformation matrix.

Similarly we can carry out the transformations for each of the elements and get the overall orientation of the arm in the global coordinate axis system.

When the end moments are changed, we can by the same procedure, compute the new orientation of the arm. The self weight of the elements is neglected throughout in our derivations.

The horizontal deflection, δ_h, at the free end can be obtained from Equation (11) as follows

$$\delta_h = L - \frac{\alpha + \beta}{M_c - \xi} \sin \left[L \frac{(M_c - \xi)}{(\alpha + \beta)} \right] \tag{12}$$

The vertical deflection at the free end can be obtained by substituting $(L-\delta_h)$ for x in Equation (5) to get

$$\delta_v = \frac{(\alpha + \beta)}{(M_c - \xi)} \left[1 - \cos \{ L \frac{(M_c - \xi)}{(\alpha + \beta)} \} \right] \tag{13}$$

Thus knowing the end moment values the end deflections δ_h and δ_v can be computed from equations (12) and (13) respectively, after the position of neutral axis and the radius of curvature have been computed.
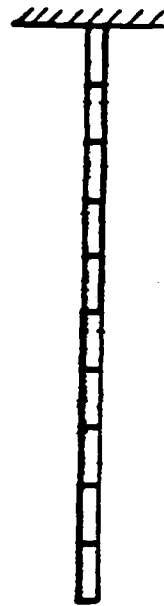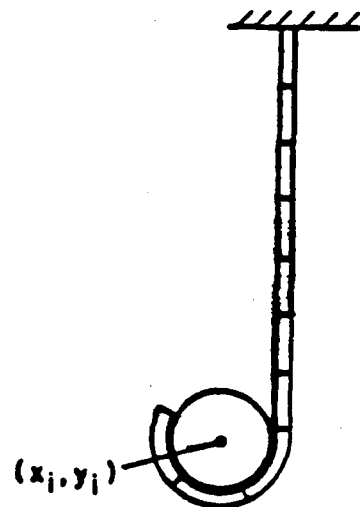
Figure 4.   Unpressurized elements (a);three end elements
            pressurized (b).

Derivation to Transfer Local End Coordinates to
Global End Coordinates
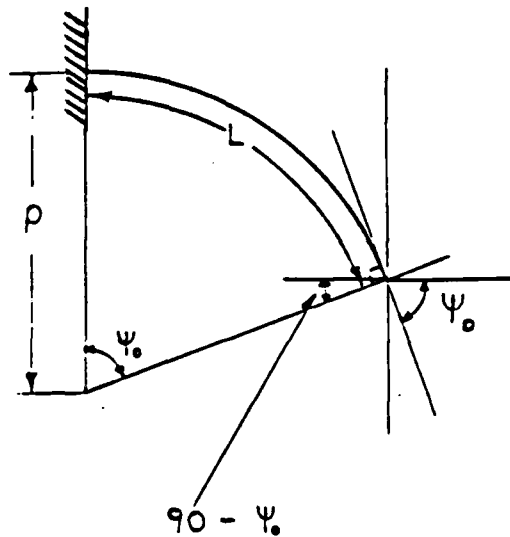
As the bending moment is constant for an element, the radius of curvature ρ is constant. It follows from the sketch above that

$$\Psi_0 = \frac{L}{\rho} \tag{14}$$

As shown in Figure 5a for the first element the global and local axis coincide.

For the remaining elements the relationship between the local and global axis system is as follows.

$$\begin{bmatrix} x \\ y \end{bmatrix} = \begin{bmatrix} x_2 \\ y_2 \end{bmatrix} + \begin{bmatrix} \cos\Psi_0 & \sin\Psi_0 \\ -\sin\Psi_0 & \cos\Psi_0 \end{bmatrix} \begin{bmatrix} x_1 \\ y_1 \end{bmatrix}$$

where

39
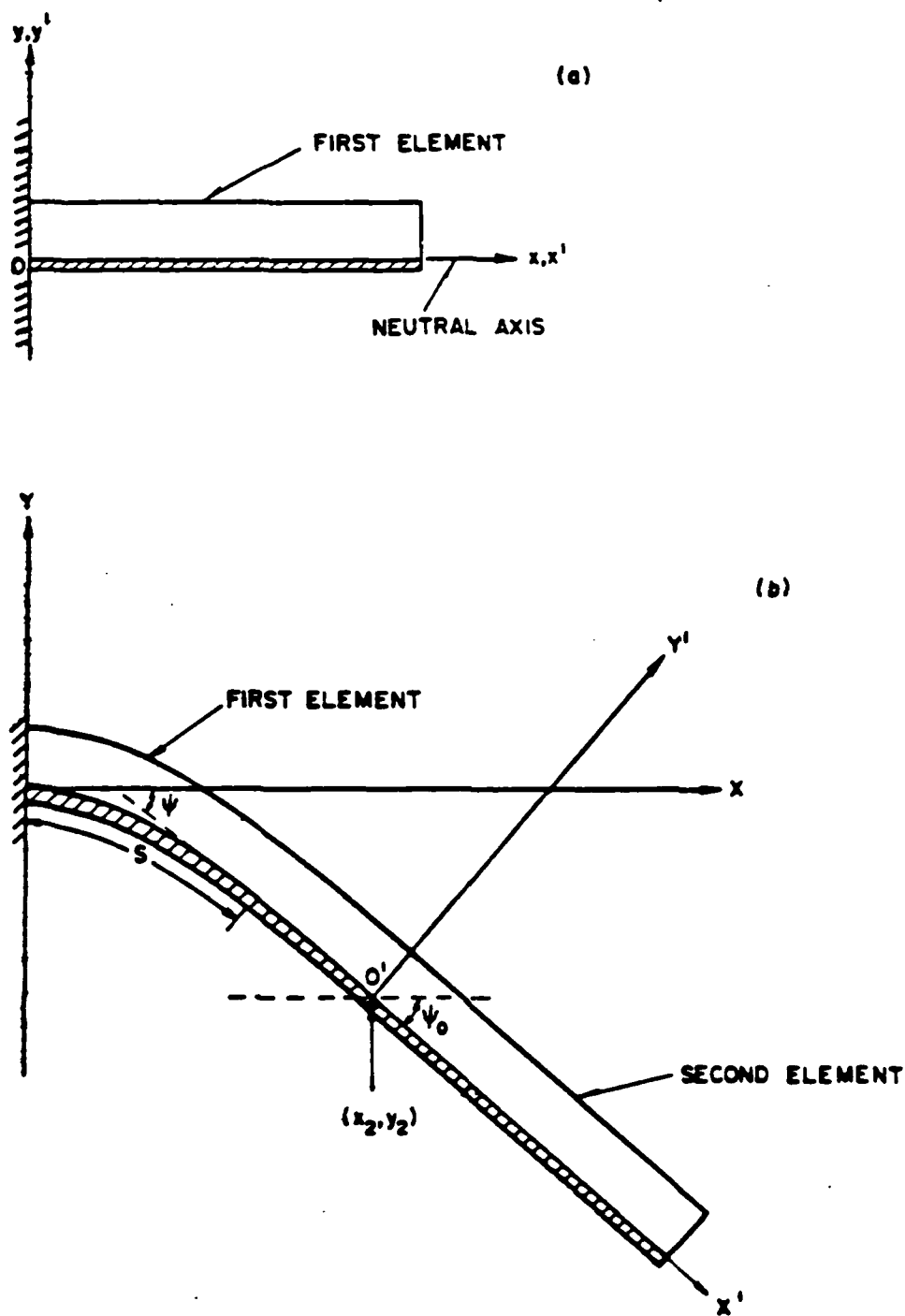
Figure 5. First element showing coincidence of local and global axes (a); and second element showing displaced local axis (b).

Ψ_0 is the angle which the x' axis, of the local coordinate axis system of the element, makes with the x axis of the global coordinate axis system.

x_2, y_2 are the coordinates of the origin of the local coordinate axis system in terms of the global coordinate axis system.

x_1, y_1 are the coordinates of any point P in the local coordinate axis system.

x, y are the coordinates of the same point P in the global coordinate axis system.

In our case the point P is the end point of the deflected element.

$$x_1 = L - \delta_h$$
$$y_1 = -\delta_v$$

(15)

where

δ_h = horizontal deflection

δ_v = vertical deflection

For the next element

$$\Psi_{on} = \Psi_{oc} + \frac{L_c}{\rho_c}$$

(16)

The subscripts n and c mean next and current, respectively. The origin for the local coordinate axis system for the next element, is the end coordinates of the current element

$$x_{2n} = x_c$$
$$y_{2n} = y_c$$

(17)

Now using the transformation matrix, the end coordinates of the next element can be converted from the local coordinate axis system to the global coordinate axis system. Similarly, this can be done for all the remaining elements.

41

Evaluation of End Moments

It is required to compute the end moments to be applied on each of the
elements such as to move the load from its initial position to the final
desired position.

An example of a manipulator arm is shown in Figures 4a and 4b. The
first five elements have the shim (or reinforcement) on the right side whereas
the remaining five elements have it on the left side. When these elements are
pressurized there will be a reversal of curvature after the fifth element.
Also by positioning the elements in this order, the arm has added capability
in moving the load over a wider region.

Initially the load is assumed to have no mass. Then the end moments
M_ρ, to elastically bend the arm and move the load to its desired position are
computed.

Secondly, after the arm has reached its final configuration, we know
the coordinates of the end point of each element and also the coordinates of
the center of gravity of the load. Thus the additional moment due to the load
M_ℓ, (the load is now supposed to have mass) can now be easily evaluated.

The total moment $\qquad M_t = M_\rho + M_\ell$

Evaluation of M_ρ

It is observed that there is no unique set of M_ρ, which can shift the
load from its initial to the final position. The moments in some elements
could be increased whereas the moments in some other elements could be
decreased and the load could possibly be still in the same position. To
overcome this problem, an iterative procedure has to be used. The iteration
steps are as follows.

a.   The end moments M_ρ to coil the last three elements around the load are first evaluated.

b.   For the remaining elements initial guess moment M_ρ values have to be provided. (In the next chapter a better approach is explained).

c.   Knowing the end moments M_ρ in each of the elements, we can compute the end deflections (δ_h and δ_v) and radius of curvature ρ, by the method discussed in Chapter II. The transformation matrices can then be used to get the overall orientation of the deflected arm (method is discussed earlier in this chapter).

d.   The present position of the center of gravity of the load is now calculated as shown in Figure 6b:

$$x_p = x_d - (R_\ell + R_1 + H) \cos (\Psi)$$

$$y_p = y_d - (R_\ell + R_1 + H) \sin (\Psi)$$

Now the following inequalities must be simultaneously satisfied for the specified tolerance limits ε_1 and ε_2, respectively.

$$|x_p - x_f| < \varepsilon_1 \tag{18}$$

$$|y_p - y_f| < \varepsilon_2 \tag{19}$$

where x_f and y_f are final desired position coordinates of the center of gravity of the load. If the inequalities (18) and (19) are not satisfied, the moments in the elements have to be varied in such a way that the load moves closer to the final desired position.

The present position of the load can be in any one of the four regions shown in Figure 7. The change in moments can be done logically as follows. Refer to Figures 6a and 7.

i.   When load is to the right and higher:

$$x_p > x_f$$

$$y_p > y_f$$

43
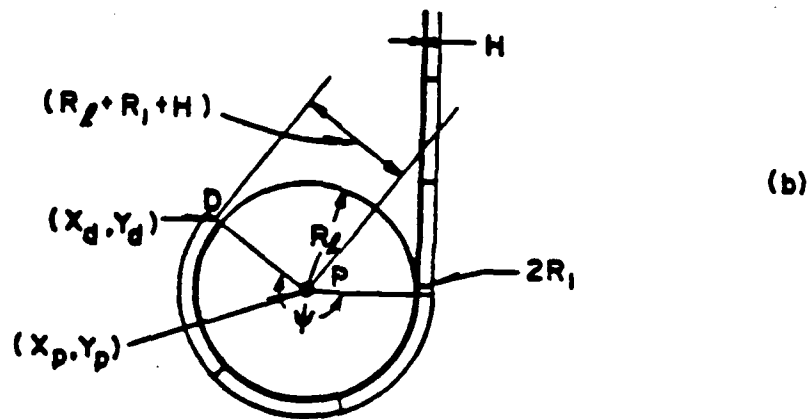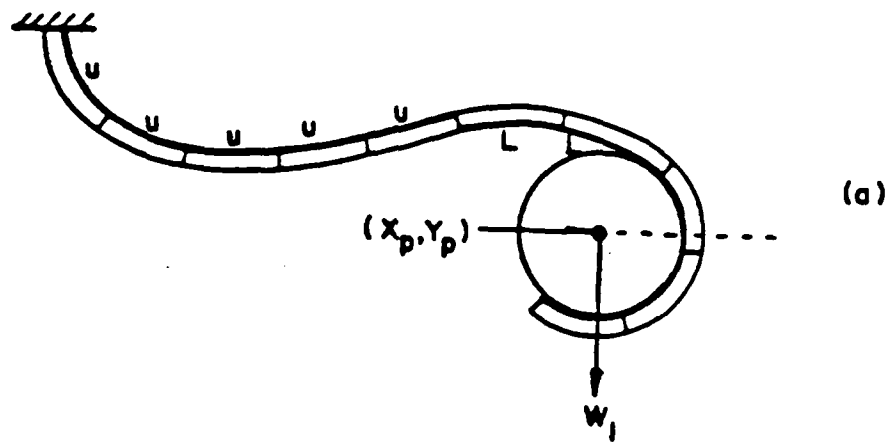
Figure 6. Global position of the load (a); and global position of the end element (b).

44
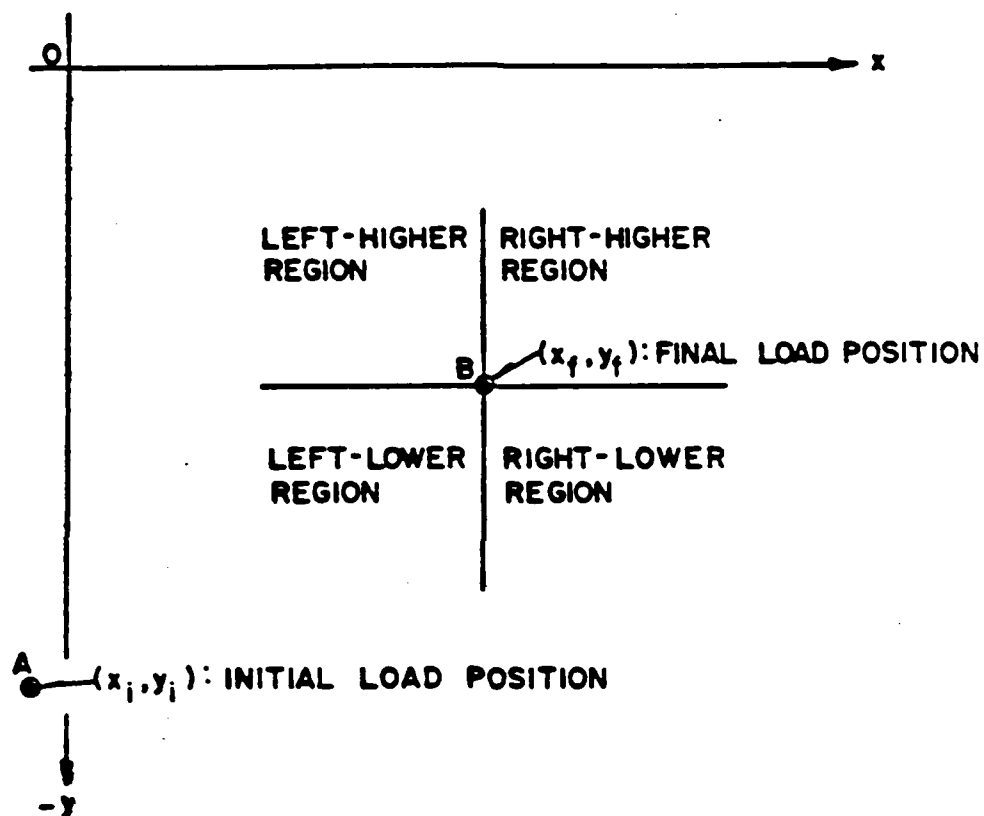
Figure 7. The four regions in which the load could be currently positioned.

Then increase the moments in the elements of the type L.

ii. When the load is to the left and higher

$$x_p < x_f$$

$$y_p > y_f$$

Then decrease the moments in the elements of type L and of type U.

iii. When the load is to the right and lower

$$x_p > x_f$$

$$y_p < y_f$$

Then increase the moments in the elements of type U and of type L.

iv. When the load is to the left and lower

$$x_p < x_f$$

$$y_p < y_f$$

Then decrease the moments in the elements of type L.

After making the requisite moment changes in the elements, which depends on the current orientation of the arm, we continue the iterative procedure from step (b) onwards, till the condition in step (d) is satisfied.

Step (a) is carried out only once as the moments required to coil the elements around the load cannot change since the dimensions of the load are fixed.

Evaluation of M_ℓ

At the end of the iteration procedure, for the evaluation of M_ρ, the load will be somewhere near the final desired position. In this orientation of the arm, we know the center of gravity of the load and the end coordinates of each element. Knowing this, we can evaluate the additional moment due to the load.

46

Since we do not precisely know the point of contact between the load and the last 3 elements coiled around it, we assume the worst case and apply an additional moment as given below.

$$M_\ell = W_1 (R_1 + R_\ell + H)$$

(For the last 3 elements M_ℓ is taken as same and is on the higher side)

We can compute the additional moments in the other elements from the free body diagram shown in Figure 8.

$$M_1 = W_1(R_1 + R_\ell + H) \cos (\theta)$$

M_ℓ for element type U, say element 5 is

$$M_\ell = W_1(x_c - x_d) - M_1$$

M_ℓ of element type L, say element 6 is

$$M_\ell = M_1 - W_1(x_c - x_e)$$

Similarly we can evaluate M_ℓ for all the elements.

Now for each of the elements we can evaluate

$$M_t = M_\rho + M_\ell$$

After the end moments required to be applied to each of the elements have been evaluated, the internal pressures required in each of the elements can easily be computed. As shown in Figure 9 (an arm with 3 elements only), there are three end moments, M_1, M_2 and M_3 and three different pressures P_1, P_2 and P_3

where

$$M_3 = P_3 \pi R_{23}^2 d_3$$

$$M_2 = (P_2 - P_3) \pi R_{22}^2 d_2$$

$$M_1 = (P_1 - P_2) \pi R_{21}^2 d_1$$

where R_{21}, R_{22}, R_{23} are the internal radii and d_1, d_2, d_3 are the distances between the center of pressure and the neutral axis for the three elements.

47
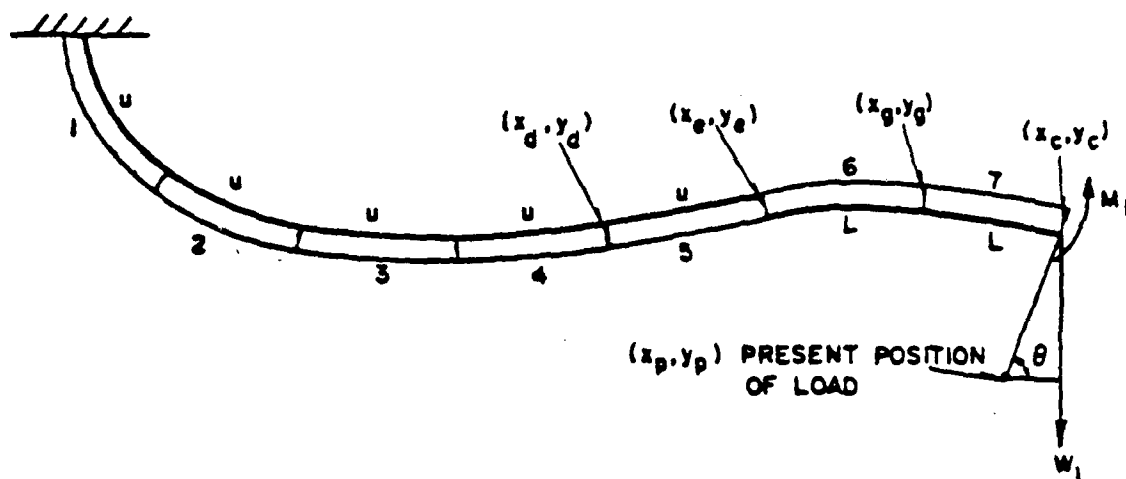
Figure 8. Free body diagram of arm without the last three elements.
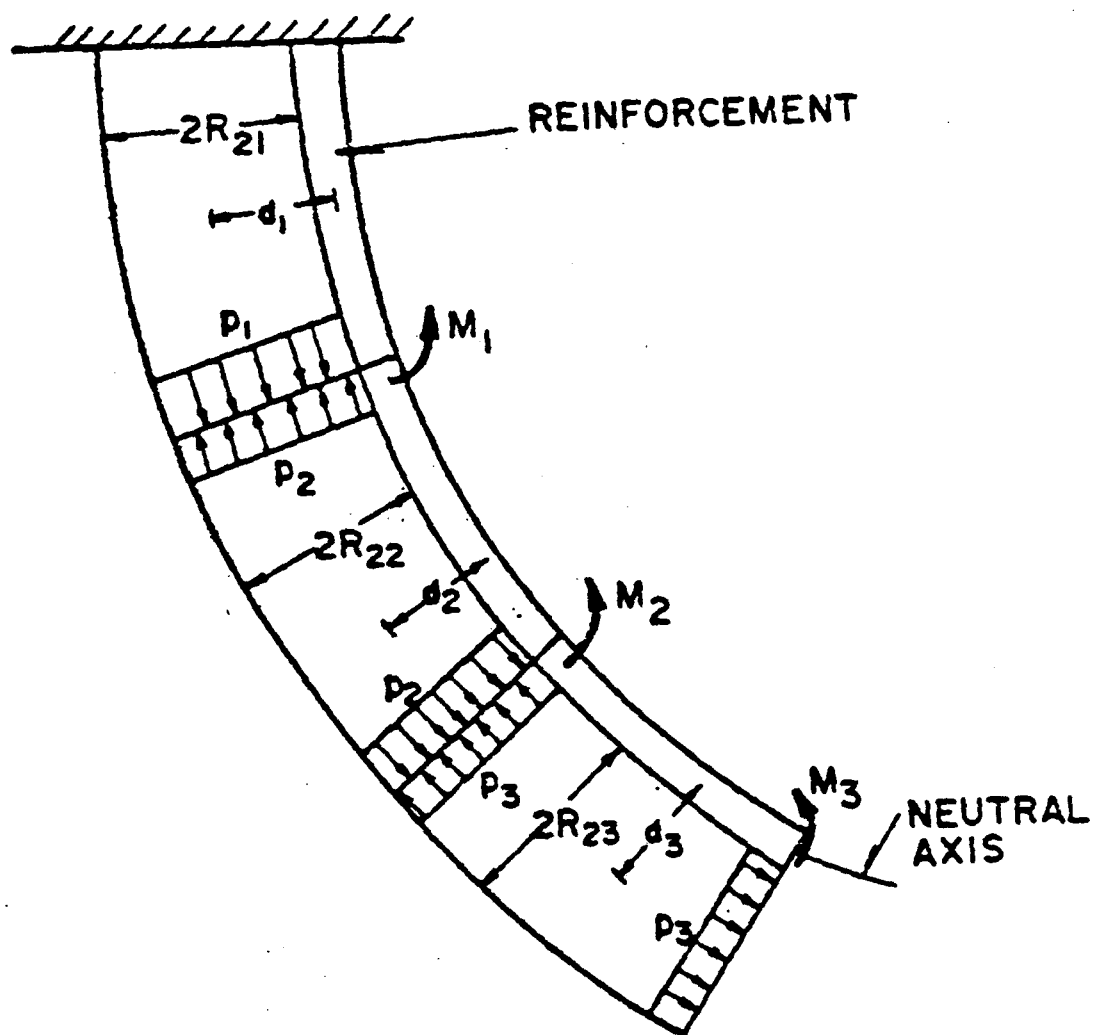
Figure 9. Relationship between internal pressures and end moments.

IMPLEMENTATION OF THE LEARNING CONCEPT

A FORTRAN program has been written to evaluate the end moments required in each of the elements, to move the load to its desired position. As mentioned in the previous chapter, apart from other input, initial guess end moment values M_ρ are required to start up the iterative procedure.

It was observed that a faster converging solution was achieved (i.e. number of iterations were reduced), the closer the guess values were to the actual solution. Also the user who wants to use the robot, initially has little or no idea about what guess values to provide. Therefore the user is liable to input guess values which could lead to numerous iterations and thereby waste expensive computer time.

As a remedial measure, it was decided that the program instead of the user should decide about the guess values. Thus the program was modified into a 'Learning Program'. The program has a data structure, which for different initial to final load positions, has the corresponding required end moment values M_ρ. Now given an initial and final load position, the program searches through its data structure to locate the 'guess' end moment values to start the iterative procedure. Everytime the program is run, at the end of the iterations, the data structure is updated appropriately, thereby increasing the apparent knowledge of the program.

A FORTRAN program has been written, which carries out all the iterative computations, matrix transformations etc., discussed in this chapter. The program also takes care of another important aspect, i.e. the user does not have to provide the initial guess end moment values M_ρ, to start the iterative procedure. As discussed in the next chapter, the program searches through its database to come up with the requisite guess values.

The data structure required to implement this 'Learning Concept', could have been appropriately implemented in a language like Pascal using tree structures. In our case as the remaining programs were in FORTRAN, we persisted with FORTRAN and had to use a five subscripted array as the data structure.

Data Structure and Search Logic:

As shown in Figure 10, given the coordinates of the initial and final positions of the load, we can uniquely define the initial and final position of the load, by the four parameters RAD, ϕ, θ and DIS. The four parameters are defined as follows

$$RAD = [x_i)^2 + (y_i)^2]^{1/2} \tag{20}$$

$$\phi = Tan^{-1}[\frac{x_i}{y_i}] \tag{21}$$

$$DIS = [(x_f - x_i)^2 + (y_f - y_i)^2]^{1/2} \tag{22}$$

$$\theta = cos^{-1}[\frac{(x_f - x_i)}{DIS}] \tag{23}$$

For each set of four such parameters we have corresponding end moment values M_ρ. Therefore when we search for the most accurate guess values, from the available data structure, a search through each of the four parameters is required. To simplify the search procedure, a five subscripted array D(I,J,K,L,N), was used where the

First subscript corresponds to - 'ϕ' values

Second subscript corresponds to - 'RAD' values

Third subscript corresponds to - 'θ' values

Fourth subscript corresponds to - 'DIS' values

Fifth subscript corresponds to - end moment values M_ρ.

51
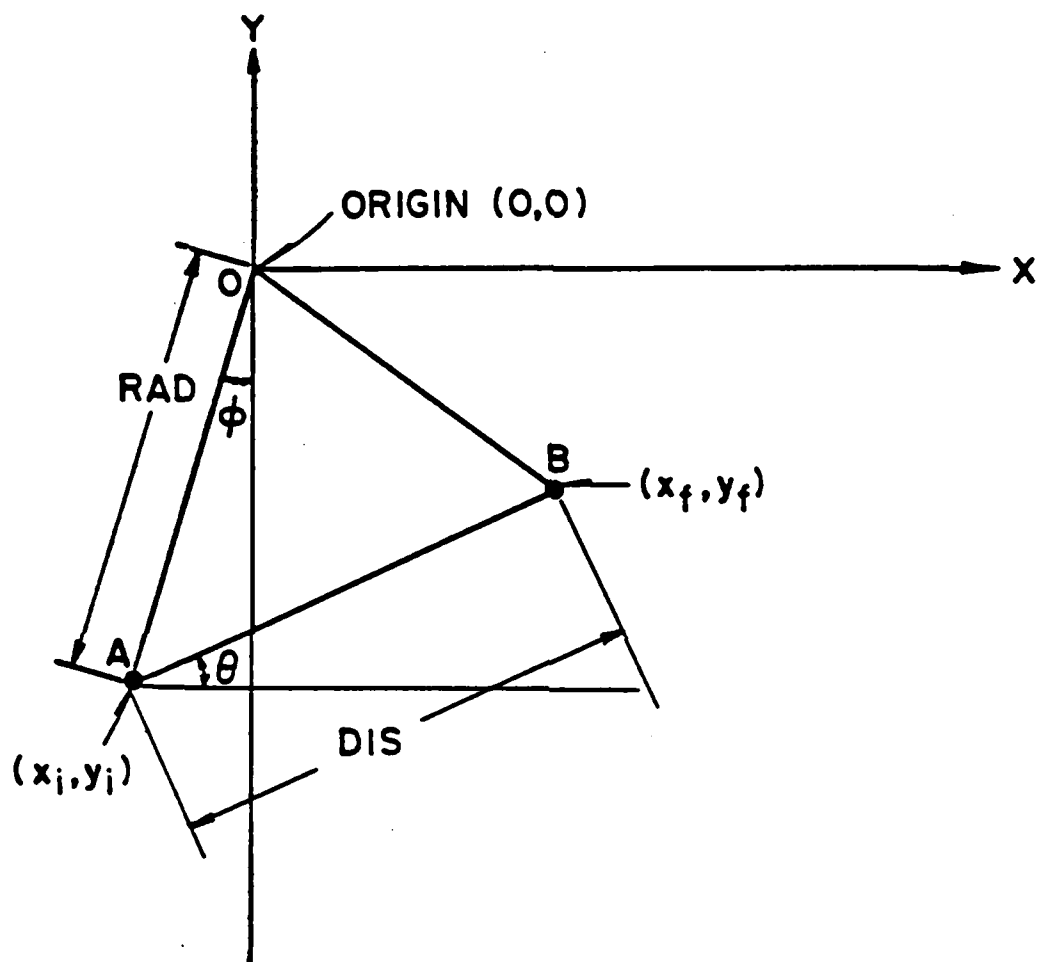
Figure 10. Initial and final position of load defined by ϕ, RAD, θ and DIS with respect to the origin.

Now it is shown in Figure 11 for each 'ϕ' we have one or more corresponding 'RAD' values. Similarly for each 'RAD' we have one or more corresponding 'θ' values and for each 'θ' we have one or more corresponding 'DIS' values. Finally for each 'DIS' we have the corresponding end moment values for each element of the robotic arm.

Therefore given an initial load position (x_i, y_i) and a final load position (x_f, y_f), using Equations (20) to (23) we can evaluate ϕ_e, RAD_e, θ_e and DIS_e (where subscript e signifies the evaluated parameters for which we wish to find best guess end moment values).

We can now search through the array $D(I,J,K,L,N)$. First, we compare 'ϕ_e' with all the 'ϕ' values in the array and choose the one which is closest to 'ϕ_e' value. Let the chosen value be 'ϕ_c'.

Next we search through all the 'RAD' values, corresponding to 'ϕ_c', value, and find the 'RAD' value closest to 'RAD_e' value. Let this chosen value be 'RAD_c'.

After this we search through all the 'θ' values, corresponding to 'RAD_c' value, and find the 'θ' value closest to 'θ_e' value. Let this chosen value be 'θ_c'.

Similarly we search through all the 'DIS', corresponding to 'θ_c' value, and find the 'DIS' value closest to 'DIS_e' value. Let this chosen value be 'DIS_c'.

The end moment values corresponding to 'DIS_c', will be our initial guess moment values for the iterative procedure. This strategy of choosing the guess values is seen to work reasonably well.

At the end of the iterative procedure, the program computes the exact end moments required to move the load from position (x_i, y_i) to position (x_f, y_f).
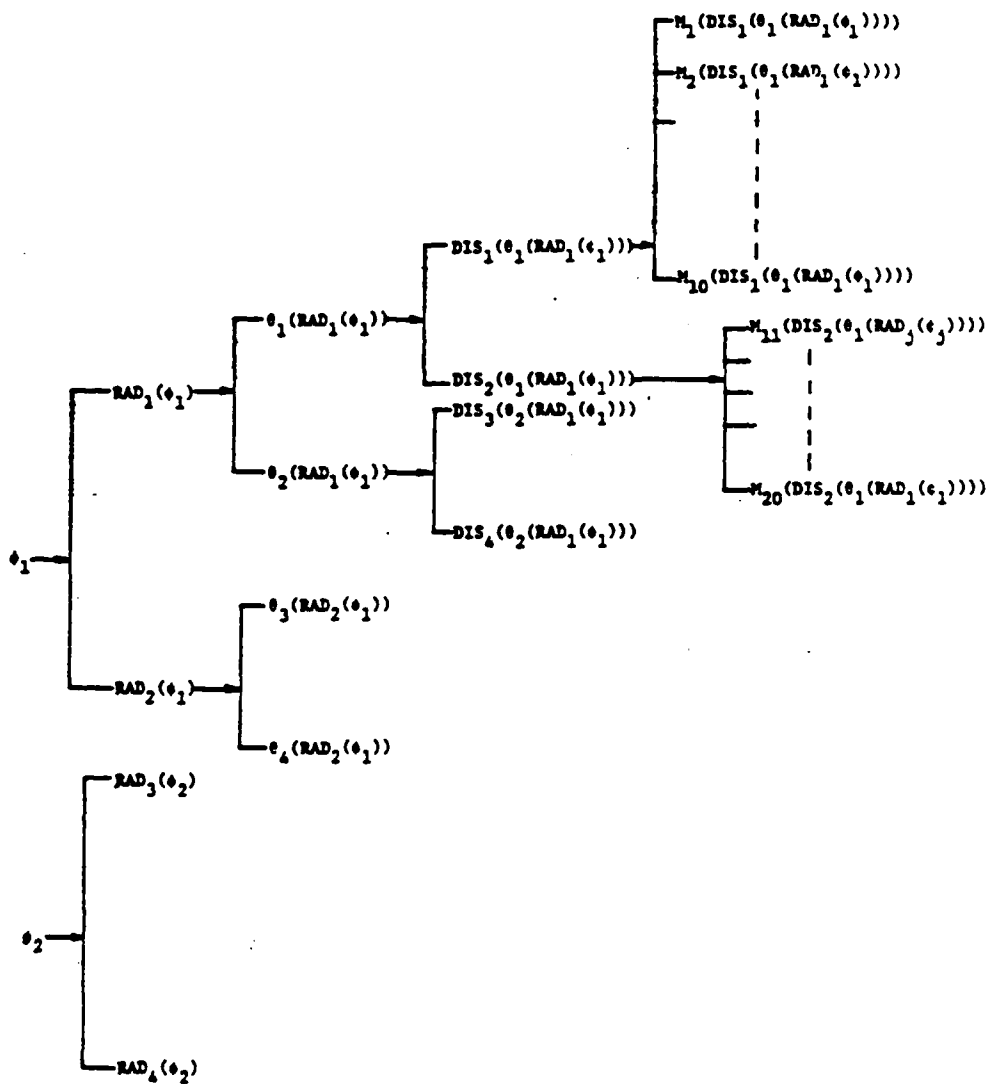
Figure 11. Data structure implementation.

The program now updates its data structure (Array $D(I,J,K,L,N)$) and ϕ_e, RAD_e, θ_e and DIS_e are inserted into the data structure in the proper places. As the array has all the values in increasing order of magnitude, insertion into the array is not difficult. The exact end moments computed by the program during the iterative procedure are also inserted into the array corresponding to ϕ_e, RAD_e, θ_e and DIS_e.

After the program has been run for several different, initial to final load positions, the data structure $D(I,J,K,L,N)$, after being repeatedly updated becomes sufficiently diverse. Now for a varied range of initial to final load positions, the guess values obtained will be sufficiently accurate.

The data structure is implemented by having a datafile. Everytime the program is run the values for array $D(I,J,K,L,N)$ are read in from this datafile. At the end of the program, after the array $D(I,J,K,L,N)$ has been updated, we overwrite the datafile with the present values of array $D(I,J,K,L,N)$. In this way the updated database is available for the next run of the program.

If the program has been run repeatedly which leads to the data structure becoming very large, the searching time may be too long. To avoid this, we can easily edit the datafile and remove the values in the range which are seldom used and leave only those values which are repeatedly used. Also after the datafile has reached an optimum size and we wish not to expand the datafile anymore, all that is required is to remove the 'write to datafile commands' from the program.

55

NUMERICAL EXAMPLES AND DISCUSSION

The program TYPEL, listed in Appendix B, carries out the single element computations discussed previously. For a prescribed end moment, the end deflections, radius of curvature and position of the neutral axis of the deflected element are computed. This program calls the IMSL subroutine DCADRE repeatedly to carry out numerical integration.

The variable list is as follows:

1) A1,B2,N = Material constants for nonlinear material, stress strain relationship $\sigma = A1\epsilon + B2\epsilon^{1/N}$

2) B1 = B = Breadth of shim

3) E = Young's modulus of steel shim or reinforcement

4) H = Thickness of shim

5) H1 = H_1 = Distance between neutral axis and point of connection between shim and tubular element

6) HDIS = δ_h = Horizontal end deflection of element

7) L = Length of an element

8) R1 = R_1 = External radius of cylindrical element

9) R2 = R_2 = Internal radius of cylindrical element

10) RHO = ρ = Radius of curvature of deflected element

11) VDIS = δ_v = Vertical end deflection of the element

56

For an element such as shown in Figures 1 and 2, made of a polymeric material with a thin steel shim, the following numerical values were chosen as input parameters.

N = 0.2	(dimensionless)	
A1 = 20.0	psi	
B2 = 50.0	psi	
R1 = 0.525	inches	
R2 = 0.475	inches	
H = 0.015	inches	
L = 2.0	inches	
B1 = 0.5	inches	
M = 3.80	lb in.	
E = 3.0×10^7	psi	

The results of the computations are as follows.

H1 = 0.00749	inches	
RHO = 1.549	inches	
VDIS = 1.121	inches	
HDIS = 0.511	inches	

It is noted that the position of the neutral axis (H1) is nearly at the midheight of the steel shim. Further, the vertical deflection at the end of the element is about one-half the element length. In this case the internal pressure p required to produce the chosen end moment M, in terms of the symbols of Figure 2, is

$$p = \frac{M}{\pi R_2^2 (R_1 + H_1)} = \frac{3.80}{\pi (0.475)^2 (0.525 + 0.00749)} = 10.1 \text{ psi}$$

Note: The remaining variables in the program hold intermediate values and are of no significance to the user.

The program LEARN, listed in Appendix B, carries out the computations discussed in Chapters III and IV. It evaluates the end moments required in each of the elements to shift the load from one position to another.

This program can handle many different options. An element in the arm may or may not be pressurized. The elements can be of varying geometry and the shim can be at top or at the underside of the element. These options allow a great variation in the motion of the arm.

Now, as previously discussed, in this program given an applied end moment on an element, it was required to know the end deflections and radius of curvature of the deflected element. To compute the end deflections and radius of curvature the previously discussed program TYPEL is required. As program LEARN goes through an iterative procedure, it would be required to run program TYPEL repeatedly. This could be extremely time consuming and expensive. Instead we input into the program a two dimensional array A(I,J). This array consists of different end moment values with their corresponding end deflections, radius of curvature, position of neutral axis, length of the element and external radius of the turbular part of the element.

The program 'LEARN' given an end moment value MI, searches through array A(I,J) and finds the two moment values (MA & MB) between which MI lies. It then linearly interpolates between MA & MB to evaluate the end deflections, radius of curvature and position of neutral axis corresponding to MI. This explanation will become clear by looking through the sample A(I,J) input.

The variable list is as follows.

1) A(I,J)   =   Array which has for different end moment values, the corresponding end deflections, radius of curvature, length of element, position of neutral axis and the external radius of element

2) ANG   =   End cumulative rotation up to that element in degrees

3) D(I,J,K,L,M) =   Holds the 'apparent knowledge' data structure

4) H   =   Thickness of shim

5) H1   =   Distance between neutral axis and point of connection between shim and turbular part

6) HDIS   =   Horizontal end deflection of a particular element

7) IDIR   =   Contains the IMOT value of previous element

8) IMOT   =   -3 means element deflects upwards
                =   +3 means element deflects downwards

9) INCK   =   to fix position of global x axis

10) IP1   =   +2 means element is pressurized
                =   -2 means element is not pressurized

11) IPCK   =   0 means no pressurized elements in the arm up till now
                =   1 means pressurized element has been encountered

12) IPLT1   =   -1 means shim on right side
                =   +1 means shim on left side

13) ITYPE   =   1 means use array A(I,J)
                =   2 means use array B(I,J)

14) LN   =   Length of an element

15) N1   =   Number of identical elements (geometrical and material properties identical and also same end moments)

59

16) NN = number of elements in the arm

17) NSHIF = shift in position of neutral axis between consecutive elements

18) NU = number of elements with shim on top

19) MM = number of data sets in A(I,J), I=1 to MM

20) R1 = outer radius of cylindrical part

21) RHO = radius of curvature of the neutral axis of an element

22) RL = radius of load

23) SI = cumulative end rotation

24) VDIS = vertical end deflection of a particular element

25) W1 = weight of load

26) X2,Y2 = end point, values for the current element w.r.t. neutral axis

27) X3,Y3 = end point, values for the current element w.r.t. mid axis of element

28) XB,YB = coordinates of c.g. of load at end of each iteration

29) XI,YI = coordinates of c.g. of load in its initial rest position

30) XF,YF = coordinates of c.g. of load in the final desired position

31) XORD(I),YORD(I)= coordinates of end points of the elements

Typical numerical results were obtained for line of ten identical elements such as shown in Figure 4(a) with all the elements unpressurized. The requirement is to lift a 2 lb load ($w_1 = 2$) from position (XI, YI) = (-2.082, -14.0) as shown in Figure 4(b), to position (XF, YF) = (8.5, -8.0) as shown in Figure 6(a). (These figures are not to scale.) The input data is as follows.

NN	=	10
MM	=	10
NU	=	5
RL	=	1.542 inch
W1	=	2 lbs
H	=	0.015 inch
XI	=	-2.082 inch
YI	=	-14.00 inch
XF	=	8.5 inch
YF	=	-8.0 inch

The chosen dimensions of the five subscripts of array D(I,J,K,L,M) are:

$$I = 1 \text{ to } N2 = 3$$
$$J = 1 \text{ to } M2 = 4$$
$$K = 1 \text{ to } N7 = 4$$
$$L = 1 \text{ to } M7 = 4$$
$$M = 1 \text{ to } MX = 13$$

The last dimension in each subscript holds a dummy value (-1000.0), so that during the search procedure the entire sparse matrix need not be searched. The overall dimensions were chosen to suit the sample problem and not waste memory space.

61

Specific data about each element has to be provided to the program. For example, IPLT1 specifies position of shim, IP1 specifies whether the element is to be internally pressurized or not. The following table specifies the properties of all ten elements in this example problem.

I = 1 to NN   NN = 10   in this example

I TYPE (I)	IP1(I)	IPLT1(I)	N1(I)	IMOT1(I)
1	+2	-1	1	-3
1	+2	-1	1	-3
1	+2	-1	1	-3
1	+2	-1	1	-3
1	+2	-1	1	-3
1	+2	+1	1	+3
1	+2	+1	1	+3
1	+2	+1	1	+3
1	+2	+1	1	+3
1	+2	+1	1	+3

For elements having similar geometry and stiffness properties, we can repeatedly run program TYPEL to obtain the results tabulated below. Now during the iterative procedure in program LEARN, given the end moment value, we can by interpolation of the array A(I,J) obtain the corresponding end deflections, radius of curvature and the other items in the table below.

Array A(I,J)

I = 1 to 10

J = 1 to 7

End Moment (lb-in)	Radius of Curvature ρ (in)	H1 (in)	HDIS (in)	VDIS (in)	Length of Element LN (in)	Radius of Element R1 (in)
1.02	5.3979	0.749255×10^{-2}	0.0455	0.3663	2.0	0.525
1.265	4.3537	0.749259×10^{-2}	0.0696	0.4514	2.0	0.525
1.705	3.2391	0.749247×10^{-2}	0.1247	0.5981	2.0	0.525
1.915	2.8904	0.74924×10^{-2}	0.1558	0.6648	2.0	0.525
2.2799	2.4409	0.749228×10^{-2}	0.2164	0.7745	2.0	0.525
2.4085	2.3165	0.749221×10^{-2}	0.2394	0.8111	2.0	0.525
2.634	2.130	0.7492×10^{-2}	0.2812	0.8702	2.0	0.525
3.159	1.807	0.74916×10^{-2}	0.3839	0.9982	2.0	0.525
3.798	1.549	0.7491×10^{-2}	0.5109	1.121	2.0	0.525
4.587	1.346	0.7489×10^{-2}	0.6592	1.232	2.0	0.525

63

The numerical results are summarized as follows.

Element No.	Total End Moment to be Applied (lb in)	Element Pressure (psi)
1	0.181×10^2	262.33
2	0.173×10^2	214.38
3	0.149×10^2	168.54
4	0.114×10^2	129.06
5	0.721×10^1	98.86
6	0.133×10^1	79.76
7	0.502×10^1	76.24
8	0.792×10^1	62.94
9	0.792×10^1	41.96
10	0.792×10^1	20.98

It is to be noted that elements 8, 9 and 10 have identical end moments. As the exact load distribution is not known, these elements are over-pressurized so that they coil around and grip the load more tightly than is required for lifting. The pressure p_i in the i-th element whose end moment is M_i was calculated from the following recursion relationships.

$$M_i = (p_i - p_{i+1}) \pi R_2^2 (R_1 + H_1)$$

It is observed that the pressures in the respective elements are higher for the ones closer to the support.

The elements in the sample problem were identical but if the arm consists of elements such that the cross-sectional area of elements decreases successively as they move away from the support (element 1 is attached to the support) then there would be no drastic decrease in pressure between successive elements.

64

There are several possible extensions of this research. For instance, the programming efficiency can be considerably improved if the program is rewritten in Pascal which offers the facility of tree type of data structure and dynamic storage. By implementing a tree type of datastructure searching and insertion of data is greatly simplified. Also, the mathematical model for plane motion as discussed here can be generalized to include out-of-plane manipulations. This can be done by the addition of torsion elements [6] at the base of element one. One torsion element can move the arm $\pm 180°$ out of the plane whereas another torsion element can move the arm $+90°$ in the plane. By judiciously pressurizing these torsion elements, the robotic arm can have a work space consisting of volume of revolutions in each of the four quadrants.

REFERENCES

1. Critchlow, Arthur J., "Introduction to Robotics," Macmillan Publishing Company, New York, 1985.

2. Safford, E. L., "Handbook of Advanced Robotics," Tab Books Inc., 1982.

3. Wilson, J. F., Mahajan U., Croner, L. J., and Wainwright, S. A., "Mechanics of an Elephant Trunk: Theory and Measurements," (submitted for publication).

4. Lewis, G. and Monasa, F., "Large Deflections of Cantilever Beams of Non-Linear Materials of the Ludwick Type Subjected to an End Moment," International Journal of Non-Linear Mechanics, Vol. 17, No. 1, pp. 1-6, 1982.

5. Popov, E. P., "Mechanics of Materials," Prentice Hall International, Inc., Englewood Cliffs, 1978.

6. Wilson, J. F. and Orgill, G., "Linear Analysis of Uniformly Stressed Orthotropic Cylindrical Shells," (submitted for publication).

III. LINEAR ANALYSIS OF UNIFORMLY STRESSED, ORTHOTROPIC CYLINDRICAL SHELLS

ABSTRACT

Within the framework of classical elasticity, the nonbuckled deformations are calculated for orthotropic, right circular, thin-walled cylinders under uniform load conditions. The principal direction of orthotropy follows parallel constant angle helices. Nondimensional system parameters involving four material constants and three loading conditions (internal pressure, longitudinal load and pure torque) are identified. Through parametric studies deformation patterns are calculated that are unique to orthotropy. Numerical examples illustrate that the proper selection of cylinder orthotropy can lead to designs with optimal deformations or load-carrying capacity. Results may be used for the design of robotic actuators driven by internal pressure.

INTRODUCTION

Improvement in the mechanical performance of cylindrical or nearly cylindrical shell-type structures may be achieved by adding reinforcement or by making small modifications in the basic structural geometry. For instance, the high pressure capacity of fire hoses is due to the reinforcing effect of the helical fibers in the rubber walls. In other cases, the buckling resistance to longitudinal loading of thin-walled cylindrical columns can be greatly improved by the use of a fluted design, or a periodic variation of the radius around the circumference. On the other hand, there are cases where high deformations are desirable as, for instance, in cylindrical bellows used as pipeline expansion joints. Here, length changes of up to 100 percent may be achieved by the use of axisymmetric, periodic corrugations along the length of a basic cylindrical shape [1]. Thus, the most flexible directions of the bellows and the thin-walled fluted column are orthogonal.

The purpose of this paper is to present a unified continuum model of such thin-walled, cylindrical shells using directional material properties. Such continuum models are especially efficient for calculating overall, nonbuckling, elastic deformations for fiber-reinforced cylinders [2] and for uniformly loaded, anisotropic, cylindrical shells [3,4]. In the present study, classical elasticity is employed to predict the nonbuckled deformations for uniform, orthotropic right circular cylinders with thin walls, subjected to three types of uniform loads: a torque T effecting rotation about the longitudinal axis, a longitudinal load P, and an internal pressure p. Strains along the geometric axes of symmetry are presented as functions of nondimensional system parameters involving these loads (applied separately and in combination), the cylinder geometry, four material properties, and the constant helix angle θ_0 that defines the direction of maximum stiffness. See Figure 1.

68
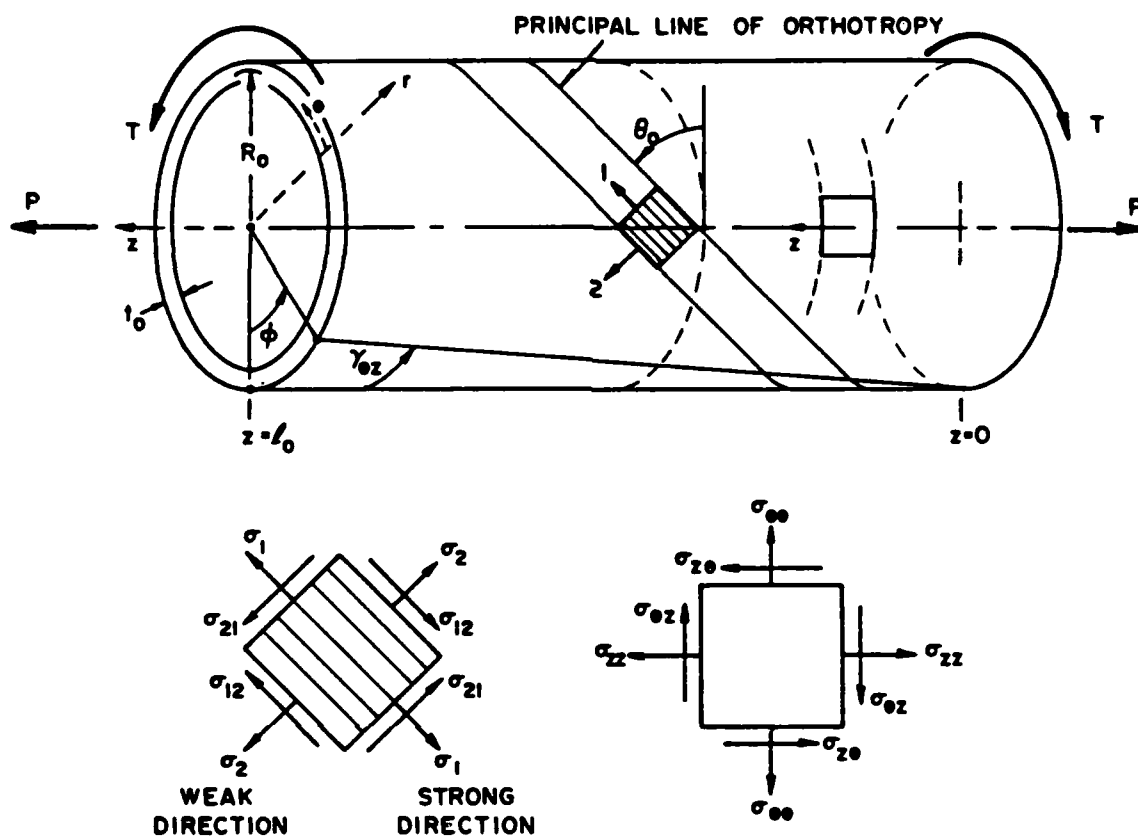
Figure 1   Definition of the orthotropic cylinder

This continuum model may describe the overall deformation characteristics of fiber-reinforced tubes as well as tubes with corrugations at arbitrary helix angles, as long as the cylindrical shape is maintained under load. Results may be used in future designs of robotic actuators that twist ($40° < \theta_0 < 80°$) or that only lengthen as for bellows ($\theta_0 = 0$) when subjected to internal pressure.

CONSTITUTIVE RELATIONSHIPS

Following the development in [5], the constitutive law for an ortho-tropic, elastic solid that relates the six strain components to the six stress components is given by

$$
\begin{bmatrix} \varepsilon_{11} \\ \varepsilon_{22} \\ \varepsilon_{33} \\ \gamma_{12} \\ \gamma_{13} \\ \gamma_{23} \end{bmatrix} = \begin{bmatrix} \frac{1}{E_{11}} & -\frac{\nu_{21}}{E_{22}} & -\frac{\nu_{31}}{E_{23}} & 0 & 0 & 0 \\ -\frac{\nu_{12}}{E_{11}} & \frac{1}{E_{22}} & -\frac{\nu_{32}}{E_{33}} & 0 & 0 & 0 \\ -\frac{\nu_{13}}{E_{11}} & -\frac{\nu_{23}}{E_{22}} & \frac{1}{E_{33}} & 0 & 0 & 0 \\ 0 & 0 & 0 & \frac{1}{G_{12}} & 0 & 0 \\ 0 & 0 & 0 & 0 & \frac{1}{G_{13}} & 0 \\ 0 & 0 & 0 & 0 & 0 & \frac{1}{G_{23}} \end{bmatrix} \begin{bmatrix} \sigma_{11} \\ \sigma_{22} \\ \sigma_{33} \\ \sigma_{12} \\ \sigma_{13} \\ \sigma_{23} \end{bmatrix} \qquad (1)
$$

Equation (1) is written with respect to the principal axis (1,2,3). The 6x6 material matrix, whose elements are designated as a_{ij}, is determined by experiments. The strains and stresses of Equation (1) are redefined using single subscription, or

70

$$\epsilon_{11} = \epsilon_1 \quad , \quad \epsilon_{22} = \epsilon_2 \quad , \quad \epsilon_{33} = \epsilon_3$$
$$\gamma_{12} = \epsilon_4 \quad , \quad \gamma_{13} = \epsilon_5 \quad , \quad \gamma_{23} = \epsilon_6 \tag{2a}$$

$$\sigma_{11} = \sigma_1 \quad , \quad \sigma_{22} = \sigma_2 \quad , \quad \sigma_{33} = \sigma_3$$
$$\sigma_{12} = \sigma_4 \quad , \quad \sigma_{13} = \sigma_5 \quad , \quad \sigma_{23} = \sigma_6 \tag{2b}$$

Using this notation, Equations (1) become

$$\epsilon_i = \sum_{j=1}^{6} a_{ij}\sigma_j \tag{3}$$

Recognizing that the total elastic energy for the orthotropic solid is invariant with respect to the coordinate system, the elements a'_{ij} of the material matrix in the (r,θ,z) coordinate system can be written in terms of a_{ij} of the $(1,2,3)$ coordinate system. That is

$$a'_{ij} = \sum_{m=1}^{6}\sum_{n=1}^{6} a_{mn}\, q_{mi}\, q_{nj} \tag{4}$$

$$i,j = 1,2,\ldots 6$$

where q_{ij} represents the direction cosines of the $(1,2,3)$ system with the (r,θ,z) coordinate system. As shown in Figure 1, the relationship is simply one of rotation of the $(1,2)$ axis to the (θ,z) axis by an angle of $-\theta_0$ in the plane r = constant. The values of q_{ij} for this rotation are listed in Table 1.

In the transformed coordinate system, the constitutive law is

$$\epsilon'_i = \sum_{j=1}^{6} a'_{ij}\, \sigma'_j \tag{5}$$

which is expressed in cylindrical coordinates as follows.

$$
\begin{bmatrix} \epsilon_{\theta\theta} \\ \epsilon_{zz} \\ \epsilon_{rr} \\ \gamma_{zr} \\ \gamma_{\theta r} \\ \gamma_{\theta z} \end{bmatrix}
=
\begin{bmatrix}
a'_{11} & a'_{12} & a'_{13} & 0 & 0 & a'_{16} \\
a'_{21} & a'_{22} & a'_{23} & 0 & 0 & a'_{26} \\
a'_{31} & a'_{32} & a'_{33} & 0 & 0 & a'_{36} \\
0 & 0 & 0 & a'_{44} & a'_{45} & 0 \\
0 & 0 & 0 & a'_{54} & a'_{55} & 0 \\
a'_{61} & a'_{62} & a'_{63} & 0 & 0 & a'_{66}
\end{bmatrix}
\begin{bmatrix} \sigma_{\theta\theta} \\ \sigma_{zz} \\ \sigma_{rr} \\ \sigma_{zr} \\ \sigma_{\theta r} \\ \sigma_{\theta z} \end{bmatrix}
\tag{6}
$$

For the types of uniform loading considered here, the shear stresses $\sigma_{\theta r}$ and σ_{zr} may be approximated as zero, an assumption consistent with the elastic theory of thin-walled cylinders [6]. From Equation (6), the remaining stress-strain relations are thus

$$
\begin{bmatrix} \epsilon_{\theta\theta} \\ \epsilon_{zz} \\ \epsilon_{rr} \\ \gamma_{\theta z} \end{bmatrix}
=
\begin{bmatrix}
a'_{11} & a'_{12} & a'_{13} & a'_{16} \\
a'_{21} & a'_{22} & a'_{23} & a'_{26} \\
a'_{31} & a'_{32} & a'_{33} & a'_{36} \\
a'_{61} & a'_{62} & a'_{63} & a'_{66}
\end{bmatrix}
\begin{bmatrix} \sigma_{\theta\theta} \\ \sigma_{zz} \\ \sigma_{rr} \\ \sigma_{\theta z} \end{bmatrix}
\tag{7}
$$

The elements a'_{ij} of the material matrix of Equation (7) are calculated from Equation (4) with a_{ij} and q_{ij} given by Equation (1) and Table 1, respectively. The results are as follows*.

---

*Note that ϕ in reference [5] is interpreted as $-\theta_0$ in Equations (8)-(17). Also, Equation (9) reflects a correction of the results reported in [5].

72

Table 1. Elements of q_{ij} for axis rotation

i \ j	1	2	3	4	5	6
1	$\cos^2\theta_0$	$\sin^2\theta_0$	0	0	0	$\sin 2\theta_0$
2	0	0	0	0	0	$-\sin 2\theta_0$
3	0	0	1	0	0	0
4	0	0	0	$\cos\theta_0$	$-\sin\theta_0$	0
5	0	0	0	$\sin\theta_0$	$\cos\theta_0$	0
6	$-\frac{1}{2}\sin 2\theta_0$	$\frac{1}{2}\sin 2\theta_0$	0	0	0	$\cos 2\theta_0$

$$a'_{11} = \frac{1}{E_{11}} \cos^4\theta_o + \left(\frac{1}{G_{12}} - \frac{2\nu_{12}}{E_{11}}\right)\sin^2\theta_o\cos^2\theta_o + \frac{1}{E_{22}}\sin^4\theta_o \tag{8}$$

$$a'_{22} = \frac{1}{E_{11}} \sin^4\theta_o + \left(\frac{1}{G_{12}} - \frac{2\nu_{12}}{E_{11}}\right)\sin^2\theta_o\cos^2\theta_o + \frac{1}{E_{22}}\cos^4\theta_o \tag{9}$$

$$a'_{33} = \frac{1}{E_{33}} \tag{10}$$

$$a'_{12} = a'_{21} = \left(\frac{1}{E_{11}} + \frac{1}{E_{22}} + \frac{2\nu_{12}}{E_{11}} - \frac{1}{G_{12}}\right)\sin^2\theta_o\cos^2\theta_o - \frac{\nu_{12}}{E_{11}} \tag{11}$$

$$a'_{23} = a'_{32} = -\frac{\nu_{23}}{E_{22}}\cos^2\theta_o - \frac{\nu_{31}}{E_{33}}\sin^2\theta_o \tag{12}$$

$$a'_{13} = a'_{31} = -\frac{\nu_{23}}{E_{22}}\sin^2\theta_o - \frac{\nu_{31}}{E_{33}}\cos^2\theta_o \tag{13}$$

$$a'_{66} = \left(\frac{4}{E_{11}} + \frac{4}{E_{22}} + \frac{8\nu_{12}}{E_{11}} - \frac{4}{G_{12}}\right)\sin^2\theta_o\cos^2\theta_o + \frac{1}{G_{12}} \tag{14}$$

$$a'_{16} = a'_{61} = \left[\frac{2}{E_{11}}\cos^2\theta_o - \frac{2}{E_{22}}\sin^2\theta_o - \left(\frac{1}{G_{12}} - \frac{2\nu_{12}}{E_{11}}\right)\cdot\right.$$

$$\left.\cdot(\cos^2\theta_o - \sin^2\theta_o)\right]\sin\theta_o\cos\theta_o \tag{15}$$

$$a'_{26} = a'_{62} = \left[\frac{2}{E_{11}}\sin^2\theta_o - \frac{2}{E_{22}}\cos^2\theta_o + \left(\frac{1}{G_{12}} - \frac{2\nu_{12}}{E_{11}}\right)\cdot\right.$$

$$\left.\cdot(\cos^2\theta_o - \sin^2\theta_o)\right]\sin\theta_o\cos\theta_o \tag{16}$$

$$a'_{36} = a'_{63} = \left(\frac{-2\nu_{31}}{E_{33}} + \frac{2\nu_{23}}{E_{22}}\right)\sin\theta_o\cos\theta_o \tag{17}$$

EVALUATION OF MATERIAL CONSTANTS

There are seven material constants that appear in Equations (8)-(17), namely E_{11}, E_{22}, E_{33}, ν_{12}, ν_{23}, ν_{31} and G_{12}. It is necessary to determine how

these constants are related to each other and then to devise meaningful tests to measure them. To insure that the strain energy is a single valued function of the strain displacements, the material matrix of Equation (1) must be symmetric. That is

$$E_{11} \nu_{21} = E_{22} \nu_{12} \tag{18}$$

$$E_{22} \nu_{32} = E_{33} \nu_{23} \tag{19}$$

$$E_{33} \nu_{13} = E_{11} \nu_{31} \tag{20}$$

Consider a tensile test for which the specimen's longitudinal axis coincides with the longitudinal or z-axis of an orthotropic cylinder, given that $\theta_0 = 90$ deg. For a uniform, applied stress $\bar{\sigma}_{zz}$ where $\sigma_{\theta\theta} = \sigma_{rr} = \sigma_{\theta z} = 0$, it follows from Equations (7)-(20) that the strains are

$$\epsilon_{\theta\theta} = -\frac{\nu_{12}}{E_{11}} \bar{\sigma}_{zz} = -\frac{\nu_{21}}{E_{22}} \bar{\sigma}_{zz} \tag{21}$$

$$\epsilon_{zz} = \frac{1}{E_{11}} \bar{\sigma}_{zz} \tag{22}$$

$$\epsilon_{rr} = -\frac{\nu_{31}}{E_{33}} \bar{\sigma}_{zz} = -\frac{\nu_{13}}{E_{11}} \bar{\sigma}_{zz} \tag{23}$$

Equation (22) shows that E_{11} is the equivalent of Young's modulus along the 1 axis. Now suppose that for $\theta_0 = 90$ deg the orthotropic tube corresponds to a fluted, thin-walled cylindrical column of a homogeneous, isotropic material with Young's modulus E and Poisson's ratio ν. This fluted column test specimen thus exhibits the same stress-strain behavior of the isotropic material in both the 1 (or z) direction and in the 3 (or r) direction. The following definitions of the orthotropic constants are consistent with Equations (21)-(23).

$$E = E_{11} = E_{33} \tag{24}$$

$$\nu = \nu_{31} = \nu_{13} = \nu_{12} \tag{25}$$

Consider a second tensile test for which the specimen's longitudinal axis again corresponds with the z-axis of an orthotropic cylinder, but now let $\theta_0 = 0$ deg. Again, the only nonzero stress is the applied, uniform tensile stress $\bar{\sigma}_{zz}$. It follows from Equations (7)-(20), (24) and (25) that

$$\varepsilon_{\theta\theta} = -\frac{\nu}{E} \bar{\sigma}_{zz} = -\frac{\nu_{21}}{E_{22}} \bar{\sigma}_{zz} \tag{26}$$

$$\varepsilon_{zz} = \frac{1}{E_{22}} \bar{\sigma}_{zz} \tag{27}$$

$$\varepsilon_{rr} = -\frac{\nu_{23}}{E_{22}} \bar{\sigma}_{zz} = -\frac{\nu_{32}}{E} \bar{\sigma}_{zz} \tag{28}$$

Observing Equation (27), it is seen that the modulus of elasticity in the 2 (or z) direction is E_{22}. Now let

$$E' = E_{22} \tag{29}$$

$$\nu' = \nu_{21} = \nu_{23} \tag{30}$$

which define respectively the effective Young's modulus and Poisson's ratio for a bellows, consistent with the assumption that $\sigma_{\theta\theta} = \sigma_{rr}$ in this tensile test. It follows, using Equations (24), (25), (29), (30), that Equations (18)-(20) are satisfied if

$$\nu = \nu_{32} \quad , \quad E\nu' = E'\nu \tag{31}$$

In a third test, a pure shear stress $\sigma_{\theta z}$ is applied to an orthotropic cylinder for which $\theta_0 = 0$. This corresponds to the application of a pure torque that rotates a bellows about its longitudinal axis. As for the previous two tests, the cylinder is orthotropic only because of its corrugations, since it is constructed of an isotropic material with elastic constants E, ν and shear modulus G. Torsion tests on such a bellows have shown that [8]

$$\gamma_{\theta z} = \frac{\sigma_{\theta z}}{G} \tag{32}$$

which indicates that the rotation and shearing stress are those predicted by

76

the theory of thin-walled tubes without corrugations. When Equation (32) is compared with the stress-strain law given by Equations (7)-(17) in this case, it is seen that

$$G = G_{12} \tag{33}$$

In summary, there are four independent material constants needed to describe the stress-strain behavior of a cylinder with corrugated walls made of an isotropic material, but modeled as an orthotropic, smooth-walled tube. The stiffest direction (modulus E) follows the corrugation lines forming constant angle helices. Orthogonal to the helices is the weakest direction (modulus E'). The independent material constants are E, E', G and ν. Given uniform stresses $\sigma_{\theta\theta}$, σ_{zz}, σ_{rr}, and $\sigma_{\theta z}$, the uniform strains are calculated from Equation (7). Using Equations (24), (25), (29-31) and (33), Equations (8)-(17) give the elements of the material matrix as follows.

$$a'_{11} = \frac{1}{E}\cos^4\theta_0 + (\frac{1}{G} - \frac{2\nu}{E})\sin^2\theta_0\cos^2\theta_0 + \frac{1}{E'}\sin^4\theta_0 \tag{34}$$

$$a'_{22} = \frac{1}{E}\sin^4\theta_0 + (\frac{1}{G} - \frac{2\nu}{E})\sin^2\theta_0\cos^2\theta_0 + \frac{1}{E'}\cos^4\theta_0 \tag{35}$$

$$a'_{33} = \frac{1}{E} \tag{36}$$

$$a'_{12} = a'_{21} = (\frac{1}{E} + \frac{1}{E'} + \frac{2\nu}{E} - \frac{1}{G})\sin^2\theta_0\cos^2\theta_0 - \frac{\nu}{E} \tag{37}$$

$$a'_{23} = a'_{32} = -\frac{\nu}{E} \tag{38}$$

$$a'_{13} = a'_{31} = -\frac{\nu}{E} \tag{39}$$

$$a'_{66} = (\frac{4}{E} + \frac{4}{E'} + \frac{8\nu}{E} - \frac{4}{G})\sin^2\theta_0\cos^2\theta_0 + \frac{1}{G} \tag{40}$$

$$a'_{16} = a'_{61} = [-\frac{2}{E'}\sin^2\theta_0 + \frac{2}{E}\cos^2\theta_0 - (\frac{1}{G} - \frac{2\nu}{E})\cdot$$
$$\cdot(\cos^2\theta_0 - \sin\theta_0)]\sin\theta_0\cos\theta_0 \tag{41}$$

77

$$a'_{26} = a'_{62} = [- \frac{2}{E} \cos^2\theta_0 + \frac{2}{E} \sin^2\theta_0 + (\frac{1}{G} - \frac{2\nu}{E}) \cdot$$

$$\cdot (\cos^2\theta_0 - \sin^2\theta_0)] \sin\theta_0 \cos\theta_0 \qquad (42)$$

$$a'_{36} = a'_{63} = 0 \qquad (43)$$

These results can be used to calculate the strains, displacements and rotations of the cylinder for the special cases of loading discussed below.

EQUILIBRIUM AND COMPATIBILITY

As shown in Figure 1, the thin-walled cylinder is subjected to three types of uniform loads: an internal pressure p, a longitudinal load P centered on the z-axis, and a pure torque T causing rotation about the z-axis. Since there are no boundary or edge constraints, the resulting uniform stresses may be derived using equilibrium conditions and elementary methods. In terms of the mean radius R_0 and shell thickness t_0, which are essentially constant during loading, the stresses are:

$$\sigma_{\theta\theta} = \frac{pR_0}{t_0} \qquad (44)$$

$$\sigma_{\theta\theta} = \frac{P}{2\pi R_0 t_0} + \frac{pR_0}{2t_0} \qquad (45)$$

$$\sigma_{\theta\theta} = \frac{T}{2\pi R_0^2 t_0} \qquad (46)$$

Consistent with the thin-wall assumption, the radial stress is negligible, or $\sigma_{rr} = 0$ [6].

Since these stresses and their corresponding strains, as given by Equations (7) and (34-43), are all uniform, they are all independent of the cylindrical coordinates (r,θ,z). Thus the 81 St. Venant strain compatibility conditions are automatically satisfied [7].

78

STRAIN-DISPLACEMENT RELATIONS

The general strain-displacement equations in polar-cylindrical coordinates given in [7] are simplified as follows to express the condition that there are no variations in displacement in the θ or circumferential direction.

$$\epsilon_{rr} = \frac{\partial U_r}{\partial r} \tag{47}$$

$$\epsilon_{\theta\theta} = \frac{1}{r}\frac{\partial U_\theta}{\partial \theta} + \frac{U_r}{R} = \frac{U_r}{r} \tag{48}$$

$$\epsilon_{zz} = \frac{\partial U_z}{\partial z} \tag{49}$$

$$\gamma_{\theta z} = \frac{\partial U_\theta}{\partial z} + \frac{1}{r}\frac{\partial U_z}{\partial \theta} = \frac{\partial U_\theta}{\partial z} \tag{50}$$

Here, U_r, U_θ, and U_z are respectively the displacements in the r, θ and z directions.

Following a procedure in [3], these relationships can be integrated in terms of three functions $f_1(r,z)$, $f_2(z)$ and $f_3(z)$ which are to be determined. From Equation (47):

$$U_r = r \, \epsilon_{rr} + f_1(r,z) \tag{51}$$

It follows from Equations (48) and (51) that:

$$f_1(r,z) = r(\epsilon_{\theta\theta} - \epsilon_{rr}) \tag{52}$$

From the last two equations, then,

$$U_r = r \, \epsilon_{\theta\theta} = R_0 \epsilon_{\theta\theta} \tag{53}$$

where $r = R_0$ for a thin-walled cylinder.

From Equation (49):

$$U_z = z \, \epsilon_{zz} + f_2(z) \tag{54}$$

where the second function of integration, $f_2(z)$, is independent of r since the cylinder wall is very thin and any variations across this thickness have no significant effect on the longitudinal deformation. Further, by imposing the

79

condition of no rigid body motion, where $U_z = 0$ at $z = 0$, and noting that U_z can be at most a linear function of z, then it is apparent that $f_2(z) = 0$. Thus Equation (54) thus yields the position $\xi = z + U_z$ of a material point originally at point z measured from one end of the cylinder, or

$$\xi = (1 + \epsilon_{zz})z \qquad (55)$$

The circumferential displacement is obtained by integrating Equation (50) and then using Equation (55). That is

$$U_\theta = \xi \, \gamma_{\theta z} + f_3(z) \qquad (56)$$

Here the function of integration is again independent of r, which is consistent with the thin-wall assumption. By imposing the condition of no rigid body rotation where $U_\theta = 0$ at $z = 0$, and noting that U_θ can at most be a linear function in z, it is evident that $f_3(z) = 0$. Thus $U_\theta = \xi \, \gamma_{\theta z}$.

In summary, the radial, circumferential and longitudinal displacements are given in terms of the strains, the mean radius, and the z-coordinate only, or

$$U_r = R_0 \, \epsilon_{\theta\theta} \quad ; \quad U_\theta = (1 + \epsilon_{zz})z\gamma_{\theta z} \quad ; \quad U_z = z \, \epsilon_{zz} \qquad (57)$$

It is noted that U_θ and U_z are the same displacements assumed [2] for the solid orthotropic cylinder rotating about the z-axis.

A further displacement of practical interest is the angle of rotation ϕ for a cross section of the cylinder at the coordinate z. Within the limits of linear theory, $\phi = U_\theta/R_0$. Thus, from Equation (57):

$$\phi = \frac{z}{R_0} (1 + \epsilon_{zz})\gamma_{\theta z} \qquad (58)$$

PARAMETRIC STUDIES

All of the calculations for the parametric studies that follow are based on Equation (7), the stresses of Equations (44)-(46), and the elements of the material matrix given by Equations (34)-(43). The specific values of $E/G = 3$

80

and $\nu = 0.5$ were chosen since they are characteristic of the polymeric and rubber-like materials to be used in future applications.

Effects of Loading without Constraint. In the first series of parametric studies, the separate effects of each loading, p, P and T on the homogeneous strains $\gamma_{\theta z}$ and ε_{zz} were investigated for an unconstrained cylinder. The goal was to determine peak strains as a function of the appropriate nondimensional system parameters.

The three nondimensional parameters involving the shear strain $\gamma_{\theta z}$ are defined by the ordinates of Figures 2 through 4, in which the only nonzero load is p, P and T, respectively. For the isotropic case ($E/E' = 1$), all three of these figures show no shear strain variations with the helix angle θ_0, a result that could be anticipated. For p loading only (Figure 2) and for P loading only (Figure 3) the negative ordinates indicate that $\gamma_{\theta z}$ is negative, or that the cylinder "unwinds" because of orthotropy ($E/E' > 1$). For T loading only (Figure 4), the positive ordinate indicates that the cylinder "winds up" if T is applied as shown in Figure 1. The interesting result is that the peak value of each respective shear strain parameter occurs at a distinctly different value of θ_0. That is:

$$\text{peak} \left(\frac{E t_0 \gamma_{\theta z}}{p R_0} \right) \text{ occurs for } \theta_0 = 53 \text{ deg}$$

$$\text{peak} \left(\frac{E t_0 R_0 \gamma_{\theta z}}{P} \right) \text{ occurs for } \theta_0 = 30 \text{ deg}$$

$$\text{peak} \left(\frac{E t_0 R_0^2 \gamma_{\theta z}}{T} \right) \text{ occurs for } \theta_0 = 45 \text{ deg}$$

For each load type, there is no shift in these respective values of θ_0 for $1 < E/E' < 100$.

81
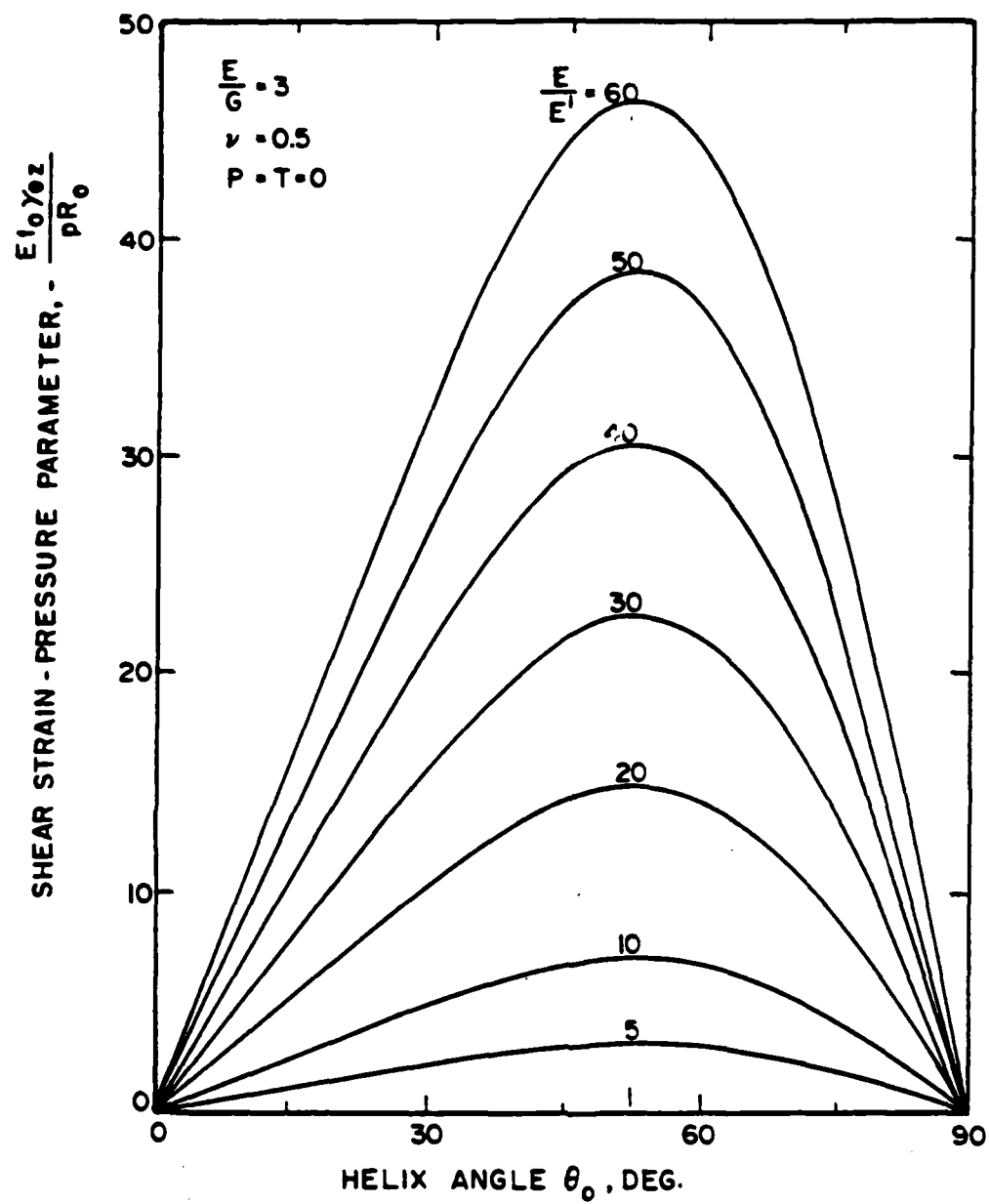
Figure 2   Unrestrained twisting due to internal pressure
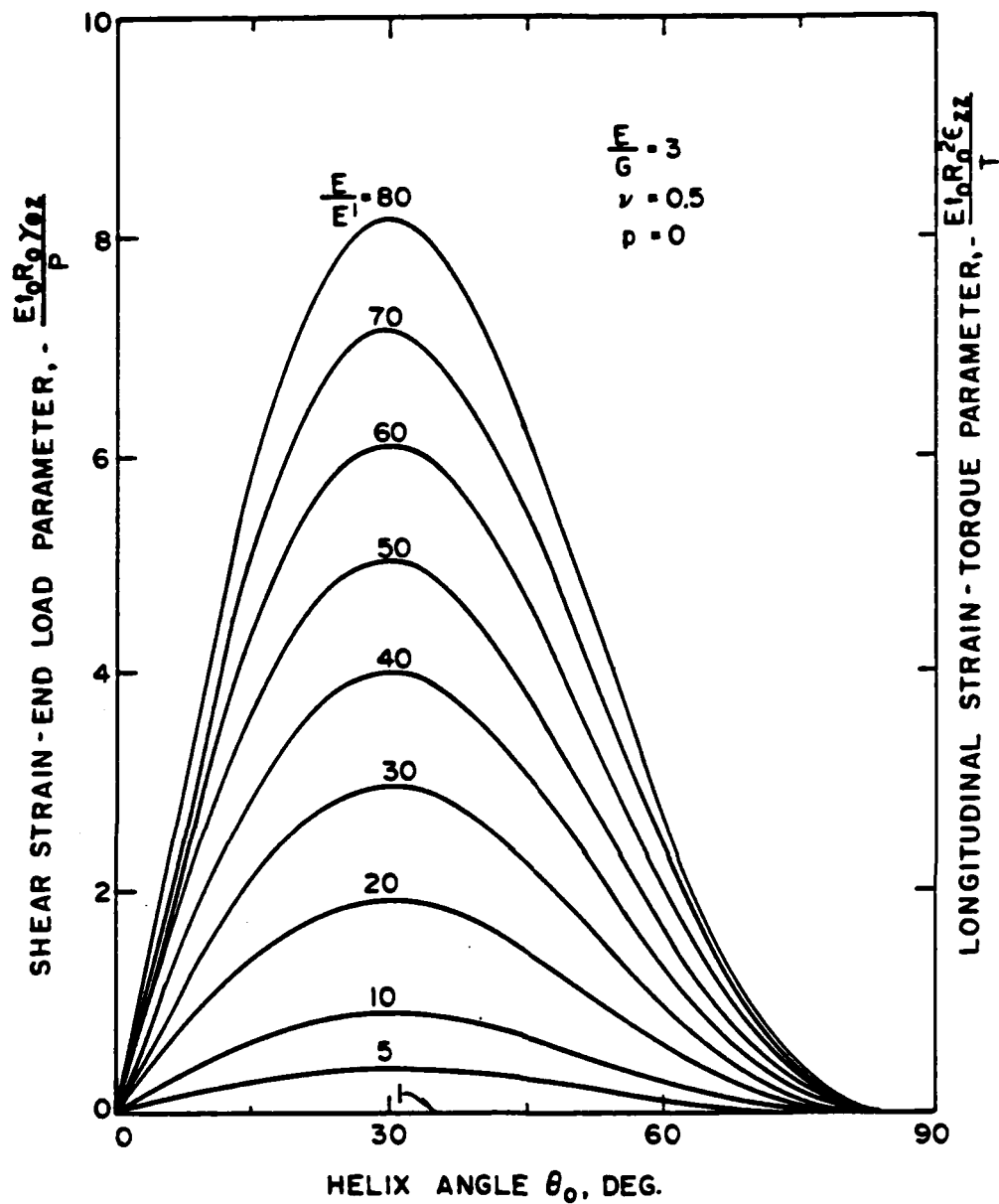
Figure 3   Unrestrained twisting due to longitudinal load (left ordinate)
              and unrestrained longitudinal strain due to pure torque (right
   ordinate)

10

$\dfrac{E}{G} = 3$

$\nu = 0.5$

$p = P = 0$

$\dfrac{E}{E'} = 60$

50

40

30

20

10

5

1

8

6

4

2

0

SHEAR STRAIN-TORQUE PARAMETER, $\dfrac{E'_0 R_0^2 \gamma_{\theta z}}{T}$

0   30   60   90

HELIX ANGLE θ_0, DEG.
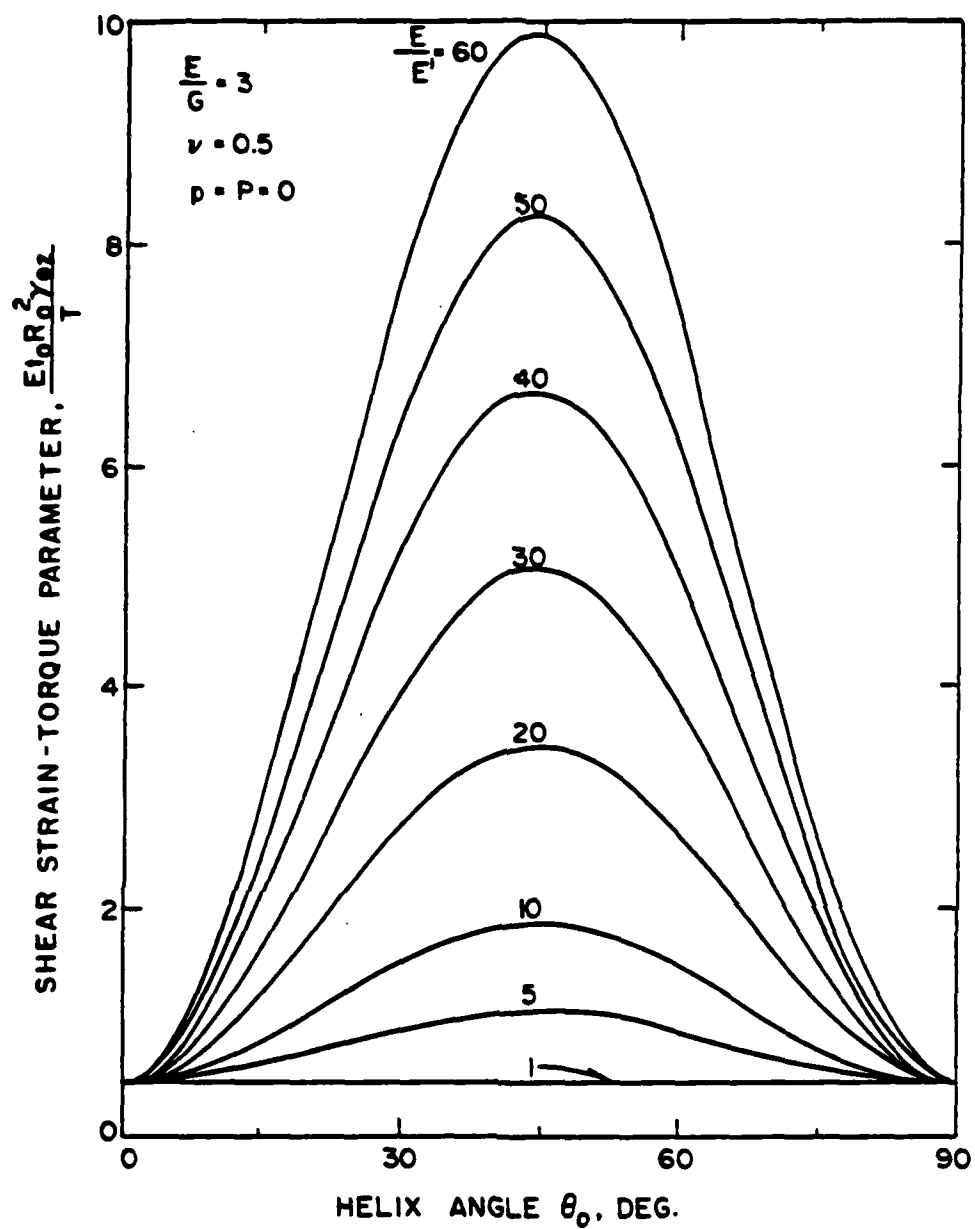
Figure 4   Unrestrained twisting due to a pure torque

84

The three nondimensional parameters involving the longitudinal strain ϵ_{zz} are defined by the ordinates of Figures 5, 6 and 3 (right ordinate), given that p, P and T are the only nonzero loads, respectively. For the isotropic case $(E/E' = 1)$, ϵ_{zz} is zero for two load cases: with the p load as a direct consequence of choosing ν as 0.5, and with the T load as expected from elementary solutions. With orthotropy, the peak values of the longitudinal strain parameters are as follows:

$$\text{peak} \left(\frac{E \, t_o \, \epsilon_{zz}}{p \, R_o}\right) \text{ occurs for } \theta_o = 0$$

$$\text{peak} \left(\frac{E \, t_o \, R_o \, \epsilon_{zz}}{P}\right) \text{ occurs for } \theta_o = 0$$

$$\text{peak} \left(\frac{E \, t_o \, R_o^2 \, \epsilon_{zz}}{T}\right) \text{ occurs for } \theta_o = 30 \text{ deg}$$

From Figures 5 and 6 it is observed that the values of these parameters are only somewhat depressed for $0 < \theta_o < 15$ deg, but that this depression increases more rapidly as E/E' increases. From Figure 3 (right ordinate) the longitudinal strain is seen to be negative, indicating the tendency of the orthotropic cylinder to shorten as it winds up under a positive torsion load.

Effects of Radial and End Constraint. While the studies above dealt with strain behavior for loadings applied one at a time, one can imagine a multitude of practical cases involving combined loads. Consider now one such case where an orthotropic cylinder is required to operate in close proximity with other mechanical parts. To avoid longitudinal and radial or circumferential expansions when pressurized, suppose that the unloaded orthotropic cylinder just fits within the confines of a rigid, closed-end tube. Under loading, then:

$$\epsilon_{zz} = \epsilon_{\theta\theta} = 0 \tag{59}$$
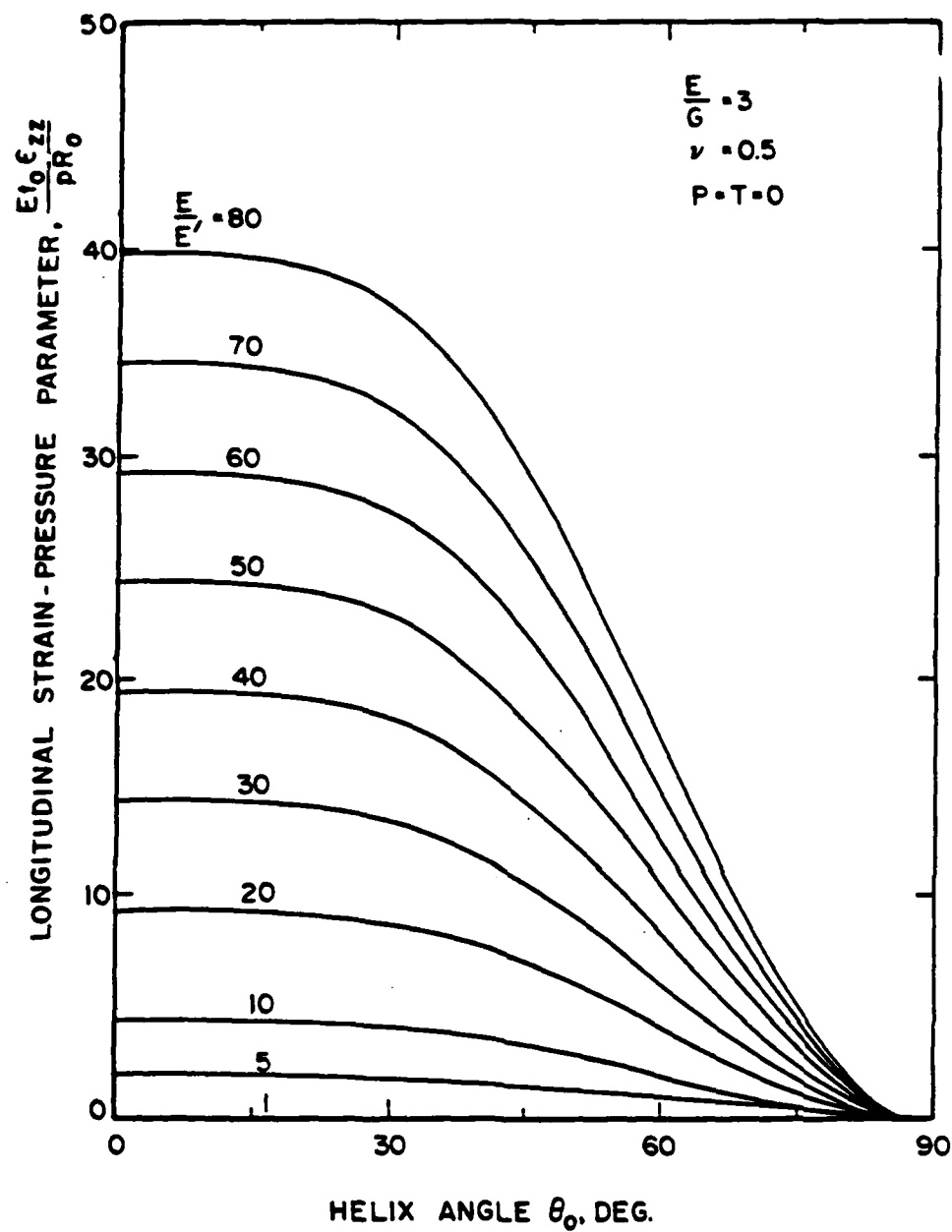
Figure 5   Unrestrained longitudinal strain due to internal pressure
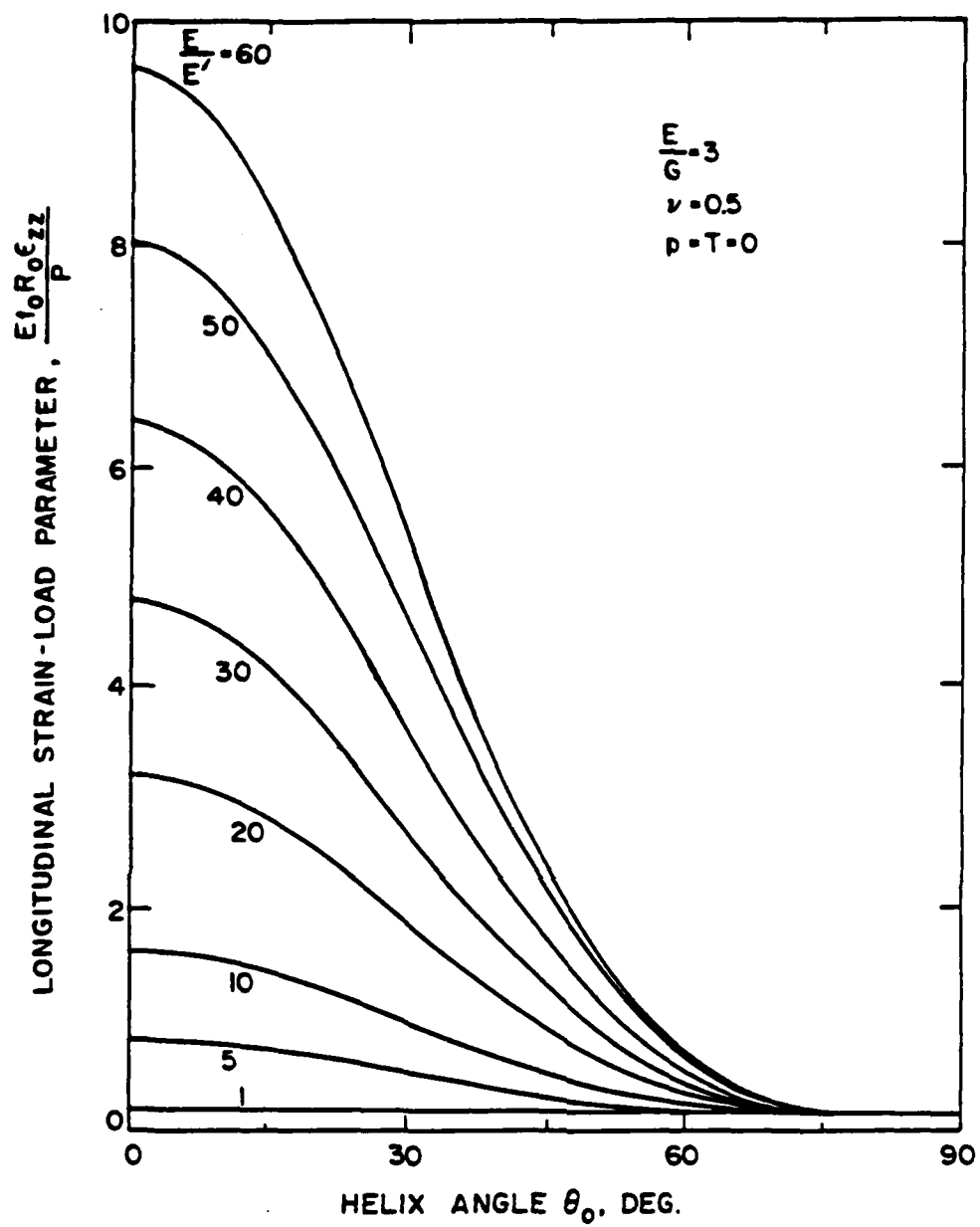
Figure 6   Unrestrained longitudinal strain due to longitudinal load

87

The confining tube has frictionless walls where its design allows for the application of a torque T to the orthotropic cylinder. The confining tube does not inhibit torsion. From Equations (7) and (44-46), the two constraints of Equation (59) become:

$$(a'_{12} + \frac{1}{2} a'_{22}) \frac{p \, R_0}{t_0} + a'_{22} \frac{p}{2\pi R_0 t} + a'_{26} \frac{T}{2\pi R_0^2 t_0} = 0 \qquad (60)$$

$$(a'_{11} + \frac{1}{2} a'_{12}) \frac{p \, R_0}{t_0} + a'_{12} \frac{p}{2\pi r_0 t} + a'_{16} \frac{T}{2\pi R_0^2 t_0} = 0 \qquad (61)$$

The compatible equation relating the loadings p and T is found by eliminating P between Equations (60) and (61), or

$$\frac{T}{pR_0^3} = 2\pi \, (\frac{a'_{12} \, a'_{12} - a'_{11} \, a'_{22}}{a'_{16} \, a'_{22} - a'_{12} \, a'_{26}}) = S \qquad (62)$$

The pressure-longitudinal load parameter is found by eliminating T between Equations (60) and (61). In terms of S of Equation (62), this is

$$\frac{P}{pR_0^2} = - 2\pi \, (\frac{a'_{12}}{a'_{22}} + \frac{1}{2} + \frac{a'_{26}}{a'_{22}} S) \qquad (63)$$

The results of Equations (62) and (63) are shown in Figures 7 and 8. Figure 7 shows that the pressure-torque parameter, the inverse of Equation (62), has a peak value at θ_0 = 50 deg for all E/E' > 1. For an imposed torque, this gives the maximum required cylinder pressure for full cylinder confinement. Figure 8 (the right ordinate) shows that the end load-pressure parameter defined by Equation (63) is independent of E/E' if that ratio exceeds unity. For a fixed pressure level p, the compatible end load P always decreases with θ_0 to maintain full cylinder confinement. It is noted that the isotropic cylinder is not shown in Figure 8 (the right ordinate) since the only
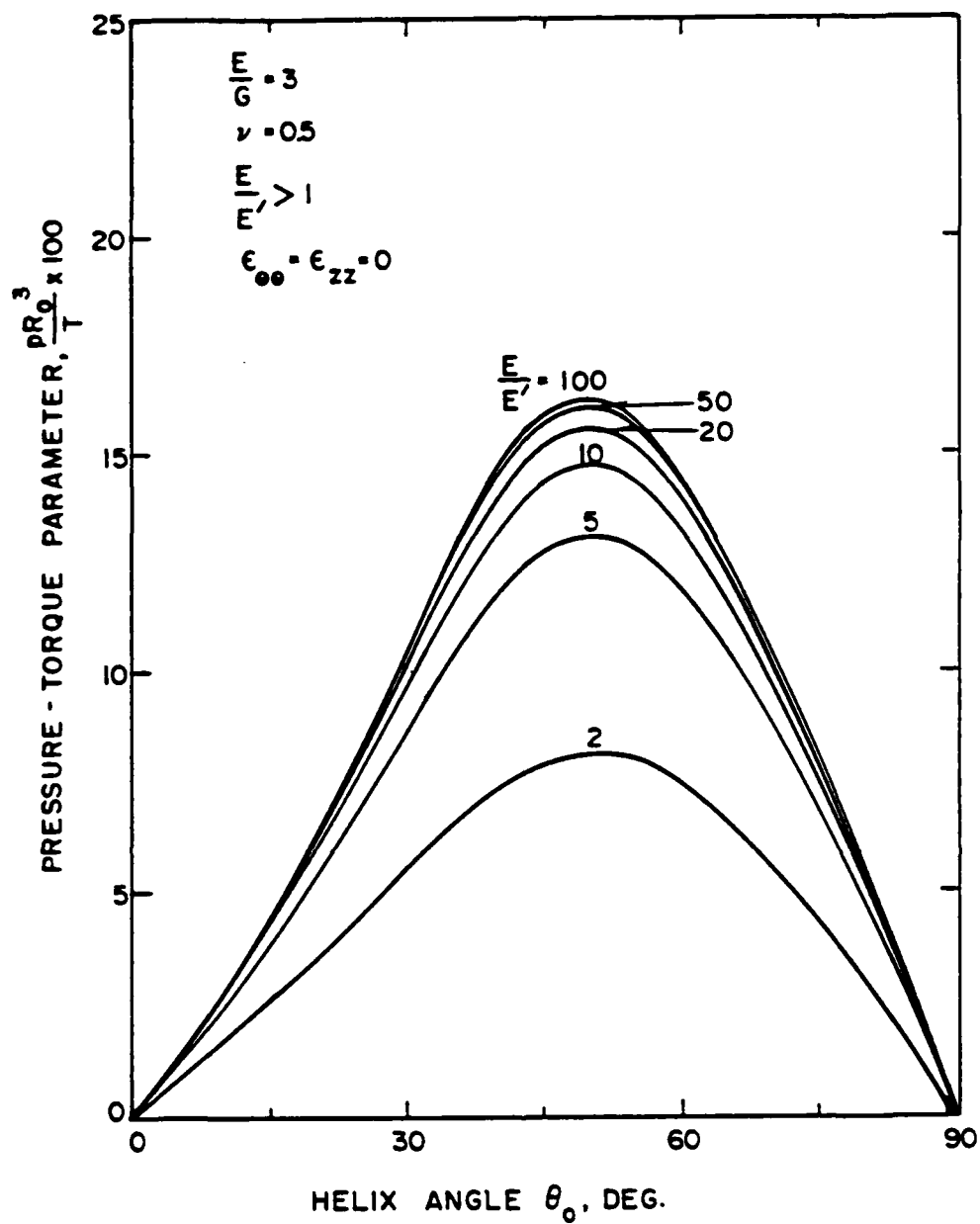
Figure 7   Pressure-torque behavior for the fully confined cylinder
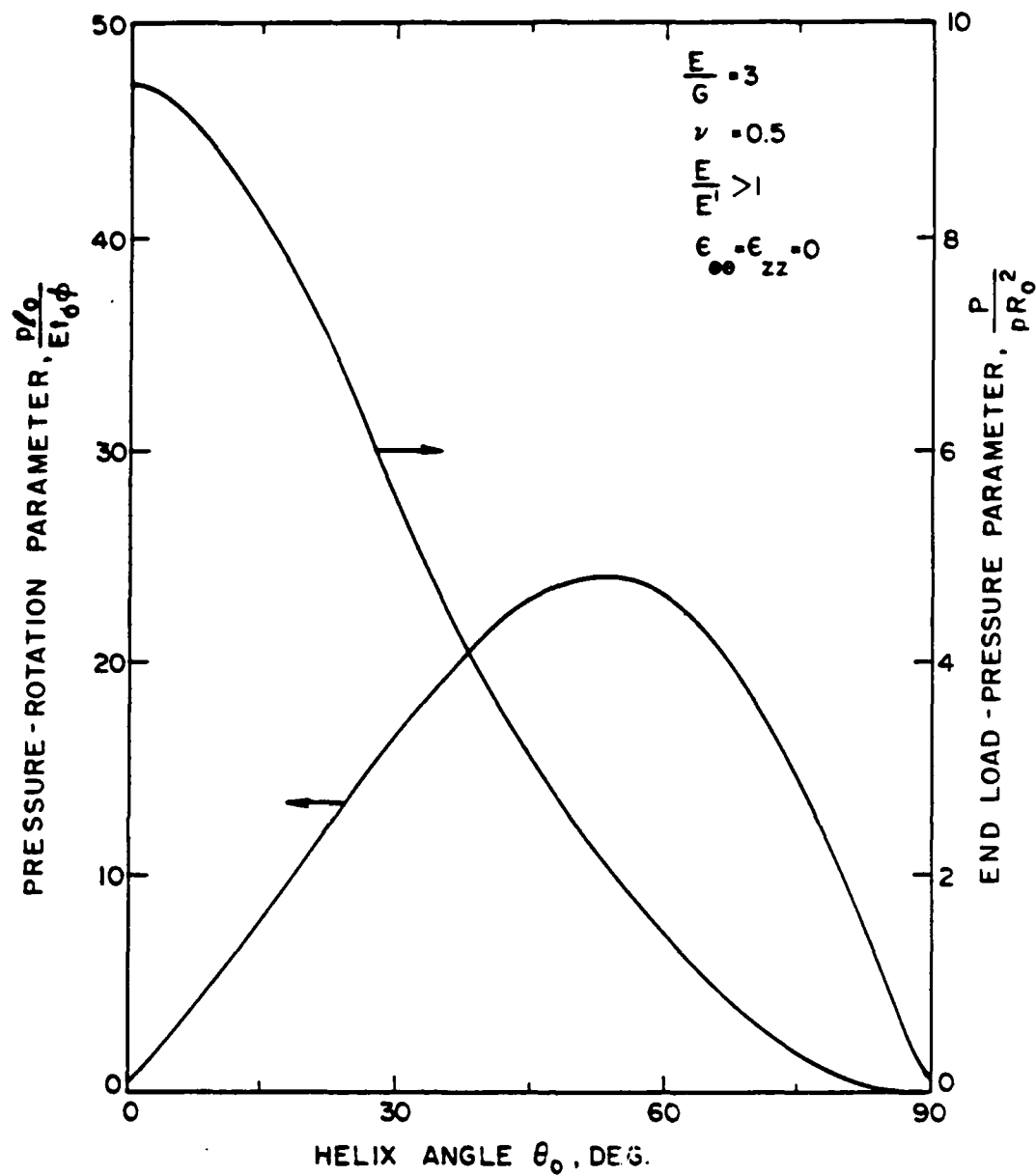
Figure 8   Rotation (left ordinate) and longitudinal load (right
            ordinate) for a pressurized and fully confined cylinder

way that full cylinder confinement can be met for $E/E' = 1$ is that $P = p = 0$. For this latter set of conditions, it is recalled that a nonzero value for T always implies full cylinder confinement; that is, Equation (59) is satisfied.

Using the results of Equations (62) and (63) it is possible to calculate the helix angle that will minimize the rotation ϕ (minimize $\gamma_{\theta z}$) at a given pressure level. The conclusion in this case, based on the results of Figure 8, left ordinate, is that $\theta_0 = 53$ deg will produce a minimum ϕ for all $E/E' > 1$.

<u>Effects of Torsional and End Constraint.</u> Consider now the special case where the orthotropic cylinder is fully restrained from rotation and also from longitudinal displacement. That is

$$\gamma_{\theta z} = \epsilon_{zz} = 0 \tag{64}$$

With Equations (7) and (34)-(46) these two constraint equations are:

$$(a'_{12} + \frac{1}{2} a'_{22}) \frac{p R_0}{t_0} + a'_{22} \frac{P}{2\pi R_0 t_0} + a'_{26} \frac{T}{2\pi R_0^2 t_0} = 0 \tag{65}$$

$$(a'_{16} + \frac{1}{2} a'_{26}) \frac{p R_0}{t_0} + a'_{26} \frac{P}{2\pi R_0 t_0} + a'_{66} \frac{T}{2\pi R_0^2 t_0} = 0 \tag{66}$$

By eliminating P between Equations (65) and (66), the torque-pressure parameter is deduced as:

$$\frac{T}{p R_0^3} = -2\pi \left(\frac{a'_{16} a'_{22} - a'_{26} a'_{12}}{a'_{22} a'_{66} - a'_{26} a'_{26}} \right) = S' \tag{67}$$

The compatible end load-pressure parameter is found by eliminating T between the same two equations. In terms of S' of Equation (67), this is

$$\frac{P}{p R_0^2} = -2\pi \left(\frac{a'_{12}}{a'_{22}} + \frac{1}{2} + \frac{a'_{26}}{a'_{22}} S' \right) \tag{68}$$

The results of these studies are shown in Figures 9 and 10. For a constant pressure p and a fixed modulus ratio E/E', it is observed that both

91
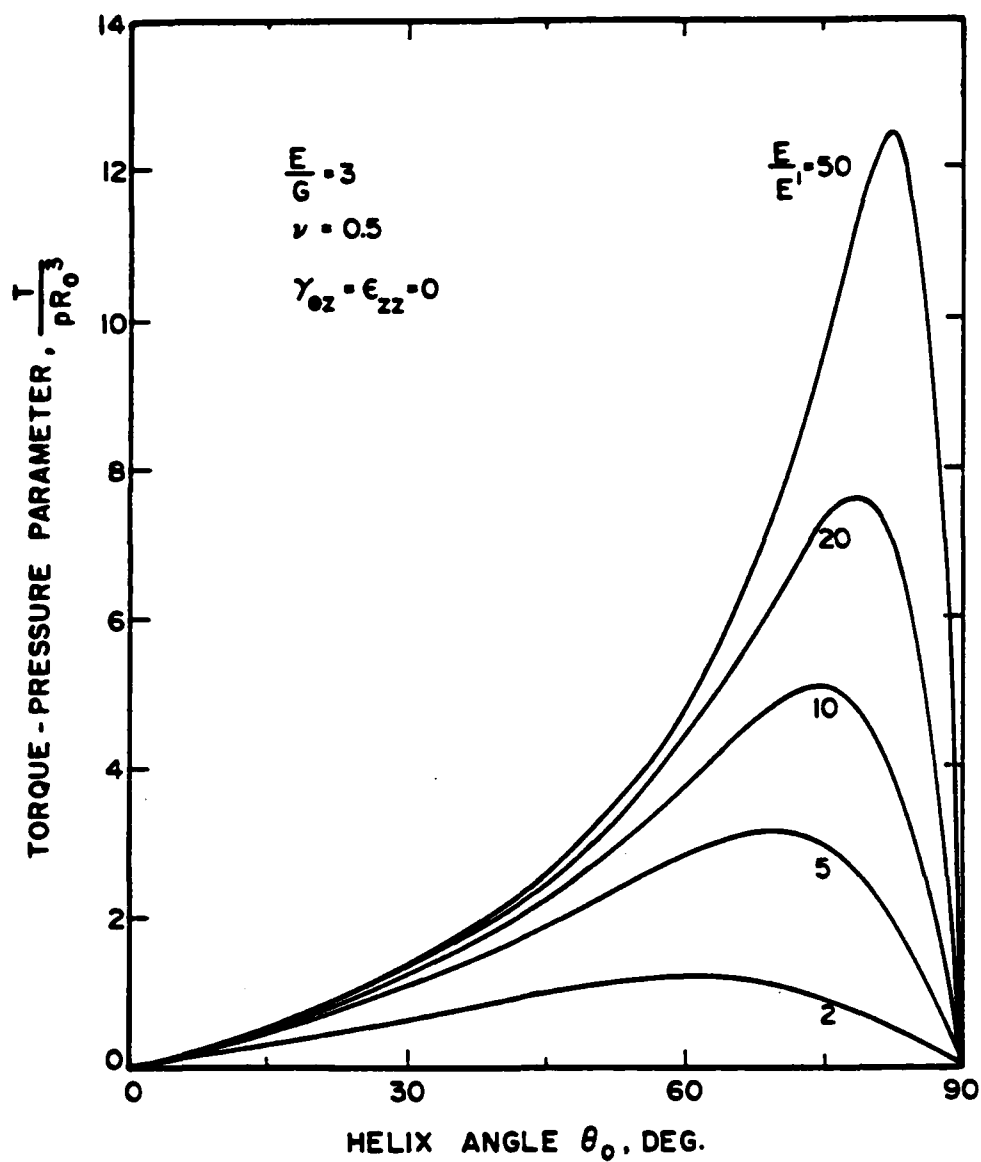
Figure 9   Torque required to supress rotation and longitudinal strain in a pressurized cylinder

92
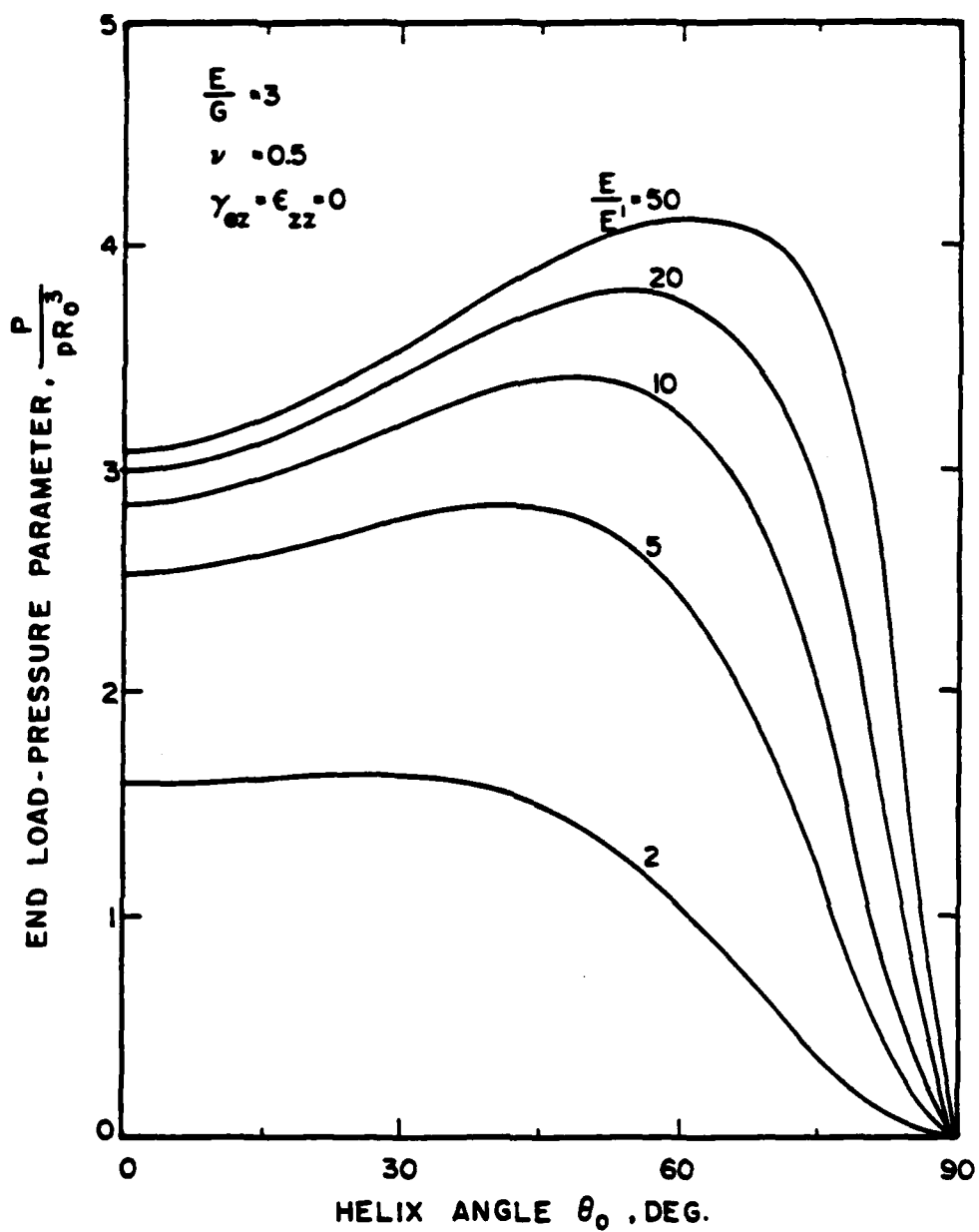
Figure 10   End load required to supress longitudinal strain and rotation
in a pressurized cylinder

the applied torque T and end load P reach peaks that are highly dependent on the helix angle. For instance, if the orthotropic cylinder were to be used as an efficient torque-exerting device, we would pick θ_0 = 60 deg if E/E' = 2, but would pick θ_0 = 80 deg if E/E' = 50. However, if this cylinder were to be used as a longitudinal or end loading device, we would choose θ_0 = 62 deg for E/E' = 50. These results are contingent, of course, on the requirement that all rotations and longitudinal motions be completely supressed.

There are three observations for this case where θ_0 = 90 deg and p > 0. First, no end load is required for the longitudinal strain to vanish, which is a direct consequence of having chosen ν = 0.5. Second, no torque is required and $\gamma_{\theta z}$ is automatically zero, a result that agrees with intuition. Third, a straightforward calculation of the circumferential strain reveals that $\varepsilon_{\theta\theta}$ reaches its peak value when θ_0 = 90 deg, for all E/E' > 1.

DESIGN EXAMPLES

The following examples show the utility of the above parametric studies in the design of special purpose configurations. The finite length cylinders are assumed to be fitted with end caps that have negligible radial stiffness so that homogeneous stresses are maintained throughout. The material and geometric properties common to all three design examples discussed below are as follows.

$$E = 1.5 \times 10^7 \text{ N/m}^2 , \quad E' = 1.5 \times 10^6 \text{ N/m}^2,$$

$$G = 5 \times 10^6 \text{ N/m}^2 , \quad \nu = 0.5,$$

$$t_0 = 1.5 \text{ mm} , \quad R_0 = 15 \text{ mm} , \quad \ell_0 = 50 \text{ mm}.$$

In the first design, θ_0 = 30 deg and the maximum allowable internal pressure is p = 1.9×10^5 N/m^2. What is the maximum torque T that such a cylinder can exert to loosen a bolt, for instance? With E/E' = 10, the value

94

of the shear strain-pressure parameter for unconstrained rotation (T = 0) is given in Figure 2 as -4.87, from which $\gamma_{\theta z}$ = -0.62 rad. The maximum torque capacity is then the value of T for which $\gamma_{\theta z}$ = +0.62 rad., corresponding to complete supression of rotation. With this shear strain and the ordinate of Figure 4, for which the shear strain-torque parameter is 1.55 at θ_0 = 30 deg and E/E' = 10, the maximum possible torque is thus calculated as T = 2.02 N-m.

For this first design, what is the length change in the cylinder for this maximum torque condition? From Figure 5, the longitudinal strain-pressure parameter is 4.2, for which ε_{zz} = 0.53 for unconstrained rotation (T = 0). For fully constrained rotation ($\gamma_{\theta z}$ = 0) let T = 2.02 N-m. The corresponding value of longitudinal strain from the right ordinate of Figure 3 is calculated, or ε_{zz} = -0.37. By superposition, the net result is ε_{zz} = 0.16, the length change of the cylinder is U_z = 8 mm and the final cylinder length is ξ = 58 mm, which are found from Equations (57) and (55) respectively for $z = \ell_0$ = 50 mm.

In the second design, the maximum allowable internal pressure is again p = 1.9 x 10^5 N/m^2. What value of θ_0 will produce the maximum end load P? The procedure is to allow the cylinder to expand freely in the longitudinal direction with a strain ε_{zz} compatible with Figure 5; and then for the same θ_0 to apply a compressive load P compatible with Figure 6 where this load completely nullifies the previous strain ε_{zz}. This is equivalent to finding the value of θ_0 that maximizes the ratio Y_5/Y_6, or the ratio of ordinates of these two respective Figures. In these terms, the peak compressive value of P is given by

$$P = \left(\frac{Y_5}{Y_6}\right)_{max} pR_0^2 = 341 \text{ N} \tag{69}$$

corresponding to θ_0 = 58 deg.

In the third design, the applied torque and the longitudinal strain are zero. What value of θ_0 will produce the maximum cylinder rotation at an arbitrary internal pressure? In this case, $\gamma_{\theta z}$ is the sum of two components: that due to the internal pressure (Figure 2) and that due to the longitudinal load (Figure 3, left ordinate). In terms of the ordinates Y_2 and Y_3 of these respective Figures, as well as the ordinates Y_5 and Y_6, the total shear strain reduces to:

$$\gamma_{\theta z} = (-Y_2 + \frac{Y_3 \, Y_5}{Y_6}) \frac{p \, R_0}{E \, t_0} \tag{70}$$

In Equation (70), the value of P was eliminated from Y_3 by the multiple Y_5/Y_6. Using a trial and error procedure, the peak value of the bracket term in Equation (70) was calculated as -4.94, for which $\theta_0 = 67$ deg. If the internal pressure is $p = 3.8 \times 10^4$ N/m^2, then the corresponding shear strain is $\gamma_{\theta z} = -0.125$ rad; and the rotational displacement and angle of rotation at $z = \ell_0$, calculated from Equations (57) and (58), are $U_\theta = -6.25$ mm and $\phi = -0.42$ rad, respectively.

SUMMARY AND CONCLUSIONS

Within the limits of linear theory, the deformation behavior of uniformly stressed, orthotropic cylindrical shells is described by several nondimensional parameters involving four independent material constants E, E', G, ν, and three loads: internal pressure, longitudinal load and pure torque. It is assumed that buckling is absent and that the cylinder is sufficiently constrained so that the cylindrical shape is always maintained. As shown in Figure 1, the principal directions of orthotropy follow constant angle helices. The more important findings of the parametric studies, unique to this type of orthotropy, are summarized as follows.

1. Longitudinal loading P and/or internal pressure p effects twisting about the longitudinal axis.

2. For P loading only, maximum twisting deformation occurs for an orthotropy angle of $\theta_0 = 30$ deg; but for p loading only, this occurs when $\theta_0 = 53$ deg.

3. For a pure torque T, maximum twisting deformation occurs when $\theta_0 = 45$ deg.

4. A pure torque T produces a change in cylinder length, which is not the case for isotropic cylinders.

5. The cylindrical strains $\gamma_{\theta z}$, $\epsilon_{\theta\theta}$ and ϵ_{zz} are all amplified for a given set of loads (p, P, T) as the magnitude of the orthotropy increases, that is, as E/E' increases, given that the geometry and other material constants remain fixed.

6. The maximum longitudinal strain ϵ_{zz} for P and p loading occurs for $\theta_0 = 0$; but ϵ_{zz} is maximum for T loading when $\theta_0 = 30$ deg.

7. The design examples show that the proper selection of cylinder orthotropy (θ_0 and E/E') can lead to optimal deformations or load-carrying capacity. Such designs, however, are highly sensitive to both the type of loading and strain constraint conditions .

The results of these studies are important to the design of versatile and efficient pressure-controlled actuators made of rubber-like materials that can sustain relatively high strains. Orthotropy may be achieved by corrugations of the wall. Robotics is a logical field of. application for such actuators.

NOMENCLATURE

E	Young's modulus in strong direction of orthotropy
E'	Young's modulus in weak direction of orthotropy
E_{ii}	Modulus of elasticity in i direction where i is one of the orthotropic axes, i = 1,2,3
G	Shear modulus of an isotropic material with Young's modulus E
G_{ij}	Shear modulus in i-j plane, where i and j are orthotropic axes, (i,j) = 1,2,3, i ≠ j
P	Longitudinal load
R_o	Mean radius of cylinder
T	Applied end torque
Y_k	Value of ordinate for Figure k, k = 2,3,...6
a_{ij}	elastic constants in orthotropic coordinate system (i,j) = 1,2,...6
a'_{ij}	Elastic constants in cylinder coordinate system (i,j) = 1,2,...6
$f_1(r,z)$	Function of integration
$f_2(z)$, $f_3(z)$	Functions of integration
ℓ_o	Length of cylinder
p	Internal pressure
q_{ij}	Direction cosine terms relating the (1,2,3) axis to (r,θ,z) axis, (i,j) = 1,2,...6
r,θ,z	Cylindrical coordinates
t_o	Wall thickness
U_r	Radial displacement
U_z	Longitudinal displacement
U_θ	Circumferential displacement
ξ	Longitudinal coordinate of material point where ξ = z at ϵ_{zz} = 0

γ_{ij}	Shear strains in i-j plane in orthotropic coordinate system, $(i,i) = 1,2,3$, $i \neq j$
γ_{zr}	Shear strain in z-r plane
$\gamma_{\theta r}$	Shear strain in θ-r plane
$\gamma_{\theta z}$	Shear strain in θ-z plane
ε_i	Strains in orthotropic coordinate system, single index notation $i=1,...6$
ε_i'	Strains in cylinder coordinate system, single index notation $i=1,...6$
ε_{ii}	Strains in orthotropic coordinate system, double index notation $i = 1,2,3$
ε_{rr}	Strain in radial direction
ε_{zz}	Strain in longitudinal direction
$\varepsilon_{\theta\theta}$	Strain in circumferential direction
θ_0	Angle between strong axis of orthotropy and circumferential direction on cylinder
ν	Poisson's ratio of isotropic material with Young's modulus E
ν_{ij}	Ratio of extensional strain in i direction to extensional strain in j direction for orthotropic coordinate system, $(i,j) = 1,2,3$, $i \neq j$
σ_i	Stresses in orthotropic coordinate system, $i=1,2,...6$
σ_i'	Stresses in cylinder coordinate system, $i = 1,2,...6$
σ_{ij}	Stresses in orthotropic coordinate system, $(i,j) = 1,2,3$
σ_{rr}	Normal stress in radial direction
σ_{zr}	Shear stress in z-r plane
σ_{zz}	Normal stress in longitudinal direction
$\sigma_{\theta r}$	Shear stress in θ-r plane
$\sigma_{\theta z}$	Shear stress in θ-z plane
$\sigma_{\theta\theta}$	Normal stress in circumferential direction
ϕ	Angle of rotation of cross-section

REFERENCES

1. Wilson, J. F., "Mechanics of Bellows: A Critical Review," _International Journal of Mechanical Sciences_, 1985 (in press).

2. Verma, P. D. S. and Rana, O. H., "Rotation of a Circular Cylindrical Tube Reinforced by Fibres Lying Along Helices," _Mechanics of Materials_, Vol. 2, pp. 353-359, 1983.

3. Reissner, E., "On Uniform Stress and Strain in Axially Homogeneous Cylindrical Shells," _International Journal of Solids and Structures_, Vol. 6, pp. 133-138, 1970.

4. Reissner, E. and Tsai, W. T., "Pure Bending, Stretching, and Twisting of Anisotropic Cylindrical Shells," _Journal of Applied Mechanics_, Vol. 41, pp. 168-174, 1974.

5. Lekhnitskii, S. G., _Theory of Elasticity of an Anisotropic Elastic Body_, Translated from Russian by P. Fern, Holden-Day, Inc., San Francisco, 1963.

6. Timoshenko, S. P. and Woinowsky-Krieger, S., _Theory of Plates and Shells_, 2nd Edition, McGraw-Hill, New York, 1959.

7. Sokolnikoff, I. S., _Mathematical Theory of Elasticity_, 2nd Edition, McGraw-Hill, New York, 1956.

8. Dahl, N. C., "Toroidal-Shell Expansion Joints," _Journal of Applied Mechanics_, Vol. 20, pp. 497-503, 1953.

APPENDIX A

COMPUTATION OF NEUTRAL AXIS

The iteration steps to compute the position of the neutral axis of the composite section of an element, given an end moment M_a, were briefly outlined in Chapter 2. The iteration steps including various formulae derivations, are now discussed in detail.

To set up the force equilibrium equation for the composite section it is needed to integrate over elemental areas across the section. For the cylindrical part as shown in Figure 2a, the area of elemental steps are as follows.

$$\text{area of strip ABCD is } 2\sqrt{A_{r1}}\ dy$$

$$\text{area of strip EFGH is} \sqrt{A_{r1}}\ dy - \sqrt{A_{r2}}\ dy,$$

where

$$A_{r1} = R_1{}^2 - (R_1 - y + H_1)^2 \qquad (A.1)$$

$$A_{r2} = R_2{}^2 - (R_1 - y + H_1)^2 \qquad (A.2)$$

The iteration steps are

a. Choose an initial value of H_1 to fix the position of the neutral axis.

b. After the neutral axis position is chosen the radius of curvature ρ of the deflected element is computed. Due to applied end moment, the part of the section above the neutral axis will be in tension, whereas below the

neutral axis the section will be in compression. Refer to Figures 2a dnd 2c.

For the linear reinforcement material the stress strain relationship is

$$\sigma = E\epsilon \qquad (A.3)$$

and strain curvature relationship is

$$\epsilon = y/\rho \qquad (A.4)$$

From Equations (A.3) and (A.4) we get

$$\sigma = E\ y/\rho \qquad (A.5)$$

For the nonlinear synthetic material the stress strain relationship is

$$\sigma = A\epsilon + B\epsilon^{1/n} \qquad (A.6)$$

From Equations (A.4) and (A.6) we get

$$\sigma = A(\tfrac{y}{\rho}) + B(\tfrac{y}{\rho})^{1/n} \qquad (A.7)$$

Now

$$F = \text{Force} = \int_A \sigma dA \qquad (A.8)$$

From Equations (A.5) and (A.8), the compressive force in the lower part of the reinforcement (below the neutral axis) is

$$F = \int_{H-H_1}^{0} E\ \tfrac{y}{\rho}\ b\ dy = \frac{-Eb(H - H_1)^2}{2\rho} \qquad (A.9)$$

Similarly the tensile force in the upper part of the reinforcement is

$$F = \int_{0}^{H_1} E\ \tfrac{y}{\rho}\ b\ dy = \frac{EB\ H_1^2}{2\rho} \qquad (A.10)$$

From Equations (A.7) and (A.8), the tensile force in the cylindrical part is

$$F = \frac{1}{\rho}\ (\gamma) + B(\tfrac{1}{\rho})^{1/n}(I) \qquad (A.11)$$

where

102

$$\gamma = 2A\left[\int_{H_1}^{R_1-R_2+H_1} y\sqrt{A_{r1}}\,dy + \int_{R_1-R_2+H_1}^{R_1+R_2+H_1} y\{\sqrt{A_{r1}} - \sqrt{A_{r2}}\}dy\right.$$

$$\left. + \int_{R_1+R_2+H_1}^{2R_1+H_1} y\sqrt{A_{r1}}\,dy\right] \tag{A.12}$$

and

$$I = 2\left[\int_{H_1}^{R_1-R_2+H_1} y^{1/n}\sqrt{A_{r1}}\,dy + \int_{R_1-R_2+H_1}^{R_1+R_2+H_1} y^{1/n}\{\sqrt{A_{r1}} - \sqrt{A_{r2}}\}dy\right.$$

$$\left. + \int_{R_1+R_2+H_1}^{2R_1+H_1} y^{1/n}\sqrt{A_{r1}}\,dy\right] \tag{A.13}$$

γ and I are evaluated using numerical integration techniques.

To have force equilibrium we know that the sum of compressive and tensile forces is equal to zero. Thus from Equations (A.9), (A.10) and (A.11) we get

$$-\frac{Eb(H - H_1)^2}{2\rho} + \frac{Eb\,H_1^2}{2\rho} + \frac{1}{\rho}\gamma + B\left(\frac{1}{\rho}\right)^{1/n} I = 0$$

$$\frac{Eb(H^2 - 2HH_1) - 2\gamma}{2\rho} = B\left(\frac{1}{\rho}\right)^{1/n} I$$

$$\frac{Eb(H^2-2HH_1) - 2\gamma}{2BI} = \left(\frac{1}{\rho}\right)^{\frac{1}{n} - 1}$$

$$\frac{1}{\rho} = \left[\frac{Eb(H^2-2HH_1) - 2\gamma}{2BI}\right]^{\frac{n}{1-n}}$$

$$\rho = \left[\frac{2BI}{Eb(H^2-2HH_1)-2\gamma}\right]^{\frac{n}{1-n}} \tag{A.14}$$

103

c. For the computed radius of curvature ρ and chosen position of neutral axis the moment of resistance of the section M_c is evaluated.

$$\text{Moment of resistance} = \int_A \sigma y\, dA \tag{A.15}$$

Using Equations (A.5) and (A.15) the moment resisted by the reinforcement is

$$M_r = \int_0^{H_1} y^2 \frac{E}{\rho} b\, dy + \int_{H_1-H}^{0} y^2 \frac{E}{\rho} b\, dy$$

$$M_r = \frac{1}{\rho}(\alpha) \tag{A.16}$$

where

$$\alpha = \frac{Eb}{3}[H_1^3 + (H - H_1)^3] \tag{A.17}$$

Using Equations (A.7) and (A.15) the moment resisted by the nonlinear cylindrical part is

$$M_n = \left(\frac{1}{\rho}\right)\beta + \left(\frac{1}{\rho}\right)^{1/n}n \tag{A.18}$$

where

$$\beta = 2A\left[\int_{H_1}^{R_1-R_2+H_1} y^2\sqrt{A_{r1}}\, dy + \int_{R_1-R_2+H_1}^{R_1+R_2+H_1} y^2\{\sqrt{A_{r1}} - \sqrt{A_{r2}}\}dy\right.$$

$$\left. + \int_{R_1+R_2+H_1}^{2R_1+H_1} y^2\sqrt{A_{r1}}\, dy\right] \tag{A.19}$$

and

$$n = 2B\left[\int_{H_1}^{R_1-R_2+H_1} y^{\frac{n+1}{n}}\sqrt{A_{r1}}\, dy + \int_{R_1-R_2+H_1}^{R_1+R_2+H_1} y^{\frac{n+1}{n}}\{\sqrt{A_{r1}} - \sqrt{A_{r2}}\}\, dy\right.$$

$$\left. + \int_{R_1+R_2+H_1}^{2R_1+H_1} y^{\frac{n+1}{n}}\sqrt{A_{r1}}\, dy\right] \tag{A.20}$$

The total moment resisted by the section

104

$$M_c = M_r + M_n$$

From Equations (A.16) and (A.18) we obtain

$$M_c = \left(\frac{1}{\rho}\right) \alpha + \left(\frac{1}{\rho}\right) \beta + \left(\frac{1}{\rho}\right)^{1/n} \eta \qquad (A.21)$$

d. If the following inequality holds for a specified tolerance limit ϵ

$$\left| \frac{M_a - M_c}{M_a} \right| < \epsilon$$

then the iterations stop. Otherwise a new position of neutral axis is chosen and steps (b) to (d) are repeated.

PROGRAM TYPEL

```
1.      // JOB
2.      // EXEC FTVCG
3.      //C.SYSIN DD *
4.      C
5.      C
6.             REAL*8 H1,H,N,B1,M,A1,B2,R1,R2,RHO,RHIN,ALPHA,
7.            1BETA,NETA,KSITA,GAMA,M1,M2,U,Z,N1,L,MM,INTGRL,
8.            2E,VDIS,HDIS,CHK,O,R
9.             READ(1,10) N,B1,H,R1,R2,L,A1,B2,M,E
10.      10 FORMAT(F3.1,F4.1,F7.4,2F6.3,F4.1,F5.1,F5.1,E9.2,E9.1)
11.             WRITE (3,10) N,B1,H,R1,R2,L,A1,B2,M,E
12.     C
13.     C     LOOP TO VARY THE APPLIED MOMENT
14.     C
15.            DO 20 I=1,5
16.            WRITE(3,63)I
17.      63 FORMAT(1H ,'I=',I2)
18.            M1=FLOAT(I)*0.2*M
19.            O=0.00056
20.            R=0.00001
21.            H1=0.5*H
22.      70 H1=H1-O*H
23.            O=O*0.95
24.            R=R*0.95
25.            GO TO 90
26.      80 H1=H1+R*H
27.            O=O*0.95
28.            R=R*0.95
29.      90 IF((H1 .LE. 0.000001) .OR. (H1 .GE. (0.5*H))) GO TO 92
30.            N1=N
31.            Z=INTGRL(H1,R1,R2,N1)
32.            Z=2.0*Z
33.            N1=1.0
34.            GAMA =INTGRL(H1,R1,R2,N1)
35.            GAMA=2.0*A1*GAMA
36.            CHK=DABS(E*B1*(H*H-2.0*H*H1)-2.0*GAMA)
37.            RHO=((2.0*Z*B2)/CHK)**(N/(1.0-N))
38.            ALPHA=E*B1*(H1**3.0+(H-H1)**3.0)/3.0
39.            N1=0.5
40.            BETA=INTGRL(H1,R1,R2,N1)
41.            BETA=2.0*A1*BETA
42.            N1=N/(N+1.0)
43.            NETA=INTGRL(H1,R1,R2,N1)
44.            NETA=2.0*B2*NETA
45.            RHIN=1.0/RHO
46.            M2=RHIN*ALPHA+RHIN*BETA+RHIN**(1.0/N)*NETA
47.            U=DABS((M1-M2)/M1)
48.            IF((U .LE. 0.1) .AND. (U .GE. 0.0)) GO TO 60
49.            WRITE(3,34) M2,H1,M1
50.      34 FORMAT(1H ,'M2=',E15.7,'H1=',E15.7,'M1=',E15.7)
51.            IF(M1 .GT. M2) GO TO 70
52.            GO TO 80
53.      60 KSITA=RHIN**(1.0/N)*NETA
54.            MM=(M2-KSITA)/(ALPHA+BETA)
55.            VDIS=(1.0-DCOS(L*MM))/MM
56.            HDIS=L-(DSIN(L*MM))/MM
57.            WRITE(3,29)
58.      29 FORMAT(1H ,5X,'H1',10X,'RHO',8X,'MOMENT',6X,'VDIS',7X,'HDIS')
59.            WRITE(3,19) H1,RHO,M2,VDIS,HDIS
```

```
60.          19 FORMAT(1H ,5E15.8)
61.             GO TO 20
62.          92 WRITE(3,95)
63.     C
64.     C       ERROR MESSAGE
65.     C
66.          95 FORMAT(1H ,'THE DATA IS UNSUITABLE FOR DESIRED STRUCTURE')
67.          20 CONTINUE
68.             STOP
69.             END
70.     C
71.     C       FUNCTION USED TO CALL INTEGRATION ROUTINE DCADRE
72.     C
73.             DOUBLE PRECISION FUNCTION INTGRL(H1,R1,R2,N1)
74.             INTEGER IER
75.             REAL*8 DCADRE,F,A,B,AERR,RERR,ERROR,H1,C1,C2,C3,C4,N2,
76.            1R1,R2,P,R3,R4,H2,N1
77.             COMMON R3,R4,N2,P,H2
78.             EXTERNAL F
79.             N2=N1
80.             R3=R1
81.             R4=R2
82.             H2=H1
83.             RERR=0.000000001
84.             AERR=0.000000001
85.             A=H2+0.000000001
86.             B=R3-R4+H2-0.000000001
87.             P=1.5
88.             C1=DCADRE(F,A,B,AERR,RERR,ERROR,IER)
89.             A=B+0.000000011
90.             B=R3+R4+H2-0.000000001
91.             C2=DCADRE(F,A,B,AERR,RERR,ERROR,IER)
92.             P=0.5
93.             A=A
94.             B=B
95.             C3=DCADRE(F,A,B,AERR,RERR,ERROR,IER)
96.             P=1.5
97.             A=B+0.000000011
98.             B=2*R3+H2-0.000000001
99.             C4=DCADRE(F,A,B,AERR,RERR,ERROR,IER)
100.            INTGRL=C1+C2-C3+C4
101.            RETURN
102.            END
103.    C
104.    C
105.            DOUBLE PRECISION FUNCTION F(Y)
106.            REAL*8 R3,R4,N2,UNDER1,UNDER2,H2,Y,P
107.            COMMON R3,R4,N2,P,H2
108.            IF(P .LE. 1.0) GO TO 14
109.            UNDER1=(2*R3*Y-Y*Y-H2*H2-2*H2*R3+2*Y*H2)**0.5
110.            F=(Y**(1.0/N2))*UNDER1
111.            GO TO 17
112.         14 UNDER2=(R4*R4+2*R3*Y-Y*Y-H2*H2-2*H2*R3+2*H2*Y-R3*R3)**0.5
113.            F=Y**(1.0/N2)*UNDER2
114.         17 RETURN
115.            END
116.    //G.SYSIN DD *
117.    0.2 0.5 0.0150 0.525 0.475 2.0 20.0 50.0  0.15E02    3.0E07
118.    /*
119.    //
```

```
1.      // JOB .REGION=1024K
2.      // EXEC FTVCG
3.      //C.SYSIN DD *
4.      C
5.      C       ................................
6.      C       * SUBROUTINE FOR PRINTING RESULTS *
7.      C       ................................
8.      C
9.              SUBROUTINE RESULT(SI,X3,Y3,RHO,M)
10.             DIMENSION XORD(25),YORD(25)
11.             COMMON XORD,YORD,X5,Y5
12.             ANG=180.0/3.1415927*SI
13.             X5=Y3
14.             Y5=-X3
15.             WRITE(3,95) ANG,X5,Y5,RHO,M
16.          95 FORMAT(1H ,'END ROTATION=',E12.4,4X,'XCOR=',E12.4,4X,
17.             1'YCOR=',E12.4,4X,'RHO=',E12.4,4X,'M=',I2)
18.             MN=M+1
19.             XORD(MN)=X5
20.             YORD(MN)=Y5
21.             RETURN
22.             END
23.     C
24.     C       ................................
25.     C       * SUBROUTINE FOR DATA INTERPOLATION *
26.     C       ................................
27.     C
28.             SUBROUTINE DTINT(RM1,ITYPE)
29.             REAL H1,HDIS,LN
30.             DIMENSION A(20,7),B(20,7),AB(20,7)
31.             COMMON /BLK1/RHO,H1,HDIS,VDIS,LN,R1,MM,A,B
32.             IF(ITYPE.EQ.1) GO TO 91
33.             IF(ITYPE.EQ.2) GO TO 45
34.          45 DO 98 I=1,MM
35.             DO 98 J=1,7
36.             AB(I,J)=B(I,J)
37.          98 CONTINUE
38.             GO TO 46
39.          91 DO 99 I=1,MM
40.             DO 99 J=1,7
41.             AB(I,J)=A(I,J)
42.          99 CONTINUE
43.          46 IF(RM1 .EQ. 0.0) GO TO 41
44.             DO 16 I=1,MM
45.             IF(AB(I,1) .GE. RM1) GO TO 92
46.          16 CONTINUE
47.             WRITE(3,18)
48.          18 FORMAT(1H ,'THE ELEMENT CANNOT SUBSTAIN DESIRED MOMENT')
49.             GO TO 93
50.          92 K=I-1
51.             RIF=(RM1-AB(K,1))/(AB(I,1)-AB(K,1))
52.             RHO=RIF*(AB(I,2)-AB(K,2))+AB(K,2)
53.             H1=RIF*(AB(I,3)-AB(K,3))+AB(K,3)
54.             HDIS=RIF*(AB(I,4)-AB(K,4))+AB(K,4)
55.             VDIS=RIF*(AB(I,5)-AB(K,5))+AB(K,5)
56.             LN=AB(1,6)
57.             R1=AB(1,7)
58.             GO TO 93
59.          41 RHO=0.0
```

```
60.          H1=0.0
61.          HDIS=0.0
62.          VDIS=0.0
63.          LN=AB(1,6)
64.          R1=0.0
65.       93 RETURN
66.          END
67.   C
68.   C      ............................
69.   C      * MAIN PROGRAM STARTS NOW *
70.   C      ............................
71.   C
72.          REAL LN,RHO,X2,Y2,VDIS,HDIS,SI,ANG,R1,R3,H1,H3,X3,Y3,NSHIF
73.          DIMENSION XORD(25),YORD(25),A(20,7),B(20,7),ITYPE1(5),IP1(20),
74.         1IPLT1(20),N1(20),IMOT1(20),RMOM(20),RMOM1(20),D(3,4,4,4,13)
75.          COMMON XORD,YORD,X5,Y5
76.          COMMON /BLK1/RHO,H1,HDIS,VDIS,LN,R1,MM,A,B
77.          READ(1,11) NN,MM,NU,RL,W1,H
78.       11 FORMAT(3I2,3E11.4)
79.          READ(1,104) XI,YI,XF,YF
80.      104 FORMAT(4E11.4)
81.          READ(1,10) (ITYPE1(I),IP1(I),IPLT1(I),N1(I),IMOT1(I),I=1,NN)
82.       10 FORMAT(5I2)
83.          READ(1,12)((A(I,J),J=1,7),I=1,MM)
84.       12 FORMAT(7E10.3)
85.          READ(1,55) N2,M2,N7,M7,MX
86.       55 FORMAT(5I4)
87.          N2=NN-3
88.          DO 26 II=1,N2
89.          RMOM(II)=0.0
90.       26 CONTINUE
91.          N2=N2+1
92.   C
93.   C
94.   C      THE DATA FILE IS READ INTO THE DATA MATRIX
95.   C
96.   C      READ ALL THE 'PHI'
97.          DO 319 I=1,N2
98.          READ(40,318) D(I,1,1,1,1)
99.      318 FORMAT(E11.4)
100.         IF(D(I,1,1,1,1).EQ.1000.0) GO TO 320
101.     319 CONTINUE
102.   C
103.   C      READ IN ALL THE 'RAD'
104.     320 DO 321 I=1,N2
105.         IF(D(I,1,1,1,1).EQ.1000.0) GO TO 324
106.         DO 322 J=2,M2
107.         READ(40,323) D(I,J,1,1,1)
108.     323 FORMAT(E11.4)
109.         IF(D(I,J,1,1,1).EQ.1000.0) GO TO 321
110.     322 CONTINUE
111.     321 CONTINUE
112.   C
113.   C      READ ALL THE 'THETA'
114.     324 DO 325 I=1,N2
115.         IF(D(I,1,1,1,1).EQ.1000.0) GO TO 330
116.         DO 326 J=2,M2
117.         IF(D(I,J,1,1,1).EQ.1000.0) GO TO 325
118.         DO 327 K=2,N7
119.         READ(40,326) D(I,J,K,1,1)
```

```
120.         328 FORMAT(E11.4)
121.             IF(D(I,J,K,1,1).EQ.1000.0) GO TO 326
122.         327 CONTINUE
123.         326 CONTINUE
124.         325 CONTINUE
125.     C
126.     C       READ ALL THE 'THETA'
127.     C
128.         330 DO 331 I=1,N2
129.             IF(D(I,1,1,1,1).EQ.1000.0) GO TO 338
130.             DO 332 J=2,M2
131.             IF(D(I,J,1,1,1).EQ.1000.0) GO TO 331
132.             DO 333 K=2,N7
133.             IF(D(I,J,K,1,1).EQ.1000.0) GO TO 332
134.             DO 334 L=2,M7
135.             READ(40,335) D(I,J,K,L,1)
136.         335 FORMAT(E11.4)
137.             IF(D(I,J,K,L,1).EQ.1000.0) GO TO 333
138.         334 CONTINUE
139.         333 CONTINUE
140.         332 CONTINUE
141.         331 CONTINUE
142.     C
143.     C       READ ALL THE 'MOM'
144.     C
145.         338 DO 339 I=1,N2
146.             IF (D(I,1,1,1,1).EQ.1000.0) GO TO 348
147.             DO 341 J=2,M2
148.             IF (D(I,J,1,1,1).EQ.1000.0) GO TO 339
149.             DO 342 K=2,N7
150.             IF(D(I,J,K,1,1).EQ.1000.0) GO TO 341
151.             DO 343 L=2,M7
152.             IF(D(I,J,K,L,1).EQ.1000.0) GO TO 342
153.             DO 344 M=2,MX
154.             READ(40,345) D(I,J,K,L,M)
155.         345 FORMAT(E11.4)
156.             IF(D(I,J,K,L,M).EQ.1000.0) GO TO 343
157.         344 CONTINUE
158.         343 CONTINUE
159.         342 CONTINUE
160.         341 CONTINUE
161.         339 CONTINUE
162.     C
163.     C       THE DATAFILE HAS BEEN READ IN
164.     C
165.         348 REWIND 40
166.             P=0.95
167.             E=0.95
168.             F=0.95
169.             G=0.95
170.     C
171.     C       TO EVALUATE MCUR REQUIRED TO GET THE LOAD FROM INITIAL
172.     C       POSITION TO THE FINAL DESIRED POSITION
173.     C
174.     C       MAIN LOOP BEGINS NOW
175.     C
176.     C
177.     C       MAXIMUM OF 25 ITERATIONS ARE ALLOWED
178.     C
179.             DO 56 KK=1,25
```

```
180.              IF(KK.NE.1) GO TO 101
181.        C
182.        C     THE MOMENT IS APPLIED ON THE LAST THREE ELEMENTS TO INITIALLY
183.        C     COIL THE ARM AROUND THE LOAD
184.              DO 102 II=NZ,NN
185.              IO=II+1
186.              RMOM(II)=D(1,2,2,2,IO)
187.          102 CONTINUE
188.        C
189.          101 SI=0.0
190.              X2=0.0
191.              Y2=0.0
192.              M=0
193.              R3=0.0
194.              H3=0.0
195.              Y4=0.0
196.              IPCK=0
197.              INCK=0
198.              MR=0
199.              NSHIF=0.0
200.              XORD(1)=0.0
201.              YORD(1)=0.0
202.        C
203.        C
204.        C     LOOP FOR FINDING THE END COORDINATES AND ROTATIONS OF
205.        C     VARIOUS ELEMENTS
206.        C
207.              DO 20 I=1,NN
208.              ITYPE=ITYPE1(I)
209.              RM1=RMOM(I)
210.              CALL DTINT(RM1,ITYPE)
211.              IF(RM1.EQ.0.0) GO TO 86
212.              IP=IP1(I)
213.              GO TO 87
214.           86 IP=-2
215.           87 IPLT=IPLT1(I)
216.              N=N1(I)
217.              IMOT=IMOT1(I)
218.              IF(I.EQ.1) GO TO 17
219.              IF(IDIR.EQ.IMOT) GO TO 17
220.              IF(SI.LT.0.0) GO TO 19
221.              MR=MR+1
222.        C     THE NUETRAL AXIS IS SHIFTED ACCORDINGLY
223.        C
224.              IF(IDIR.EQ.-3) GO TO 21
225.              IF(MR.EQ.1) NSHIF=R3+H3+R1+H1
226.              X2=X2+NSHIF*SIN(SI)
227.              Y2=Y2+NSHIF*COS(SI)
228.              NSHIF=0.0
229.        C
230.        C     TO CHECK IF PRESSURIZED OR NOT
231.        C
232.              IF(IP.EQ.-2) GO TO 23
233.              X2=X2+(LN-HDIS)*COS(SI)+VDIS*SIN(SI)
234.              Y2=Y2-(LN-HDIS)*SIN(SI)+VDIS*COS(SI)
235.              SI=SI-LN/RHO
236.              IF(SI.LT.0.0) GO TO 24
237.              X3=X2-(R1+H1)*SIN(SI)
238.              Y3=Y2-(R1+H1)*COS(SI)
239.              GO TO 25
```

111

```
240.          24 X3=X2+(R1+H1)*SIN(-SI)
241.             Y3=Y2-(R1+H1)*COS(-SI)
242.          25 M=M+1
243.             CALL RESULT(SI,X3,Y3,RHO,M)
244.             R3=R1
245.             H3=H1
246.             GO TO 20
247.          23 X2=X2+LN*COS(SI)
248.             Y2=Y2-LN*SIN(SI)
249.             X3=X2-(R3+H3)*SIN(SI)
250.             Y3=Y2-(R3+H3)*COS(SI)
251.             M=M+1
252.             CALL RESULT(SI,X3,Y3,RHO,M)
253.             GO TO 20
254.     C
255.     C       WHEN REVERSE CURVATURE MOTION IS IN OPP DIRECTION
256.     C
257.          21 IF(MR.EQ.1) NSHIF=R3+H3+R1+H1
258.             X2=X2+NSHIF*SIN(SI)
259.             Y2=Y2-NSHIF*COS(SI)
260.             NSHIF=0.0
261.             IF(IP.EQ.-2) GO TO 33
262.             X2=X2+(LN-HDIS)*COS(SI)+VDIS*SIN(SI)
263.             Y2=Y2+(LN-HDIS)*SIN(SI)-VDIS*COS(SI)
264.             SI=SI-LN/RHO
265.             IF(SI.LT.0.0) GO TO 34
266.             X3=X2-(R1+H1)*SIN(SI)
267.             Y3=Y2+(R1+H1)*COS(SI)
268.             GO TO 35
269.          34 X3=X2+(R1+H1)*SIN(-SI)
270.             Y3=Y2+(R1+H1)*COS(-SI)
271.          35 M=M+1
272.             CALL RESULT(SI,X3,Y3,RHO,M)
273.             R3=R1
274.             H3=H1
275.             GO TO 20
276.          33 X2=X2+LN*COS(SI)
277.             Y2=Y2+LN*SIN(SI)
278.             X3=X2-(R3+H3)*SIN(SI)
279.             Y3=Y2+(R3+H3)*COS(SI)
280.             M=M+1
281.             CALL RESULT(SI,X3,Y3,RHO,M)
282.             GO TO 20
283.          19 SI=-SI
284.          17 IDIR=IMOT
285.             DO 15 J=1,N
286.     C
287.     C       TO CHECK IF THE ELEMENT IS PRESSURIZED OR NOT
288.     C
289.             IF(IP .EQ. -2) GO TO 30
290.             IPCK=1
291.     C
292.     C       TO CHECK IF THE PLATE IS AT TOP OR BOTTOM
293.     C
294.             IF(IPLT .EQ. -1) GO TO 40
295.             IF(INCK .EQ. 0)Y4=R1+H1
296.             INCK=1
297.             M=M+1
298.             IF(M .EQ. 1) GO TO 39
299.             NSHIF=(R1+H1)-(R3+H3)
```

112

```
300.          X2=X2-NSHIF*SIN(SI)
301.          Y2=Y2-NSHIF*COS(SI)
302.       39 X2=X2+(LN-HDIS)*COS(SI)-VDIS*SIN(SI)
303.          Y2=Y2-(LN-HDIS)*SIN(SI)-VDIS*COS(SI)
304.          SI=SI+LN/RHO
305.          X3=X2+(R1+H1)*SIN(SI)
306.          Y3=Y2+(R1+H1)*COS(SI)-Y4
307.          R3=R1
308.          H3=H1
309.          CALL RESULT(SI,X3,Y3,RHO,M)
310.          GO TO 15
311.       40 M=M+1
312.          IF(INCK.EQ.0)Y4=-(R1+H1)
313.          INCK=1
314.          IF(M .EQ. 1) GO TO 49
315.          NSHIF=(R1+H1)-(R3+H3)
316.          X2=X2-NSHIF*SIN(SI)
317.          Y2=Y2+NSHIF*COS(SI)
318.       49 X2=X2+(LN-HDIS)*COS(SI)-VDIS*SIN(SI)
319.          Y2=Y2+(LN-HDIS)*SIN(SI)+VDIS*COS(SI)
320.          SI=SI+LN/RHO
321.          X3=X2+(R1+H1)*SIN(SI)
322.          Y3=Y2-(R1+H1)*COS(SI)-Y4
323.          R3=R1
324.          H3=H1
325.          CALL RESULT(SI,X3,Y3,RHO,M)
326.          GO TO 15
327.    C
328.    C     TO CHECK DIRECTION OF MOTION OF STRUCTURE
329.    C
330.       30 IF(IPCK .EQ. 0) GO TO 53
331.          IF(IMOT .EQ. -3) GO TO 51
332.    C
333.    C     THE TRANSFORMATION FOR DOWNWARD TRANSLATION
334.    C
335.          X2=X2+LN*COS(SI)
336.          Y2=Y2-LN*SIN(SI)
337.          X3=X2+(R3+H3)*SIN(SI)
338.          Y3=Y2+(R3+H3)*COS(SI)-Y4
339.          M=M+1
340.          INCK=1
341.          CALL RESULT(SI,X3,Y3,RHO,M)
342.          GO TO 15
343.       51 X2=X2+LN*COS(SI)
344.          Y2=Y2+LN*SIN(SI)
345.          X3=X2+(R3+H3)*SIN(SI)
346.          Y3=Y2-(R3+H3)*COS(SI)-Y4
347.          M=M+1
348.          INCK=1
349.          CALL RESULT(SI,X3,Y3,RHO,M)
350.          GO TO 15
351.    C
352.    C     WHEN ELEMENTS IN THE BEGINNING ARE NOT PRESSURIZED
353.    C
354.       53 X2=X2+LN
355.          Y2=0.0
356.          M=M+1
357.          INCK=1
358.          X3=X2
359.          Y3=Y2
```

113

```
360.          CALL RESULT(SI,X3,Y3,RHO,M)
361.       15 CONTINUE
362.    C     LOOP FOR IDENTICAL ELEMENTS IS COMPLETE
363.       20 CONTINUE
364.    C     LOOP FOR FINDING END COORDINATES FOR ALL THE ELEMENTS
365.    C     IS COMPLETE
366.    C
367.          MN=M+1
368.          CALL PICSIZ(20.0,11.0)
369.          CALL ORIGIN(5.0,10.5)
370.          CALL FACTOR(2.0,2.0)
371.          CALL AXIS(-3.0,0.0,23.0,'POSITION OF STRUCTURE IN XDIRECTION_'
372.         1,0.0,2.0,-3.0,20.0)
373.          CALL AXIS(-3.0,0.0,20.0,'POSITION OF STRUCTURE IN YDIRECTION_'
374.         1,-90.0,2.0,0.0,-20.0)
375.          CALL SYMBOL(2.0,-4.0,0.2,
376.         1'DEFORMED ROBOTIC ARM ON INTERNAL PRESSURIZATION_',0.0)
377.          CALL PLOT(XORD,YORD,MN)
378.    C
379.          WRITE(3,84) (RMOM(IY),IY=1,NN)
380.       84 FORMAT(1H ,'MOMENT AT PRESENT=',E12.5)
381.    C
382.    C*************************************************************
383.    C
384.    C     NOW TO CHECK THE CURRENT POSITION OF THE LOAD W.R.T THE
385.    C     THE FINAL DESIRED POSITION AND THEREBY VARY THE MOMENTS
386.    C     IN THE ELEMENTS
387.    C
388.          IF(KK.EQ.1) GO TO 69
389.          P1=P
390.          E1=E
391.          F1=F
392.          G1=G
393.    C
394.    C     TO EVALUATE THE COORDINATES OF THE CENTER OF THE LOAD
395.    C
396.          XB=X5-(RL+R1+H)*COS(SI)
397.          YB=Y5+(RL+R1+H)*SIN(SI)
398.          WRITE(3,85) XB,YB,XF,YF
399.       85 FORMAT(1H ,'XB=',E12.5,5X,'YB=',E12.5,5X,'XF=',E10.3,5X,
400.         1'YF=',E10.3)
401.          XDIS=XB-XF
402.          YDIS=YB-YF
403.          IF((ABS(XDIS).LE.1.0).AND.(ABS(YDIS).LE.1.0)) GO TO 60
404.    C
405.    C     NOW TO CHECK THE CURRENT POSTION OF LOAD W.R.T FINAL POSITION
406.    C
407.          IF((XDIS.LT.0.0).AND.(YDIS.LT.0.0)) GO TO 62
408.          IF((XDIS.LT.0.0).AND.(YDIS.GT.0.0)) GO TO 63
409.          IF((XDIS.GT.0.0).AND.(YDIS.LT.0.0)) GO TO 64
410.    C
411.    C     WHEN LOAD IS TO THE RIGHT AND HIGHER
412.    C
413.          NA=NU+1
414.          NB=NN-3
415.          P1=P1/(2.0*((NN-3)-NU))
416.          P2=P1
417.          DO 65 I=NA,NB
418.          RMOM(I)=RMOM(I)+RMOM(I)*D1
419.          P1=P1+P2
```

114

```
420.          65 CONTINUE
421.             P=P-P*0.05
422.             GO TO 83
423.       C
424.       C     WHEN LOAD IS TO THE LEFT AND LOWER
425.       C
426.          62 NC=NU+1
427.             ND=NN-3
428.             E1=E1/((2.0*(NN-3)-NU))
429.             E2=E1
430.             DO 66 I=NC,ND
431.             RMOM(I)=RMOM(I)-RMOM(I)*E1
432.             E1=E1+E2
433.          66 CONTINUE
434.             E=E-E*0.05
435.             GO TO 83
436.       C
437.       C     WHEN THE LOAD IS TO THE LEFT AND HIGHER
438.       C
439.          63 F1=F1/(2.0*NU)
440.             F2=F1
441.             DO 67 I=1,NU
442.             RMOM(I)=RMOM(I)-RMOM(I)*F1
443.             F1=F1+F2
444.          67 CONTINUE
445.             F=F-F*0.05
446.             GO TO 83
447.       C
448.       C     WHEN LOAD IS TO THE RIGHT AND LOWER
449.       C
450.          64 G1=G1/(2.0*NU)
451.             G2=G1
452.             DO 68 I=1,NU
453.             RMOM(I)=RMOM(I)+RMOM(I)*G1
454.             G1=G1+G2
455.          68 CONTINUE
456.             G=G-G*0.05
457.             GO TO 83
458.       C
459.       C     THE DATA MATRIX IS SEARCHED TO PROVIDE THE GUESS VALUE
460.       C
461.       C     TO EVALUATE PHI,RAD,THETA & DIS FOR THE GIVEN COORDINATES
462.          69 RAD=(ABS(XI)**2.0-ABS(YI)**2.0)**0.5
463.             DIS=((ABS(XF-XI))**2.0+(ABS(YF-YI))**2.0)**0.5
464.             THETA=ACOS((XF-XI)/DIS)
465.             IF(XI.LE.0.0) GO TO 360
466.             PHI=ATAN(XI/ABS(YI))
467.             GO TO 361
468.         360 PHI=-ATAN(XI/YI)
469.       C     THE SEARCHING STARTS NOW
470.       C
471.       C     TO FIND THE CLOSEST PHI
472.         361 I=0
473.         362 I=I+1
474.             IF(PHI.GT.D(I,1,1,1,1)) GO TO 362
475.             K=I-1
476.             DIFF=ABS(PHI-D(K,1,1,1,1))
477.             DIFF2=ABS(D(I,1,1,1,1)-PHI)
478.             IF(DIFF.GT.DIFF2) GO TO 363
479.             I=K
```

115

```
480.    C
481.    C       TO FIND THE CLOSEST RAD
482.       363 J=1
483.       364 J=J+1
484.           IF(RAD.GT.D(I,J,1,1,1)) GO TO 364
485.           L=J-1
486.           IF((RAD-D(I,L,1,1,1)).GT.(D(I,J,1,1,1)-RAD)) GO TO 365
487.           J=L
488.    C
489.    C       TO FIND THE CLOSEST THETA
490.       365 K=1
491.       366 K=K+1
492.           IF(THETA.GT.D(I,J,K,1,1)) GO TO 366
493.           M=K-1
494.           IF((THETA-D(I,J,M,1,1)).GT.(D(I,J,K,1,1)-THETA)) GO TO 367
495.           K=M
496.    C
497.    C       TO FIND THE CLOSEST DIS
498.       367 N=1
499.       368 N=N+1
500.           IF(DIS.GT.D(I,J,K,N,1)) GO TO 368
501.           L=N-1
502.           IF((DIS-D(I,J,K,L,1)).GT.(D(I,J,K,N,1)-DIS)) GO TO 369
503.           N=L
504.    C
505.    C       TO TRANSFER THE GUESS VALUE 'MOMENTS' IN THE MEMBERS TO
506.    C       START THE ITERATIVE PROCEDURE
507.    C
508.       369 DO 370 M1=1,NN
509.           M=M1+1
510.           RMOM(M1)=D(I,J,K,N,M)
511.       370 CONTINUE
512.    C
513.    C       THE GUESS MOMENT VALUES HAVE BEEN LOCATED
514.    C
515.        83 WRITE(3,57)KK
516.        57 FORMAT(1H ,'ITERATION NO ',I2,' IS COMPLETE')
517.        56 CONTINUE
518.    C       MAIN LOOP ENDS NOW
519.    C       THE MCUR HAS BEEN EVALUATED WITHIN 25 ITERATIONS
520.    C
521.    C
522.           WRITE(3,97)
523.        97 FORMAT(1H ,'NOT POSSIBLE TO REACH GOAL IN 25 STEPS')
524.           GO TO 172
525.    C
526.        60 CALL PICSIZ(0.0,0.0)
527.    C
528.    C*****************************************************************
529.    C
530.    C       ********************************************************
531.    C       * THE DATABASE IS CHECKED AND THE PRESENT RESULTS ARE   *
532.    C       * INSERTED IN THE PROPER PLACE IN THE DATABASE IF NEEDED *
533.    C       ********************************************************
534.    C
535.           DIS=((XB-XI)**2.0+(YE-YI)**2.0)**0.5
536.           THETA=ACOS((XB-XI)/DIS)
537.    C       TO PUT PHI IN PROPER PLACE IF REQUIRED
538.           I=0
539.       127 I=I+1
```

116

```
540.              IF(ABS(PHI-D(I,1,1,1,1)).LE.O.00009) GO TO 126
541.      C       NO NEED TO INSERT
542.              IF(PHI.GT.D(I,1,1,1,1)) GO TO 127
543.      C       TO INSERT AND PUSH THE DATA DOWN SUCCESSIVELY
544.              IP=I
545.              DO 150 I=1,N2
546.              IF(D(I,1,1,1,1).EQ.1000.0) GO TO 151
547.          150 CONTINUE
548.          151 IK=I+1
549.              IF(IK.GT.N2) GO TO 169
550.      C       THE INSERTION AND SHIFTING LOOP STARTS NOW
551.              D(IK,1,1,1,1)=D(I,1,1,1,1)
552.              IK=IK-1
553.              I=I-1
554.              IP5=IP-1
555.          167 IF(I.EQ.IP5) GO TO 166
556.              D(IK,1,1,1,1)=D(I,1,1,1,1)
557.              DO 152 J=2,M2
558.              D(IK,J,1,1,1)=D(I,J,1,1,1)
559.              IF(D(I,J,1,1,1).EQ.1000.0) GO TO 153
560.          152 CONTINUE
561.          153 JJ=J-1
562.              DO 154  J=2,JJ
563.              DO 155  K=2,N7
564.              D(IK,J,K,1,1)=D(I,J,K,1,1)
565.              IF(D(I,J,K,1,1).EQ.1000.0) GO TO 156
566.          155 CONTINUE
567.          154 CONTINUE
568.          156 KK=K-1
569.              DO 157 J=2,JJ
570.              DO 158 K=2,KK
571.              DO 159 L=2,M7
572.              D(IK,J,K,L,1)=D(I,J,K,L,1)
573.              IF(D(I,J,K,L,1).EQ.1000.0) GO TO 160
574.          159 CONTINUE
575.          158 CONTINUE
576.          157 CONTINUE
577.          160 LL=L-1
578.              DO 161 J=2,JJ
579.              DO 162 K=2,KK
580.              DO 163 L=2,LL
581.              DO 164 LM=2,MX
582.              D(IK,J,K,L,LM)=D(I,J,K,L,LM)
583.              IF(D(I,J,K,L,LM).EQ.1000.0) GO TO 165
584.          164 CONTINUE
585.          163 CONTINUE
586.          162 CONTINUE
587.          161 CONTINUE
588.      C       TO GO UP ONE INDEY AND PUSH DOWN
589.          165 IF(IK.EQ.IP) GO TO 166
590.              IK=IK-1
591.              I=I-1
592.              GC TO 167
593.      C       SHIFTING IS COMPLETE
594.          166 D(IK,1,1,1,1)=PHI
595.              D(IK,2,1,1,1)=RAD
596.              D(IK,3,1,1,1)=1000.0
597.              D(IK,2,2,1,1)=THETA
598.              D(IK,2,3,1,1)=1000 0
599.              D(IK,2,2,2,1)=DIS
```

117

```
600.            D(IK,2,2,3,1)=1000.0
601.            MC=NN+1
602.            DO 168 IB=2,MC
603.            KK=IB-1
604.            D(IK,2,2,2,IB)=RMOM(KK)
605.      168 CONTINUE
606.            MC=MC+1
607.            D(IK,2,2,2,MC)=1000.0
608.    C     INSERTION COMPLETE GO TO WRITE FILE AREA
609.            GO TO 170
610.    C
611.    C     ERROR MESSAGE IF FIRST DIMENSION WAS EXCEEDED
612.      169 WRITE(3,171)
613.      171 FORMAT(1H ,'THE FIRST DIMENSION WAS EXCEEDED')
614.    C     GO TO END OF PROGRAM
615.            GO TO 172
616.    C
617.    C     IF PHI WAS NOT INSERTED SEARCH TO SEE IF RAD NEEDS
618.    C     TO BE INSERTED IN THE DATABASE
619.      126 J=1
620.      174 J=J+1
621.            IF(ABS(RAD-D(I,J,1,1,1)).LE.0.009) GO TO 173
622.            IF(RAD.GT.D(I,J,1,1,1)) GO TO 174
623.    C     TO INSERT RAD
624.            JP=J
625.            DO 175 J=2,M2
626.            IF(D(I,J,1,1,1).EQ.1000.0) GO TO 176
627.      175 CONTINUE
628.      176 JK=J+1
629.            IF(JK.GT.M2) GO TO 177
630.            D(I,JK,1,1,1)=D(I,J,1,1,1)
631.            JK=JK-1
632.            J=J-1
633.            JP1=JP-1
634.      188 IF(J.EQ.JP1) GO TO 187
635.            D(I,JK,1,1,1)=D(I,J,1,1,1)
636.            DO 178 K=2,N7
637.            D(I,JK,K,1,1)=D(I,J,K,1,1)
638.            IF(D(I,J,K,1,1).EQ.1000.0) GO TO 179
639.      178 CONTINUE
640.      179 KK=K-1
641.            DO 180 K=2,KK
642.            DO 181 L=2,M7
643.            D(I,JK,K,L,1)=D(I,J,K,L,1)
644.            IF(D(I,J,K,L,1).EQ.1000.0) GO TO 182
645.      181 CONTINUE
646.      180 CONTINUE
647.      182 LL=L-1
648.            DO 183 K=2,KK
649.            DO 184 L=2,LL
650.            DO 185 LM=2,M7
651.            D(I,JK,K,L,LM)=D(I,J,K,L,LM)
652.            IF(D(I,J,K,L,LM).EQ.1000.0) GO TO 186
653.      185 CONTINUE
654.      184 CONTINUE
655.      183 CONTINUE
656.    C     GO UP AND PUSH DOWN AGAIN
657.    C
658.      186 IF(JK.EQ.JP) GO TO 187
659.            JK=JK-1
```

```
660.            J=J-1
661.            GO TO 188
662.        187 D(I,JK,1,1,1)=RAD
663.            D(I,JK,2,1,1)=THETA
664.            D(I,JK,3,1,1)=1000.0
665.            D(I,JK,2,2,1)=DIS
666.            D(I,JK,2,3,1)=1000.0
667.            MC=NN+1
668.            DO 189 IB=2,MC
669.            KK=IB-1
670.            D(I,JK,2,2,IB)=RMOM(KK)
671.        189 CONTINUE
672.            MC=MC+1
673.            D(I,JK,2,2,MC)=1000.0
674.            GO TO 170
675.     C      THE SECOND DIMENSION WAS EXCEEDED
676.        177 WRITE(3,190)
677.        190 FORMAT(1H ,'THE SECOND DIMENSION HAS BEEN EXCEEDED')
678.     C      GO TO THE END OF PROGRAM WITHOUT REWRITING THE DATAFILE
679.            GO TO 172
680.     C
681.     C      IF PHI & RAD WERE NOT INSERTED, CHECK FOR THETA
682.     C
683.        173 K=1
684.        192 K=K+1
685.            IF(ABS(THETA-D(I,J,K,1,1)).LE.0.00009) GO TO 191
686.            IF(THETA.GT.D(I,J,K,1,1)) GO TO 192
687.     C      TO INSERT THETA
688.            KP=K
689.            DO 193 K=2,N7
690.            IF(D(I,J,K,1,1).EQ.1000.0) GO TO 194
691.        193 CONTINUE
692.        194 KK=K+1
693.            IF(KK.GT.N7) GO TO 195
694.            D(I,J,KK,1,1)=D(I,J,K,1,1)
695.            KK=KK-1
696.            K=K-1
697.            KP1=KP-1
698.        202 IF(K.EQ.KP1) GO TO 201
699.            D(I,J,KK,1,1)=D(I,J,K,1,1)
700.            DO 196 L=2,M7
701.            D(I,J,KK,L,1)=D(I,J,K,L,1)
702.            IF(D(I,J,K,L,1).EQ.1000.0) GO TO 197
703.        196 CONTINUE
704.        197 LL=L-1
705.            DO 198 L=2,LL
706.            DO 199 LM=2,MX
707.            D(I,J,KK,L,LM)=D(I,J,K,L,LM)
708.            IF(D(I,J,K,L,LM).EQ.1000.0) GO TO 200
709.        199 CONTINUE
710.        198 CONTINUE
711.     C      GO UP AND PUSH DOWN AGAIN
712.        200 IF(KK.EQ.KP) GO TO 201
713.            K=K-1
714.            KK=KK-1
715.            GO TO 202
716.        201 D(I,J,KK,1,1)=THETA
717.            D(I,J,KK,2,1)=DIS
718.            D(I,J,KK,3,1)=1000.0
719.            MC=NN+1
```

```
720.              DO 272 IB=2,MC
721.              MZ=IB-1
722.              D(I,J,KK,2,IB)=RMOM(MZ)
723.          272 CONTINUE
724.              MC=MC+1
725.              D(I,J,KK,2,MC)=1000.0
726.     C        INSERTION COMPLETE GO TO WRITE FILE AREA
727.              GO TO 170
728.     C        THE THIRD DIMENSION HAS BEEN EXCEEDED
729.          195 WRITE(3,203)
730.          203 FORMAT(1H ,'THE THIRD DIMENSION HAS BEEN EXCEEDED')
731.     C        GO TO END OF PROGRAM WITHOUT REWRITING THE DATAFILE
732.              GO TO 172
733.     C
734.     C        IF PHI,RAD & THETA WERE NOT INSERTED, CHECK FOR DIS
735.     C
736.          191 L=1
737.          205 L=L+1
738.              IF(ABS(DIS-D(I,J,K,L,1)).LE.0.00009) GO TO 237
739.              IF(DIS.GT.D(I,J,K,L,1)) GO TO 205
740.     C        TO INSERT DIS
741.              LP=L
742.              DO 206 L=2,M7
743.              IF(D(I,J,K,L,1).EQ.1000.0) GO TO 207
744.          206 CONTINUE
745.          207 LK=L+1
746.              IF(LK.GT.M7) GO TO 208
747.              D(I,J,K,LK,1)=D(I,J,K,L,1)
748.              LK=LK-1
749.              L=L-1
750.              LP1=LP-1
751.          212 IF(L.EQ.LP1) GO TO 211
752.              D(I,J,K,LK,1)=D(I,J,K,L,1)
753.              DO 209 LM=2,MX
754.              D(I,J,K,LK,LM)=D(I,J,K,L,LM)
755.              IF(D(I,J,K,L,LM).EQ.1000.0) GO TO 210
756.          209 CONTINUE
757.     C        GO UP AND PUSH DOWN AGAIN
758.          210 IF(LK.EQ.LP) GO TO 211
759.              LK=LK-1
760.              L=L-1
761.              GO TO 212
762.          211 MC=NN+1
763.              DO 213 IB=2,MC
764.              MZ=IB-1
765.              D(I,J,K,LK,IB)=RMOM(MZ)
766.          213 CONTINUE
767.              MC=MC+1
768.              D(I,J,K,LK,MC)=1000.0
769.     C        INSERTION COMPLETE GO TO WRITE FILE AREA
770.              GO TO 170
771.     C        THE FOURTH DIMENSION WAS EXCEEDED
772.          208 WRITE(3,214)
773.          214 FORMAT(1H ,'THE FOURTH DIMENSION HAS BEEN EXCEEDED')
774.     C        GO TO END OF PROGRAM WITHOUT REWRITING DATAFILE
775.              GO TO 172
776.     C
777.     C
778.     C        TO OVERWRITE THE DATAFILE WITH THE NEW DATA
779.     C
```

```
780.      C      WRITE ALL THE 'PHI' FIRST
781.      C
782.      170 DO 215 I=1,N2
783.          WRITE(40,216) D(I,1,1,1,1)
784.      216 FORMAT(E11.4)
785.          IF(D(I,1,1,1,1).EQ.1000.0) GO TO 217
786.      215 CONTINUE
787.      C
788.      C      WRITE ALL THE 'RAD'
789.      C
790.      217 DO 218 I=1,N2
791.          IF(D(I,1,1,1,1).EQ.1000.0) GO TO 219
792.          DO 220 J=2,M2
793.          WRITE(40,221) D(I,J,1,1,1)
794.      221 FORMAT(E11.4)
795.          IF(D(I,J,1,1,1).EQ.1000.0) GO TO 218
796.      220 CONTINUE
797.      218 CONTINUE
798.      C
799.      C      WRITE ALL THE 'THETA'
800.      C
801.      219 DO 222 I=1,N2
802.          IF(D(I,1,1,1,1).EQ.100C.0) GO TO 223
803.          DO 224 J=2,M2
804.          IF(D(I,J,1,1,1).EQ.1000.0)  GO TO 222
805.          DO 225 K=2,N7
806.          WRITE(40,226) D(I,J,K,1,1)
807.      226 FORMAT(E11.4)
808.          IF(D(I,J,K,1,1).EQ.1000.0) GO TO 224
809.      225 CONTINUE
810.      224 CONTINUE
811.      222 CONTINUE
812.      C
813.      C      WRITE ALL THE 'DIS'
814.      C
815.      223 DO 228 I=1,N2
816.          IF(D(I,1,1,1,1).EQ.1000.0) GO TO 229
817.          DO 230 J=2,M2
818.          IF(D(I,J,1,1,1).EQ.1000.0) GO TO 228
819.          DO 231 K=2,N7
820.          IF(D(I,J,K,1,1).EQ.1000.0) GO TO 230
821.          DO 233 L=2,M7
822.          WRITE(40,234) D(I,J,K,L,1)
823.      234 FORMAT(E11.4)
824.          IF(D(I,J,K,L,1).EQ.1000.0) GO TO 231
825.      233 CONTINUE
826.      231 CONTINUE
827.      230 CONTINUE
828.      228 CONTINUE
829.      C
830.      C      WRITE ALL THE ELEMENT MOMENTS
831.      C
832.      229 DO 236 I=1,N2
833.          IF(D(I,1,1,1,1).EQ.1000.0) GO TO 237
834.          DO 238 J=2,M2
835.          IF(D(I,J,1,1,1).EQ.1000.0) GO TO 236
836.          DO 239 K=2,N7
837.          IF(D(I,J,K,1,1).EQ.100C.0) GO TO 238
838.          DO 241 L=2,M7
839.          IF(D(I,J,K,L,1).EQ.1000.0) GO TO 239
```

121

```
840.          DO 243 M=2,MX
841.          WRITE(40,244) D(I,J,K,L,M)
842.      244 FORMAT(E11.4)
843.          IF(D(I,J,K,L,M).EQ.1000.0) GO TO 241
844.      243 CONTINUE
845.      241 CONTINUE
846.      239 CONTINUE
847.      238 CONTINUE
848.      236 CONTINUE
849.    C
850.    C*****************************************************************
851.    C
852.    C      ***********************************************************
853.    C      * TO CALCULATE THE ADDITIONAL MOMENT DUE TO THE LOAD *
854.    C      * TO CALCULATE THE X-COORDINATE OF POINT C           *
855.    C      ***********************************************************
856.    C
857.      237 GAMA=ABS(SI-3*LN/RHO)
858.          RM3=W1*(RL+R1+H)
859.          XC=XB+(RL+R1+H)*COS(GAMA)
860.          RM2=W1*(RL+R1+H)*COS(GAMA)
861.          DO 70 J=1,NU
862.          RMOM(J)=RMOM(J)-RM2+W1*(XC-XORD(J))
863.       70 CONTINUE
864.          NF=NU+1
865.          NG=NN-3
866.          DO 71 J=NF,NG
867.          RMOM(J)=RMOM(J)+RM2-W1*(XC-XORD(J))
868.       71 CONTINUE
869.          NH=NN-2
870.          DO 72 J=NH,NN
871.          RMOM(J)=RMOM(J)+RM3
872.       72 CONTINUE
873.          WRITE(3,59) (RMOM(I),I=1,NN)
874.       59 FORMAT(1H ,'TOTAL MOMENT= ',E10.3)
875.      172 STOP
876.          END
877.    /*
878.    //G.FT40F001 DD DSN=DU.DO6.ZU2142.UMESH.LDATA,DISP=OLD
879.    //G.DUKEPLOT DD SYSOUT=C
880.    //G.SYSIN DD *
881.    1010 5 0.1944E+01    0.2E+01    0.11E-01
882.    -0.*951E+01  -0.14E+02    0.8E+01   -0.9E+01
883.       1+2-1 1-3
884.       1+2-1 1-3
885.       1+2-1 1-3
886.       1+2-1 1-3
887.       1+2-1 1-3
888.       1+2+1 1+3
889.       1+2+1 1+3
890.       1+2+1 1+3
891.       1+2+1 1+3
892.       1+2+1 1+3
893.       0.2E+02 0.115E+02    0 5E-02 0.101E-01 0.173E+00   0.2E+01   0.5E+00
894.       0.25E+02 C 764E+01 C 499E-02 C.228E-01  0.26E+00   0.2E+01   0.5E+00
895.       0.3E+02 0 573E+01 0 498E-02 0.404E-01 0.346E+00   0.2E+01   0.5E+00
896.       0.75E+02 0 458E+01 0.497E-02 0.630E-01  0.43E+00   0.2E+01   0.5E+00
897.       C 4E+02 0 382E+01 0.496E-02 0.901E-01 0.512E+00   0.2E+01   0.5E+00
898.       C 45E+02 0.327E+01 0.495E-02 0.123E+00 0.593E+00   0.2E+01   0.5E+00
899.       0 5E+02 0.287E+01 0 494E-02 0.158E+00 0.669E+00   0.2E+01   0.5E+00
```

122

```
900.        0.55E+02 0.255E+01 0.493E-02 0.199E+00 0.745E+00    0.2E+01    0.5E+00
901.        0.6E+02 0.229E+01 0.492E-02 0.245E+00 0.819E+00    0.2E+01    0.5E+00
902.        0.7E+02 0.191E+01 0.491E-02 0.346E+00 0.955E+00    0.2E+01    0.5E+00
903.         3     4     4     4    13
904.     /*
905.     //
```